

How Machine Learning Predicts and Explains the Performance of Perovskite Solar Cells

Yiming Liu, Wensheng Yan,* Shichuang Han, Heng Zhu, Yiteng Tu, Li Guan,* and Xinyu Tan*

Characterizing the electrical parameters of perovskite solar cells (PSCs) usually requires a lot of time to fabricate complete devices. Here, machine learning (ML) is used to reduce the device fabrication process and predict the electrical performance of PSCs. Using ML algorithms and 814 valid data cleaned from 2735 peer-reviewed publications, ML prediction models are built for bandgap, conduction band minimum, valence band maximum of perovskites, and electrical parameters of PSCs. These prediction models have excellent accuracy, and the root mean square error of the prediction models for bandgap and power conversion efficiency (PCE) reaches 0.064 eV and 1.58%, respectively. Among the many factors that affect the performance of PSCs, those factors play a major role in the lack of comprehensive explanation. Through the prediction model of electrical parameters and Shapley Additive explanations theory, the factors affecting the PCE of PSCs are explained and analyzed. It can not only verify the objective physical laws from the perspective of ML, but also conclude that among the 13 features, the content of formamidinium/ $\text{NH}_2\text{CHNH}_2^+$ plays the most important role in improving the PCE of PSCs. These results show that ML has great application possibilities in the PSC field.

1. Introduction

As a representative of the third generation of solar cells, perovskite solar cells (PSCs) have experienced rapid development in the past 12 years, and the certified power conversion efficiency

(PCE) of single-junction PSC has now reached 25.5%.^[1] The PCE of PSCs can be improved so quickly in a short time, which is inseparable from the excellent properties of the perovskite material itself (tunable bandgap, faster carrier mobility, high absorption coefficients, lower exciton binding energy, etc.).^[2–6] Of course, it is even more inseparable from the optimization design of PSCs by many scholars, such as the optimization of energy-level alignment; the development of new transport layer materials; the passivation of material defects.^[7–9] However, without exception, these require a lot of time and resources for trial and error experiments. To overcome this problem, some simulation software based on density functional theory (DFT) have been developed, which can simulate the structure and chemical composition of materials.^[10–12] Nevertheless, researchers need to have a lot of computing resources and rich knowledge of quantum chemistry, and most simulation calculations are aimed at the material itself. As the studied system becomes complex, such as devices (systems) composed of various chemical materials, these methods are no longer applicable.

The behavior that computers use data to analyze, learn and summarize is called artificial intelligence,^[13] and ML belongs to an important branch of artificial intelligence.^[14] It can infer potential rules and relationships among materials, and between materials and the features of the complex system composed of materials only through the data itself without knowing the physical laws. Machine learning (ML) has broad prospects in the field of materials science, such as searching for virtual materials; reducing the amount of calculation required for DFT; reducing experimental procedures and time, etc.^[15–17] Although ML has been used in the field of materials, the research in the field of PSCs is still in the preliminary exploration stage,^[18,19] such as the prediction of the formability and stability of perovskites,^[20] the screening of lead-free perovskite materials suitable for cells,^[21] and the judgment of the features affecting the stability of PSCs,^[22] and so on. According to the way of data acquisition, the research of ML in the field of perovskite can be divided into two types: ML analysis based on simulated data generated by DFT theory or experimental data from real experiments.^[23,24] In which, Saidi et al. used structural information of 380 perovskite compositions, which were generated by DFT

Y. Liu, W. Yan, H. Zhu, Y. Tu, X. Tan
College of Electrical Engineering & New Energy
Hubei Provincial Collaborative Innovation Center for New Energy
Microgrid
China Three Gorges University
Yichang 443002, China
E-mail: tanxin@ctgu.edu.cn

W. Yan
Electronics and Information College
Hangzhou Dianzi University
Hangzhou 310018, China
E-mail: wensheng.yan@hdu.edu.cn

S. Han, L. Guan
Department of Physics Science and Technology
Hebei University
Baoding 071000, China
E-mail: lguan@hbu.edu.cn

 The ORCID identification number(s) for the author(s) of this article can be found under <https://doi.org/10.1002/solr.202101100>.

DOI: 10.1002/solr.202101100

and convolutional neural networks (CNN) to predict bandgaps, lattice constants, and octahedral angles.^[25] Shahzada, Ahmad et al used the random forest (RF) algorithm to predict the bandgap and PCE of PSCs based on UV-vis absorption and J-V spectra data^[26]. The aforementioned articles mostly use ML tools to screen unknown materials or predict their performance. The explanations of ML models and the mining of potential physical laws between features are rarely involved.

Our contributions mainly include the following three aspects: 1) We cleaned 814 data with bandgap, CBM, VBM, perovskite composition, and carrier mobility from 4812 published research articles and further established device-level database of bandgap and electrical parameters with 8/11/13 dimensional features; 2) Through the aforementioned 2 databases and 7 ML algorithms, we have built 49 prediction models and selected 7 prediction models with the best performance ($\text{Bandgap}_{\text{XGBoost}}$, $\text{CBM}_{\text{XGBoost}}$, $\text{VBM}_{\text{XGBoost}}$, PCE_{RF} , V_{ocRF} , J_{scRF} , and FF_{RF} , where the subscript is the ML algorithm used in the prediction model) based on root mean square error (RMSE) and Pearson correlation coefficient. The features required by the electrical parameter prediction models can also be input through $\text{Bandgap}_{\text{XGBoost}}$, $\text{CBM}_{\text{XGBoost}}$, and $\text{VBM}_{\text{XGBoost}}$ to reduce the amount of features that need to be actually characterized; and 3) Exploring the predictive mechanisms of ML models may lead to some unexpected findings that can be used to guide further research directions. Global and local explanations of samples and prediction models are carried out through the SHapley Additive exPlanations (SHAP) explainer. At the global level, the SHAP values of each feature under different algorithms and data structures are calculated, and the feature importance ranking affecting the PCE of ABX₃-type PSCs is obtained. At the local level, the samples with low and high efficiency in the database are explained,

respectively, and the reasons for low and high PCE are found. Finally, it is found that the content of FA is essential for single-junction high-performance ABX₃-type PSCs.

2. Build Models

As shown in Figure 1, the present work establishes and explains the prediction model according to the following process. It mainly includes model explanation, establishment of database, feature extraction, model selection, model evaluation, and model application.

2.1. Model Explanation

As the complexity of ML models increases, some ML models gradually lose explainability while gaining superior predictive ability, and these models are called “black-box models.” For example, RF, gradient boosting decision tree (GBDT), Xtreme Gradient boosting (XGBoost). SHAP originated from cooperative game theory. In 2017, Lundberg and Lee’s article used SHAP values to explain various ML models, making the ML models explicable.^[27] SHAP is a cumulative explainable tool. Suppose the i th sample is x_i , the j th feature of the i th sample is $x_{i,j}$, the predicted value of the model for the i th sample is $f(x_i)$, and the base value of the model (the mean of the dependent variable for all samples) is f_{base} , then the SHAP value obeys the following equation

$$f(x_i) = f_{\text{base}} + \sum_{j=1}^n \varphi(x_{i,j}) \quad (1)$$

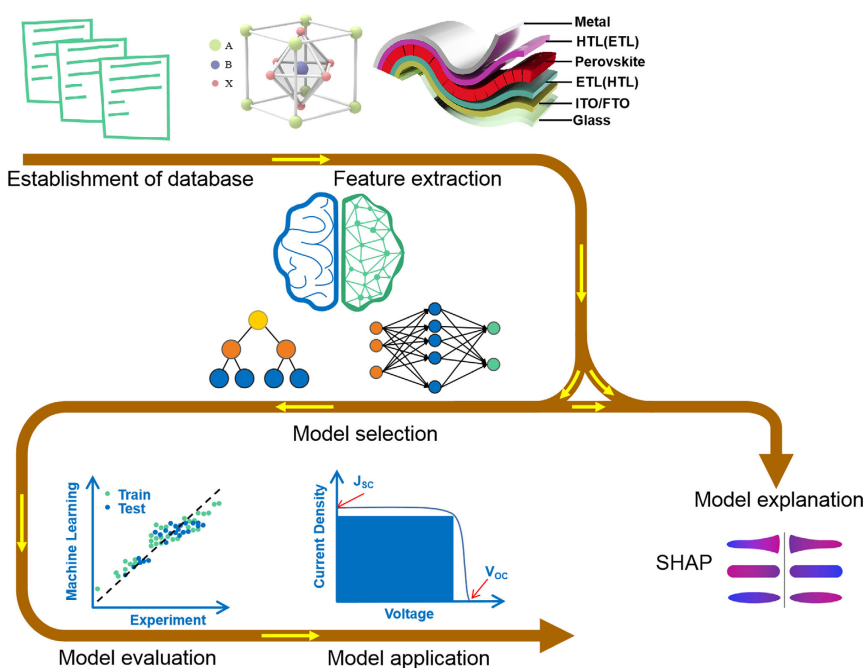


Figure 1. The flowchart of establishing and explaining for the prediction model.

$\varphi(x_{i,j})$ is the contribution of the j th feature in the i th sample to the predicted value, namely, SHAP value.

As shown in Figure 2, when $\varphi(x_{i,j}) > 0$, it means that the feature boosts the predictive value, corresponding to the red area; conversely, it means that the feature lowers the predictive value, corresponding to the blue area. The greatest advantage of SHAP is that it reflects the influence of the feature of each sample, and also shows the negative and positive contribution of this influence. We make two kinds of explanations by SHAP. 1) Global explanations. Rank the importance of all features and visually represent the contribution of each feature when it changes; and 2) Local features and sample explanations. Explaining the influence of features on predicted values under a single feature or two-feature interactions. Interpretable dimensionality reduction was performed using principal component analysis (PCA) and SHAP values to analyze the features that had the greatest impact on the first and second principal components. The explanatory analysis is performed for the main features that affect the predicted value of a single sample.

2.2. Establishment of Database

2.2.1. Data Preparation

Articles that contain the keywords “perovskite energy level,” “perovskite bandgap,” and “perovskite mobility” were downloaded from Wiley, Elsevier, Springer Nature, and other publishers, totaling 4812 articles. Only articles published after 2014 were retained, totaling 3224 articles. To ensure a sufficient amount of data and the practicability of the ML model, we only retained articles about the perovskite solar cell that has ABX_3 -type structure. In the end, there were only 2735 articles left. The monovalent cation at the A position is usually cesium (Cs^+), methylammonium ($MA^+/CH_3NH_3^+$), formamidinium ($FA^+/NH_2CHNH_2^+$); the divalent metal ion at the B position is usually lead (Pb^{2+}), Tin (Sn^{2+}); the halogen anion at the X position is iodide (I^-), bromide (Br^-), chloride (Cl^-). For the structure of single-junction PSCs, we chose the most common structure (with photoanode, single-electron transport layer,

single-perovskite layer, single-hole transport layer, and metal cathode). The active areas of PSCs are about 0.1 cm^2 .

2.2.2. Data Cleaning

The first step is to delete the duplicate and abnormal data, such as the duplicate bandgap data under the same chemical composition and the data with too low PCE and fill factor (FF) due to immature technological means.^[28] The second step is to ensure the standardization of data sources that the bandgap, CBM, and VBM of perovskite materials are obtained by experimental means. The electrical parameters of PSCs were measured under AM1.5G sunlight at 100 mW cm^{-2} . The carrier mobility is uniformly measured by the space-charge-limited current method (SCLC), and considering the influence of doping on the carrier mobility of the material, ensure that the state of the material used in the device (whether doped) is consistent with the state of the material during SCLC test. The third step is data supplement. As shown in Table S1, Supporting Information, common material features that are not mentioned in the literature but are used in modeling are uniformly supplemented.

2.3. Feature Extraction

The properties of materials or devices are determined by some factors, which are also called features. Feature extraction usually follows three principles: highly relevant to the output, easy to obtain, and minimal number.^[29,30] For ABX_3 -type perovskites, the information of bandgap, CBM, and VBM are mainly determined by the chemical compositions due to the fixed structure. Therefore, we select eight chemical compositions (MA, FA, CS, Pb, Sn, Br, Cl, I) as the features of the bandgap, CBM, and VBM prediction models. The electrical performances of PSCs are determined by numerous features such as the high absorption coefficient and high carrier mobility of perovskite, the transport and blocking effect of transport layer for holes and electrons, the effect of energy offsets alignment at the interface for carrier transfer, etc. However, considering the principles of feature extraction, cell structure, and energy conversion theory (exciton generation, carrier separation, and collection), we constructed a

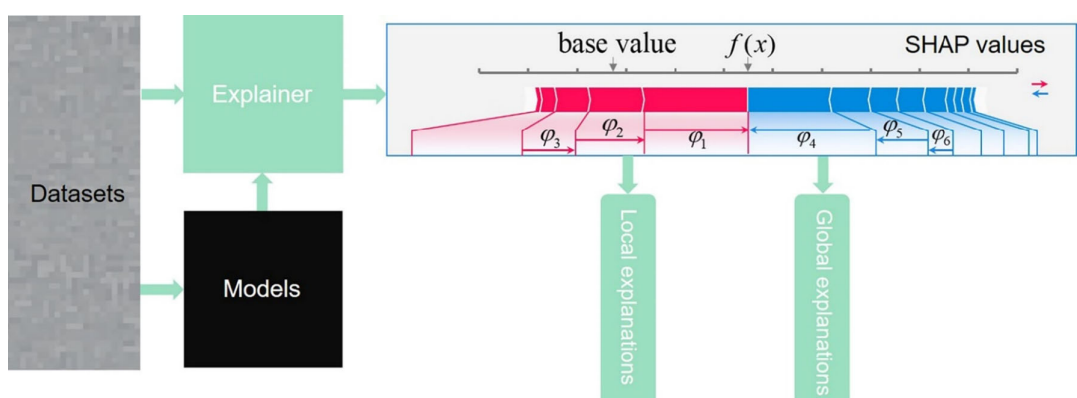


Figure 2. Schematic representation of SHAP explanation. $f(x)$ is the final predicted value of a sample, base value is the average of the predicted values of all samples. The red and blue areas represent the positive and negative contributions to the final predicted value of the sample, φ_x is the contribution value of the X_{th} feature.

set of representative features. Taking into account the properties of perovskite itself, we choose eight chemical compositions and bandgap of ABX₃-type perovskites as the features of absorber layer properties(MA, FA, Cs, Pb, Sn, Br, Cl, I, bandgap). The energy-level alignment at the interface is considered to act as a barrier and energy loss for the transfer of electrons and holes. We use energy-level alignment H ($H = \text{HTL}_{\text{HOMO}} - \text{Perovskite}_{\text{VBM}}$) and L ($L = \text{Perovskite}_{\text{CBM}} - \text{ETL}_{\text{LOMO}}$) as a feature representing the energy-level alignment at the interface (HTL/perovskite, ETL/perovskite, highest occupied molecular level for HOMO, and lowest unoccupied molecular level for LOMO). The transport layer can promote carrier transport and inhibit recombination. Taking into account the role of the transport layer on carrier transport, we use electron and hole mobility to represent the features of the transport layer material. Therefore, we constructed a set of 13-dimensional features as the inputs of the electrical parameter prediction models (MA, FA, Cs, Pb, Sn, Br, Cl, I, bandgap, H, L, electron mobility, hole mobility). Finally, we established device-level database, including 103 and 248 sets of data, respectively. The databases are shown in Table S2 and S3 (Supporting Information). The 11-dimensional feature database of electrical parameters (except electron mobility and hole mobility) used only for data dimension comparison and model explanation contains 463 groups of data, as shown in Table S4, Supporting Information. The 13 features were chosen for an explanation as shown in Table S19, Supporting Information.

2.4. Model Selection

Prediction models and SHAP explainer are built using scikit-learn and SHAP toolkit on PyCharm platform.^[31] Each prediction model is optimized by seven ML algorithms,^[32] which are linear regression (LR), K-nearest neighbor (KNN),^[33] support vector regression (SVR)^[34] random forest (RF),^[35] multilayer perceptron (MLP), gradient boosting decision tree (GBDT)^[36] and XGBoost.^[37] Linear regression (LR) is the simplest regression algorithm based on supervised learning, which uses the best linear function between the independent variable and the dependent variable for fitting. KNN is often used for classification problems, and its principle is simply summarized as “those who are close to each other are red, and those who are close to each other are black.” The K known “neighbors” closest to the unknown sample are used to vote, and then the unknown sample is predicted according to the majority-voting rule and the information of K “neighbors.” The K value of the KNN algorithm is regulated by the n_neighbors parameter in scikit-learn. SVR is an application of SVM for nonlinear regression problems that maps the data to the required feature space using kernel function. SVR creates a “spacing band” on both sides of the linear function, with a spacing of ϵ (an empirical value set manually). The loss is not calculated for all samples falling into the spacing band. Finally, the optimized model is obtained by minimizing the total loss and maximizing the spacing. MLP is also known as a feedforward neural network, which consists of an input layer, hidden layer, and output layer. Each layer is fully connected to the next layer. It has three basic elements: weights, biases, and activation functions. RF is an ensemble of independent tree learners.

First, multiple training sets are generated by the bootstrap method, and then, for each training set, a decision tree is constructed. When the nodes of the tree need to be split, a part of the features is randomly extracted from the total features, and the optimal solution is found among the extracted features, which are applied to the nodes and split. Due to the idea of bagging, its over-fitting and anti-interference ability are relatively strong. For regression problems, the final result depends on the average of the prediction results of all tree learners. Unlike RF, GBDT is an iterative algorithm that uses decision trees as learners, where all decision trees are regression trees. Its core is to use the residuals left by K-1 regression trees before fitting the Kth regression tree, thus continuously reducing the error of the model. The basic idea of XGBoost is the same as that of GBDT, but some optimizations are made, such as default missing value processing, adding second-order derivative information, regular term, and parallel computing. Among them, RF, GBDT, XGBoost are originated from ensemble learning ideas.

2.5. Model Evaluation

The relevant hyper-parameter search and model evaluation was performed by the “GridSearchCV” and “Fivefold cross-validation.” The evaluation metrics are RMSE and Pearson's correlation coefficient (r value). RMSE is the most popular regression evaluation indicator, which can be used to judge the accuracy of the ML model. To prevent overfitting,^[17,38] the RMSE of the training set shall not be less than 70% of the RMSE of the test set. Pearson's correlation coefficient is used to judge the correlation between the predicted values output by the ML model and the collected experimental values. The r value between 0.8 and 1 is a very strong correlation, and the correlation decreases every 0.2 for strong correlation, moderate correlation, and weak correlation, respectively.

2.6. Model Application

Based on the established database and ML algorithm, we selected 7 models from 49 prediction models to predict parameters of PSCs (Bandgap, CBM, VBM, PCE, J_{sc} , V_{oc} , FF). The PCE prediction model is used to perform SHAP explanations and analysis, and then find the main factors affecting PCE of PSCs among 13 influencing factors.

3. Results and Discussion

Prediction performance of bandgap, CBM, and VBM. First, 20% of the total data in Table 2 is randomly selected as the test set while the remaining 80% is used as the training set (the training set and the test set are mutually exclusive), and then use 7 ML algorithms for model training. As shown in Table S5-S7, Supporting Information, we list the optimal algorithm, hyper-parameters, r -value of the test set, RMSE of the training set and test set under each prediction model. The RMSE of the training set represents the learning performance of the model. The lower the RMSE value of the training set, the better the learning performance of the model. However, too much difference from the RMSE of the test set may lead to over-fitting. The r -value

Table 1. Comparison of the performance for different prediction models and their parameters under the XGBoost algorithm (using Table S2, Supporting Information, as the database).

Models	Hyper-parameters	Train RMSE [eV]	Test RMSE [eV]	r value (Test)
Band gap _{XGBoost}	'colsample_bytree':0.7,'gamma':0,'learning_rate':0.1,'max_depth':2,'min_child_weight':3, 'n_estimators':300,'reg_alpha':0,'reg_lambda':1,'subsample': 0.8	0.044	0.064	0.96
CBM _{XGBoost}	'colsample_bytree':0.5,'gamma':0.1,'learning_rate':0.15,'max_depth':4,'min_child_weight':3, 'n_estimators':5000,'reg_alpha':0,'reg_lambda':1,'subsample': 0.9	0.134	0.133	0.78
VBM _{XGBoost}	'colsample_bytree':0.7, 'gamma':0.1,'learning_rate': 0.15,'max_depth':4,'min_child_weight':4, 'n_estimators':5000,'reg_alpha':0,'reg_lambda':2,'subsample': 0.9	0.149	0.178	0.71

and RMSE of the test set represent the prediction ability of the model for unknown materials. High *r*-value and low RMSE indicate that the model has strong prediction ability. It can be seen from Table S5–S7, Supporting Information, that as the ML algorithm becomes more and more complex, the fitting situation and predictive ability of the model become more perfect. Among them, the top three prediction performances are three algorithms (RF, GBDT, XGBoost) under the ensemble learning framework. Because ensemble learning builds multiple “learners” to make combined predictions together, which has a strong accuracy for some tabular data that are not strongly related in the spatial and temporal dimensions. Of course, the best performing algorithm is XGBoost for the database we built. **Table 1** shows the three models with the best prediction performance for Bandgap, CBM, and VBM (Bandgap_{XGBoost}, CBM_{XGBoost}, VBM_{XGBoost}). As shown in Table 1, the training and test sets RMSE of Band gap_{XGBoost}, CBM_{XGBoost}, VBM_{XGBoost} are 0.044 and 0.064 eV, 0.134 and 0.133 eV, 0.149, and 0.178 eV. This shows that these models have a perfect fit and satisfactory predictive ability. The RMSE of a similar training set and test set shows that the model is not over-fitting. The *r*-value of each model is above 0.7, indicating that the predicted value of our model has a strong correlation with the experimental value. In other words, the predictive model we build has a better predictive ability for the bandgaps of unknown composition. **Figure 3** shows the fitting performance of our ML model. The prediction values of the three prediction models are very close to the

experimental values in published articles, which represents the superiority of the prediction model we built.

Prediction performance of four electrical parameters. As shown in Table S3, Supporting Information, 13 features (MA, FA, Cs, Pb, Sn, Br, Cl, I, Bandgap, H, L, electron mobility, hole mobility) have been used to predict four electrical parameters (PCE, J_{sc} , V_{oc} , FF). The division of training and test sets is the same as aforementioned. The optimal hyper-parameters, algorithms, and training results under the four electrical parameters are shown in Table S8–S11, Supporting Information. Because the nature of the data is similar to that of Table S2, Supporting Information, the best performance is also the three algorithms under the ensemble learning. As shown in Table S8, Supporting Information, the RMSE of the training set and test set are decreased from 2.34% and 2.96% to 1.17% and 1.58%, in other words, the accuracy of the ML model increased by more than 40%, and the *r*-value of the test set increased from 0.61 to 0.86, which further illustrates the superiority of the complex ML models. As shown in Table S9, Supporting Information, the RMSE of V_{oc} predicted value are also significantly reduced through the filtering of the algorithm, the RMSE of the training set is reduced from 0.077 to 0.036 V, the RMSE of the test set is reduced from 0.093 to 0.051 V, and the *r* value is increased from 0.76 to 0.93. As shown in Table S10, Supporting Information, the *r*-value under each algorithm is above 0.9, which indicates that the features we built can well correlate with the changes of J_{sc} . Of course, the RMSE of training and test sets can also be reduced

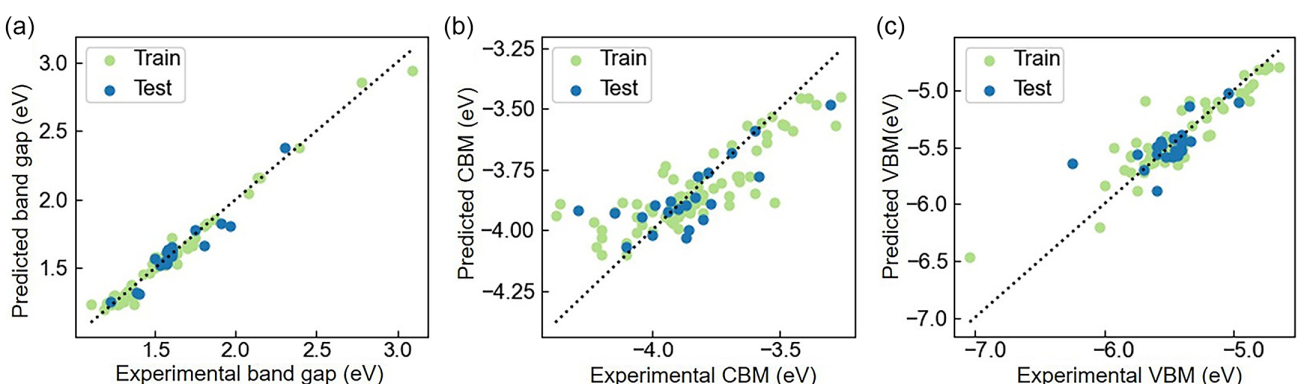
**Figure 3.** Comparison of experimental values and ML prediction values using XGBoost algorithm. The horizontal axis represents the experimental data collected from published articles, and the vertical axis represents the predicted value output by our prediction model. The green and blue dots are the training and test dataset. a) Predicted bandgap versus experimental bandgap. b) Predicted CBM versus experimental CBM. c) Predicted VBM versus experimental VBM.

Table 2. Comparison of the performance for different prediction models and their parameters under the RF algorithm (using Table S3, Supporting Information, as the database).

Models	Hyper-parameters	Train RMSE	Test RMSE	r value (Test)
PCE _{RF}	n_estimators = 50,max_features = 'auto',max_depth = 10,min_samples_split = 3,min_samples_leaf = 1,	1.15%	1.58%	0.86
Voc _{RF}	n_estimators = 500,max_features = 'sqrt',max_depth = 10,min_samples_split = 3,min_samples_leaf = 1,	0.036 V	0.051 V	0.93
Jsc _{RF}	n_estimators = 50,max_features = 'auto',max_depth = 10,min_samples_split = 3,min_samples_leaf = 1,	0.85 mA cm ⁻²	1.04 mA cm ⁻²	0.96
FF _{RF}	n_estimators = 20,max_features = 'sqrt',max_depth = 110,min_samples_split = 5,min_samples_leaf = 3,	0.034	0.046	0.63

with this highly correlated data. As shown in Table S11, Supporting Information, although the RMSE of the training set and the test set are also low (from training set: 0.049 to 0.033, test set: 0.073 to 0.046) and the r-value has increased considerably from 0.18 to 0.63, the r-value is the lowest of the four-parameter predictions. There are two reasons for this: We artificially deleted some data with low FF to prevent the influence of defects and fabrication processes on the prediction; Due to the difficulty of collecting some features that can represent FFs, we chose to give up, resulting in our built features being insensitive for predicting FF values. For this point, we can also use the three parameters predicted and the formula of photoelectric conversion efficiency to calculate. The best predictive models of electrical parameters (PCE_{RF}, Voc_{RF}, Jsc_{RF}, FF_{RF}) are shown in Table 2. The optimal algorithm is RF algorithm. The training

and test sets RMSE of PCE_{RF}, Voc_{RF}, Jsc_{RF} and FF_{RF} are 1.15% and 1.58%, 0.036 V and 0.051 V, 0.85 and 1.04 mA cm⁻², 0.034 and 0.046, respectively. Figure 4 shows the fitting performance of the training set and the test set of four electrical parameters prediction models, and the predicted values of the four electrical parameters are very close to the experimental values without over-fitting. Based on Table 2 and Figure 4, it can be demonstrated that our prediction models not only fit the known training data well but also predicts the electrical parameters for massive unknown materials of ABX₃ perovskite solar cells. Despite the exciting prediction performance of the prediction models, it has to be admitted that there is still some error in the predicted values from the experimental values. We consider the differences of the cell fabrication process as one main reason for the error, although we use some means to

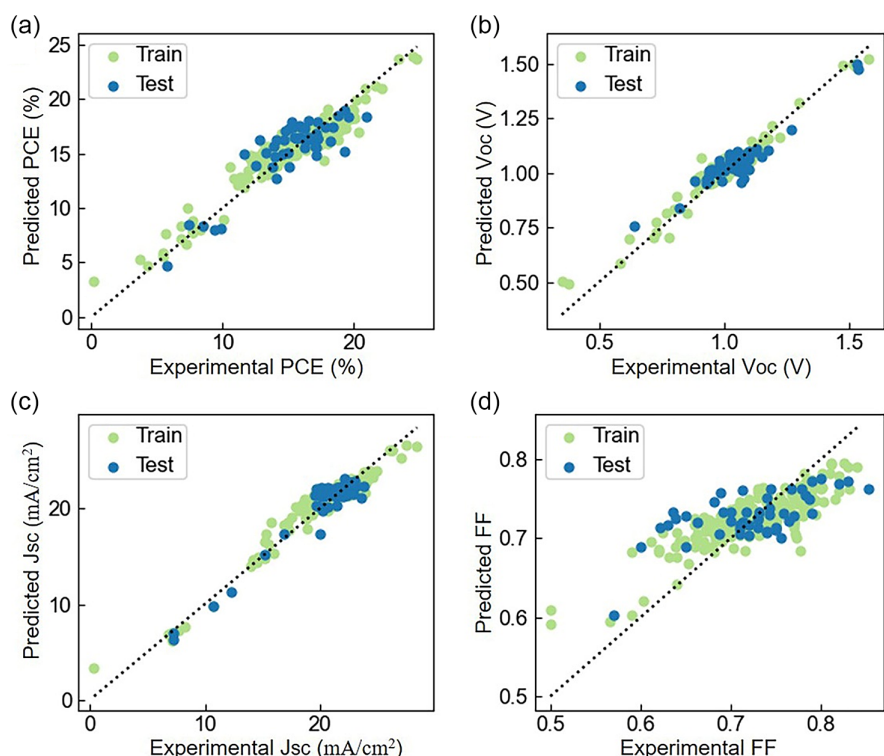


Figure 4. Comparison of experimental values and ML prediction values using RF algorithm. The horizontal axis represents the experimental data collected from published articles, and the vertical axis represents the predicted value output by our prediction model. The green and blue dots are the training and test dataset. a) Predicted PCE versus experimental PCE. b) Predicted Voc versus experimental Voc. c) Predicted Jsc versus experimental Jsc. d) Predicted FF versus experimental FF.

avoid it as much as possible (collecting the latest published data; avoiding data under immature processes; collecting data with detailed experimental details, etc.).

$\text{Bandgap}_{\text{XGBoost}}$, $\text{CBM}_{\text{XGBoost}}$, $\text{VBM}_{\text{XGBoost}}$ are the inputs of PCE_{RF} , V_{ocRF} , J_{scRF} , FF_{RF} . Using $\text{Bandgap}_{\text{XGBoost}}$, $\text{CBM}_{\text{XGBoost}}$, $\text{VBM}_{\text{XGBoost}}$ predicted bandgap, CBM, VBM as the inputs of four electrical parameter prediction models (PCE_{RF} , V_{ocRF} , J_{scRF} , FF_{RF}), to test the feasibility of combining the models. We randomly select 27 sets of experimental data from Table S3, Supporting Information, then replace the three features of Bandgap, H, and L with predicted values, and finally, predict four electrical parameters. Note that we use the same prediction model as in Table 1 and 2, making only changes in the data. The fitting performance is shown in Figure S1, Supporting Information, and the specific prediction parameters are shown in Table S13, Supporting Information. Table S13, Supporting Information, includes the comparison between the predicted and experimental values of the bandgap, PCE, J_{sc} , V_{oc} , and FF. We found that the accuracy of the model when the two models are combined to predict electrical parameters is not much different from that when 13 experimental values are used as features. When the model is combined, the RMSE and r -value of the predicted and experimental values of PCE, V_{oc} , J_{sc} , FF are 1.06% and 0.96, 0.059 V, and 0.96, 1.03 mA cm⁻² and 0.98, 0.041, and 0.62, respectively. This shows the feasibility of the model combination. The combination of models can significantly reduce the collection of experimental values (features). For devices where the transport layer is a material with unknown properties, we only need to collect the electron mobility and LOMO of the electron transport layer, and the hole mobility and HOMO of the hole transport layer to predict the electrical parameters of the device. When the composition of the ABX₃ perovskite and the material of the transport layer are known in the device, the collection of experimental values is not even required. The prediction model we built can also assist in the experimental work. For example, for the development of new materials of the transport layer, if the properties of the materials meet the expectations, but there are problems in the device PCE, this may be caused by energy level misalignment. At this time, the change of perovskite compositions and energy level alignment can be carried out through the above ML model to find the ABX₃ perovskite compositions most suitable for this material. To verify the accuracy of the model for bandgap and PCE prediction, we collected 7 latest reports. The five bandgap components and two hole transport materials have never existed in our database. As shown in Table S20 and S21, Supporting Information, our model is able to make excellent predictions.

Unlike traditional analysis methods, we can use the SHAP tool to find the main factors that influence the PCE of PSCs in a context when the underlying physical laws are not clear. To ensure that the factors affecting the PCE of PSCs found by SHAP theory are consistent with the real experimental conditions. First, we choose an electrical parameter prediction model (PCE_{RF}) with 13 experimental values as features for SHAP explanation, and the algorithm of PCE_{RF} used is the RF algorithm with the highest accuracy. Then, we verify whether the explanation obtained through the SHAP theory conforms to the physical facts.

As shown in Figure 5a,b, Supporting Information, the red dashed frames are the area where the SHAP value is positive

(positive contribution area). When the energy-level difference is 0 eV, the SHAP value of H and L is the largest, representing the maximum gain effect on PCE of PSCs at this time. With the increase of energy-level difference, the SHAP value changes from positive to negative and shows an obvious downward trend, which shows that the increase of energy-level difference has a significant negative effect on the PCE of PSCs, and further shows that good energy level alignment can effectively increase the PCE of PSCs. As shown in Figure 5c,d, the SHAP value of electron and hole mobility changes sharply from a negative value to a positive value within a range. Most samples with high mobility have a positive range of SHAP value, but the SHAP value changes little with the increase of mobility. This indicates that too low mobility will significantly reduce the PCE of PSCs. The increase of mobility can appropriately improve the PCE of PSCs, but when the mobility increases more than a certain level, it has little effect on the change of PCE for PSCs. Figure 5 proves that the model explanation obtained by the SHAP explanation conforms to the objective physical facts.

As shown in Figure 6a, the change trend of FA content with bandgap is not obvious. The samples with a band gap in the range of 1.5–1.55 eV and high FA content have the highest SHAP value. With the increase or decrease of bandgap, the SHAP value has an obvious downward trend, indicating that high FA content and appropriate bandgap have an obvious gain contribution to the PCE of PSCs. As shown in Figure 6b, bandgap has an obvious decreasing trend with the increase of Sn content. The PSC with bandgap in the range of 1.5–1.55 eV and low Sn content has the highest SHAP value, which indicates that the content of Sn can significantly affect the change of bandgap, and low bandgap and high content of Sn are the killers of high PCE. Therefore, it is necessary to have an appropriate bandgap, increase the addition of FA and reduce the content of Sn as much as possible for PSC with high PCE. See the following section for specific analysis.

Global explanations for factors affecting PCE of PSCs by SHAP theory. As shown in Figure 7, the PCE_{RF} is explained and 13 features that affect the PCE of PSCs are analyzed. The top five features with greater impact are FA, hole mobility, Sn, bandgap, and I in order. The decrease of hole mobility has a greater negative effect than the positive effect when it increases on the PCE of PSCs, which shows that the low PCE of PSCs are generally caused by low hole mobility, but this factor is not the most important factor leading to high PCE of PSCs. FA content has the most important influence among the 13 features. The decrease of FA content has a little negative impact on the PCE of PSCs, but the increase of FA content has an obvious gain trend on the PCE of PSCs, indicating that FA content plays a major role in the PSCs with high PCE. The increase of Sn content and the decrease of I content can significantly reduce the PCE of PSCs, which may be due to the content of Sn and I having an impact on the bandgap of perovskites, as well as the change of bandgap has an impact on both J_{sc} and V_{oc} of PSCs, and finally affects the PCE of PSCs. This indicates that PSCs with high PCE should increase the content of FA and select the appropriate bandgap as much as possible. We further explained different data and ML models by changing the algorithm and feature dimension to see whether similar findings could be explored. As algorithm comparison, we chose the prediction models

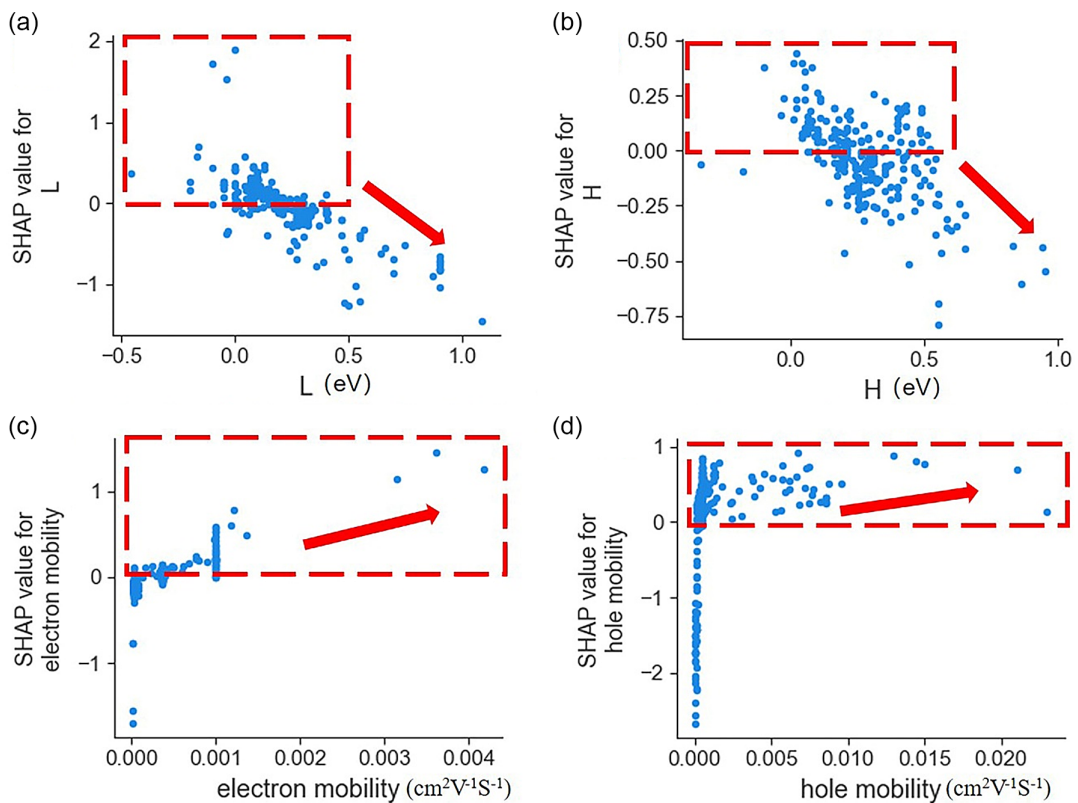


Figure 5. Dependence plot of a single feature versus its SHAP value in the PCE_{RF} . SHAP value represents the contribution of each feature to make a predicted value, the SHAP value increases as the contribution increases. the positive and negative SHAP values represent the gain and deduction contribution to the predicted value. a) L versus its SHAP value. b) H versus its SHAP value. c) Electron mobility versus its SHAP value. d) Hole mobility versus its SHAP value.

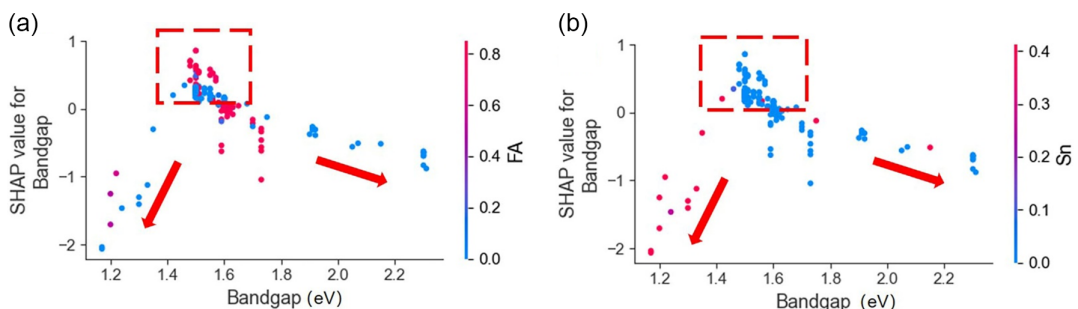


Figure 6. SHAP dependence plot of bandgap versus its SHAP value in the PCE_{RF} . a) Variation with FA. b) Variation with Sn.

(PCE_{GBDT} , $\text{PCE}_{\text{XGBoost}}$) whose prediction effect is second only to PCE_{RF} for an explanation. As shown in Figure S2 and S3, Supporting Information, the top five features that have the greatest impact when using PCE_{GBDT} are FA, I, hole mobility, bandgap, I. When the $\text{PCE}_{\text{XGBoost}}$ is used, the top five features with greater impact are FA, hole mobility, Pb, bandgap, MA. As a data comparison, we have established an electrical parameter database with 11 features, which contains 463 sets of data (Table S4, Supporting Information). The PCE prediction model is built by Table S4, Supporting Information. The specific parameters and algorithm comparisons are shown in Table S12,

Supporting Information. The top three models with the best accuracy are PCE_{RF11} , $\text{PCE}_{\text{XGBoost11}}$ and $\text{PCE}_{\text{GBDT11}}$. We perform a SHAP explanation on these three models. As shown in Figure S4, Supporting Information, when the PCE_{RF11} is used, the top 5 features with greater impact are FA, bandgap, Sn, Pb, H. As shown in Figure S5, Supporting Information, when using $\text{PCE}_{\text{XGBoost11}}$, the top five features that have great influence are FA, Pb, L, H and bandgap in turn. As shown in Figure S6, Supporting Information, FA, Pb, H, L, and bandgap are the top five features that have great influence when using $\text{PCE}_{\text{GBDT11}}$. By explaining the different data and algorithm

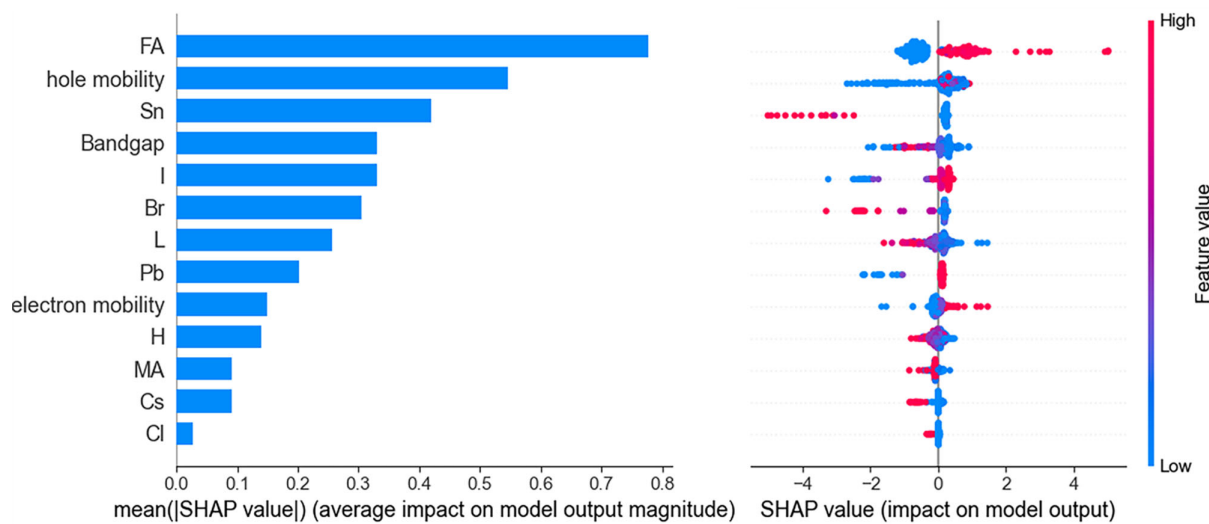


Figure 7. Feature importance ranking plot based on SHAP value (the model used is PCE_{RF}). Left: bar chart of the average absolute value of the SHAP value magnitude. Right: each point represents a sample, and each row represents a feature. The order of the features is in descending order of the average absolute value of the SHAP value. Crowded places indicate a large number of samples accumulated. The color indicates the size of the feature value (red indicates high feature value, blue indicates low feature value), and the horizontal axis represents positive and negative SHAP values.

models, we can get some similar findings, for example, FA has the most important influence, bandgap exists in the top five features, three of which represent the perovskite material itself. This indicates that more attention should be paid to the composition engineering of perovskite, especially to the proper addition of FA, to improve the PCE of PSCs. Because the above comparative analysis proves that FA has the greatest impact on the PCE of PSCs, in other words, the content of FA is essential for PSCs with high PCE.

Interpretable dimensionality reduction for PCE_{RF}. PCA is used to extract the 13 features affecting PCE, which can retain most of the information of the original influence factor matrix and greatly reduce the feature dimension. As shown in Table S14, Supporting Information, the variance contribution rates of the first principal component and the second principal component are 34% and 26%, respectively. Among them, the original feature with the largest weight of the first principal component is Sn, and the original feature with the largest weight of the second principal component is FA. As shown in Figure 8, the

top two principal components of the explanation embedding highlight two distinct features for the difference with an average value of PCE (i.e., the difference between the PCE value of a single sample and the average PCE value of samples). In the interpretation space, the distribution of all samples is roughly "V"-shaped as shown in Figure 8. At the same time, through color rendering, it can be found that the difference with the average value of PCE increases from bottom to top along the "V"-shaped left direction, while the right direction decreases from bottom to top (Figure 8a). The difference with the average value of PCE can be regarded as the clustering of the SHAP values of FA, Sn, and 11 other features. Figure 8b shows that the SHAP value of FA (i.e., the contribution of the FA value of a single sample to the predictive value of its PCE) is almost unchanged from bottom to top along the "V"-shaped right direction, while the left direction increases from bottom to top; Figure 8c shows that the SHAP value of Sn (i.e., the contribution of the Sn value of a single sample to the predictive value of its PCE) decreases along the "V"-shaped right direction from

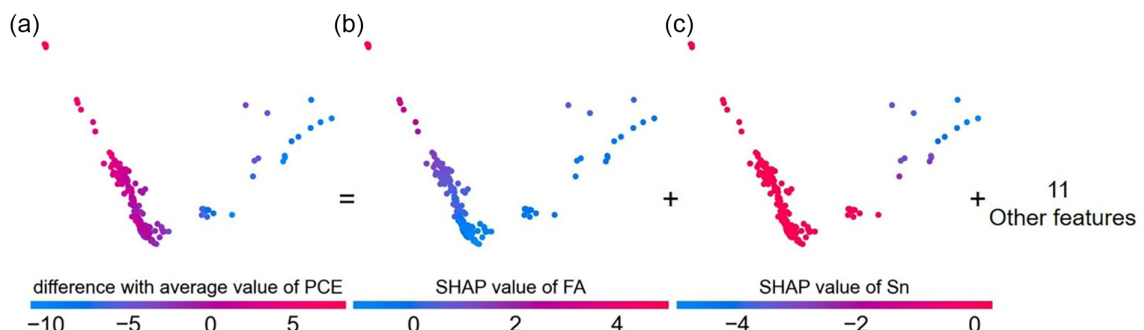


Figure 8. Interpretable dimensionality reduction (the model used is PCE_{RF}). A local explanation embedding of PCE cast onto two principal components. Local feature SHAP values can be viewed as an embedding of the samples into a space where each dimension corresponds to a feature. a-c) shows the distribution of the samples after dimensionality reduction by PCA. a) Difference with an average value of PCE. b) SHAP value of FA. c) SHAP value of Sn.

bottom to top, while the left direction has almost no change from bottom to top. The combination of Figure 8b,c can partially explain the distribution of difference with the average value of PCE, that is, the change along the left direction follows the FA feature, and the change along the right direction follows the Sn feature. Figure 8 reveals the two features that have a major impact on the difference with the average value of PCE, and also supports that FA and Sn have greater weights on the top two principal components than other features in Table S14, Supporting Information.

Sample explanations for factors affecting PCE of PSCs by SHAP theory. **Figure 9** is a sample with lower PCE in the database. The perovskite composition is $\text{MAPb}_{0.25}\text{Sn}_{0.75}\text{I}_3$. The predicted PCE value is 5.16%, and the experimental value is 3.74%. By analyzing the SHAP values of each feature, Sn, Pb, bandgap and L have the greater contribution to the loss (with a large negative SHAP), which indicates that the main reasons for the low PCE are excessive Sn content, low bandgap, and energy-level misalignment. Figure S8, Supporting Information, is a sample with higher PCE in the database. The perovskite composition is FAPbI_3 . The predicted value of PCE is 23.53% and the experimental value is 24.82%. It can be seen that the gain contribution of FA, hole mobility and bandgap is the greatest (with a larger positive SHAP value). This indicates that the reason for higher PCE is the high content of FA, higher hole mobility, and suitable bandgap.

Explaining the influence of FA on PSCs by DFT calculations. The above SHAP explanation shows that FA plays a crucial role for high-performance PSCs, and for further physical explanation we need to use DFT calculations. As shown in Table S15, Supporting Information, we used the Vienna ab initio simulation package (VASP) for the calculation of the effective masses of holes and electrons, and exciton binding energies. Compared with MAPbI_3 , the effective masses of holes and electrons in $\text{MA}_x\text{FA}_{1-x}\text{PbI}_3$ are significantly lower, where the exciton binding energy tends to decrease significantly as the doping ratio of FA increases (from 19.50 to 4.57 meV). This indicates that the doping of FA facilitates the transport and separation of holes and electrons. As shown in Figure S7, Supporting Information, we proceeded to calculate the optical properties of $\text{MA}_x\text{FA}_{1-x}$

PbI_3 . With the doping of FA, the absorption spectrum has been significantly improved, and the absorption intensity also increases with the increase in the proportion of FA. This is consistent with the reference.^[39] Details of DFT calculations can be found in Supporting Information.

In conclusion, we built 49 ML models using 814 real experimental data from the literature and 7 ML algorithms in order to predict the performance of PSCs, and finally selected 7 optimal models. The experimental PCE and predicted PCE obtained from the RF algorithm have relatively high correlation and low RMSE, with r value of 0.86, RMSE of 1.58%. These ML models show excellent prediction performance that can assist the fabrication of PSCs, and reduce the probability of experimental errors and the computational resources required for simulation calculations. For the first time, we propose a series of new explainable strategies for PCE, including the global feature importance ranking, the influence of single feature and two feature interaction on PCE, interpretable dimensionality reduction for PCE, etc. Through these explanations, we found that the most important influence on PCE is the features of the perovskite material itself, especially the addition of FA. The prediction models can be widely applied to the prediction of the performance of ABX_3 perovskite solar cells. the SHAP explanation strategies can yield generalized and common findings which explore the physical laws and chemical meaning behind the features and further inspires the discovery of new materials.

Supporting Information

Supporting Information is available from the Wiley Online Library or from the author.

Acknowledgements

Thanks to the support of the National Natural Science Foundation of China(U1765105, 52007104) and the 111 Project(D20015) of China.

Conflict of Interest

The authors declare no conflict of interest.

Data Availability Statement

The data that support the findings of this study are available in the supplementary material of this article.

Keywords

machine learning, perovskites, power conversion efficiencies, SHAP

Received: December 29, 2021

Revised: February 13, 2022

Published online: March 7, 2022

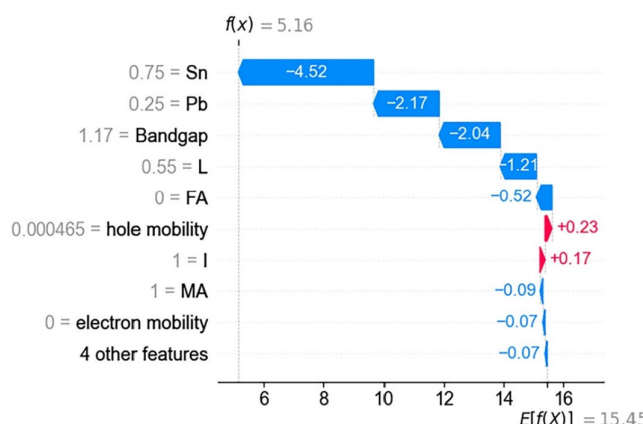


Figure 9. Evaluation process of a single sample. Perovskite composition is $\text{MAPb}_{0.25}\text{Sn}_{0.75}\text{I}_3$.

- [1] National Renewable Energy Lab, *Best research-cell efficiency chart. Photovoltaic Research*, NREL, <https://www.nrel.gov/pv/cell-efficiency.html> (accessed: August 2021).

- [2] R. Azmi, S. Y. Namb, S. Sinaga, Z. A. Akbara, C. L. Lee, S. C. Yoon, I. H. Jung, S. Y. Jang, *Nano Energy* **2017**, *44*, 191.
- [3] S. A. Veldhuis, P. P. Boix, N. Yantara, M. J. Li, T. Sum, N. Mathews, S. G. Mhaisalkar, *Adv. Mater.* **2016**, *28*, 6804.
- [4] Y. N. Wang, Y. Tang, J. Z. Jiang, Q. Zhang, J. Sun, Y. F. Hu, Q. H. Cui, F. Teng, Z. D. Lou, Y. B. Hou, *J. Mater. Chem. C* **2020**, *8*, 5399.
- [5] J. S. Huang, Y. B. Yuan, Y. C. Shao, Y. F. Yan, *Nat. Rev. Mater.* **2017**, *2*, 17042.
- [6] J. S. Huang, Y. C. Shao, Q. F. Dong, *J. Phys. Chem. Lett.* **2015**, *6*, 3218.
- [7] B. Chen, P. N. Rudd, S. Yang, Y. B. Yuan, J. S. Huang, *Chem. Soc. Rev.* **2019**, *48*, 3842.
- [8] S. Wang, T. Sakurai, W. J. Wen, Y. B. Qi, *Adv. Mater. Interface* **2020**, *7*, 2000423.
- [9] W. Fei, Y. H. Shan, J. H. Qiao, C. Zhong, R. Wang, Q. L. Song, L. N. Zhu, *ChemSusChem* **2017**, *10*, 3833.
- [10] A. Jain, G. Hautier, S. P. Ong, K. Persson, *J. Mater. Res.* **2016**, *31*, 977.
- [11] C. Kim, T. D. Huan, S. Krishnan, R. Ramprasad, *Sci. Data* **2017**, *4*, 170057.
- [12] X. Zhang, J. X. Shen, M. E. Turiansky, C. G. Walle, *Nat. Mater.* **2021**, *20*, 971.
- [13] A. Agrawal, A. Choudhary, *APL. Mater.* **2016**, *4*, 053208.
- [14] M. I. Jordan, T. M. Mitchell, *Science* **2015**, *349*, 255.
- [15] W. Sun, Y. J. Zheng, K. Yang, Q. Zhang, A. A. Shah, Z. Wu, Y. Y. Sun, L. Feng, D. Y. Chen, Z. Xiao, S. R. Lu, Y. Li, K. Sun, *Sci. Adv.* **2019**, *5*, eaay4275.
- [16] V. Stanev, C. Osés, A. G. Kusne, E. Rodriguez, J. Paglione, S. Curtarolo, I. Takeuchi, *npj. Comput. Mater.* **2018**, *4*, 29.
- [17] J. Schmidt, M. R. G. Marques, S. Botti, M. A. L. Marques, *npj. Comput. Mater.* **2019**, *5*, 83.
- [18] N. Hartono, J. Thapa, A. Tiihonen, F. Oviedo, C. Batali, J. J. Yoo, Z. Liu, R. Li, D. F. Marrón, M. G. Bawendi, T. Buonassisi, S. J. Sun, *Nat. Commun.* **2020**, *11*, 5675.
- [19] M. Saliba, *Adv. Energy. Mater.* **2019**, *9*, 1803754.
- [20] Z. Z. Li, Q. C. Xu, Q. D. Sun, Z. F. Hou, W. J. Yin, *Adv. Funct. Mater.* **2019**, *29*, 1807280.
- [21] S. H. Lu, Q. H. Zhou, Y. X. Ouyang, Y. L. Guo, Q. Li, J. L. Wang, *Nat. Commun.* **2018**, *9*, 3405.
- [22] Ç. Odabas, R. Yıldırım, *Sol. Energy Mater. Sol. Cells* **2020**, *205*, 110284.
- [23] M. L. Agiorgousis, Y. Y. Sun, D. H. Choe, D. West, S. B. Zhang, *Adv. Theor. Simul.* **2019**, *2*, 1800173.
- [24] F. Oviedo, Z. Ren, S. J. Sun, C. Settens, Z. Liu, N. T. P. Hartono, S. Ramasamy, B. L. DeCost, S. I. P. Tian, G. Romano, A. G. Kusne, T. Buonassisi, *npj Comput Mater.* **2019**, *5*, 60.
- [25] W. A. Saidi, W. Shadid, I. E. Castelli, *npj. Comput. Mater.* **2020**, *6*, 36.
- [26] E. C. Gok, M. O. Yildirim, M. P. U. Haris, E. Eren, M. Pegu, N. H. Hemasiri, P. Huang, S. Kazim, A. U. Oksuz, S. Ahmad, *Sol. RRL* **2021**, 2100927.
- [27] S. M. Lundberg, S. I. Lee, *Adv. Neural Inf. Process. Syst.* **2017**, *30*, 4765.
- [28] C. Chen, Y. X. Zuo, W. K. Ye, X. G. Li, Z. Deng, S. Y. Ong, *Adv. Energy. Mater.* **2020**, *10*, 1903242.
- [29] R. Ramprasad, R. Batra, G. Pilania, A. M. Kanakkithodi, C. Kim, *npj. Comput. Mater.* **2017**, *3*, 54.
- [30] T. Zhou, Z. Song, K. Sundmacher, *Engineering* **2019**, *5*, 1017.
- [31] F. Pedregosa, G. Varoquaux, A. Gramfort, V. Michel, B. Thirion, *J. Mach. Learn. Res.* **2011**, *12*, 2825.
- [32] N. V. Orupattur, S. H. Mushrif, V. Prasad, *Comput. Mater. Sci.* **2020**, *174*, 109474.
- [33] N. S. Altman, *Am. Stat.* **1992**, *46*, 175.
- [34] C.-C. Chang, C.-J. Lin, *ACM Trans. Intell. Syst. Technol.* **2011**, *2*, 1.
- [35] T. K. Ho, *IEEE. Trans. Pattern Anal. Mach. Intell.* **1998**, *20*, 832.
- [36] J. H. Friedman, *Ann. Stat.* **2001**, *29*, 1189.
- [37] T. Chen, C. Guestrin, in *Proc. of the 22nd ACM SIGKDD Inter. Conf. on Knowledge Discovery and Data Mining*, Association for Computing Machinery, USA **2016**, p. 785, <https://doi.org/10.1145/2939672.2939785>.
- [38] K. T. Butler, D. W. Davies, H. Cartwright, O. Isayev, A. Walsh, *Nature* **2018**, *559*, 547.
- [39] W. Li, M. U. Rothmann, Y. Zhu, W. J. Chen, C. Q. Yang, Y. B. Yuan, Y. Y. Choo, X. Wen, Y. B. Cheng, U. Bach, J. Etheridge, *Nat. Energy* **2021**, *6*, 624.

Supporting Information

How machine learning predicts and explains the performance of perovskite solar cells

Yiming Liu, Wensheng Yan^{*}, Shichuang Han, Heng Zhu, Yiteng Tu, Li Guan^{*}, Xinyu Tan^{*}

Dr. Y. Liu, H. Zhu, Y. Tu, Prof. X. Tan and Prof. W. Yan

College of Electrical Engineering & New Energy, Hubei Provincial Collaborative Innovation Center for New Energy Microgrid, China Three Gorges University, 8 University Avenue, Yichang, 443002, China

Email: tanxin@ctgu.edu.cn

Prof. W. Yan

Electronics and Information College, Hangzhou Dianzi University, Hangzhou 310018, China

Email: yws118@163.com

C. Han and L. Guan

Department of Physics Science and Technology, Hebei University, Baoding, 071000, China

Email: lguan@hbu.edu.cn

Table S1. electron and hole mobility of popular materials

Electron Transport Layer			Hole Transport Layer		
Material	Electron mobility(cm ² V ⁻¹ S ⁻¹)	Ref	Material	Hole mobility(cm ² V ⁻¹ S ⁻¹)	Ref
TiO ₂	3.3×10 ⁻⁵	[1]	Spiro-OMeTAD	4.65×10 ⁻⁴ (doped)	[6]
SnO ₂	9.92×10 ⁻⁴	[2]	PTAA	1.2×10 ⁻³ (doped)	[7]
PCBM	3.69×10 ⁻⁴	[3]	PEDOT:PSS	3.3×10 ⁻⁴	[8]
ZnO	4×10 ⁻⁴	[4]	P3HT	8.56×10 ⁻³	[9]
C ₆₀	8×10 ⁻⁵	[5]	NiO _x	2.49×10 ⁻⁴	[10]

Table S2. 8-dimensional feature database for ML prediction models(Bandgap、CBM、VBM)

ID	Cation A				Cation B			Halogen X		Bandgap (eV)	CBM (eV)	VBM (eV)
	MA	FA	Cs	Pb	Sn	Br	Cl	I				
1	1	0	0	1	0	0	0	1	1.55	-3.9	-5.45	
2	0	0	1	1	0	0	0	1	1.8	-3.6	-5.4	
3	0	0	1	1	0	0.33	0	0.67	1.91	-3.69	-5.6	
4	0	0	1	1	0	1	0	0	2.3	-3.3	-5.6	
5	0.5	0.5	0	0.5	0.5	0	0	1	1.25	-4.15	-5.4	
6	1	0	0	1	0	0	0	1	1.61	-4.06	-5.67	
7	1	0	0	1	0	0.33	0	0.67	1.8	-3.85	-5.64	
8	0	0	1	1	0	0.33	0	0.67	1.82	-3.76	-5.58	
9	0	0	1	1	0	0.67	0	0.33	2.08	-3.92	-6	
10	0	0	1	0.4	0.6	0.2	0	0.8	1.35	-3.86	-5.21	
11	0	0	1	0.4	0.6	0	0	1	1.3	-3.66	-4.96	
12	0	0	1	0.4	0.6	0.1	0	0.9	1.33	-3.76	-5.09	
13	0	0	1	0.4	0.6	0.333	0	0.667	1.42	-4.06	-5.48	
14	1	0	0	0	1	0.333	0	0.667	1.56	-3.96	-5.52	

15	1	0	0	0	1	0.667	0	0.333	1.75	-3.78	-5.53
16	1	0	0	0	1	1	0	0	2.15	-3.39	-5.54
17	1	0	0	0.95	0.05	0	0	1	1.5	-3.82	-5.32
18	1	0	0	0.9	0.1	0	0	1	1.46	-3.66	-5.12
19	1	0	0	1	0	0	0	1	1.6	-3.85	-5.45
20	1	0	0	0.75	0.25	0	0	1	1.38	-3.58	-4.96
21	1	0	0	0.5	0.5	0.2	0	0.8	1.35	-3.73	-5.08
22	0.75	0.25	0	0	1	0	0	1	1.28	-3.53	-4.81
23	0.5	0.5	0	0	1	0	0	1	1.3	-3.55	-4.85
24	0	1	0	0	1	0	0	1	1.36	-3.52	-4.88
25	1	0	0	0	1	0	0	1	1.26	-3.48	-4.74
26	0.25	0.75	0	0	1	0	0	1	1.33	-3.55	-4.88
27	0.1	0.9	0	1	0	0.1	0	0.9	1.6	-4	-5.6
28	0.85	0.15	0	1	0	0.15	0	0.85	1.75	-3.9	-5.65
29	0	0	1	1	0	0	1	0	2.78	-3.26	-6.04
30	0	0	1	1	0	1	0	0	2.39	-3.36	-5.75
31	0	0	1	1	0	0	0	1	1.73	-3.45	-5.18
32	1	0	0	1	0	0	0	1	1.51	-3.88	-5.39
33	1	0	0	0.7	0.3	0	0	1	1.31	-3.81	-5.12
34	1	0	0	0.5	0.5	0	0	1	1.28	-3.67	-4.95
35	1	0	0	0.3	0.7	0	0	1	1.23	-3.69	-4.92
36	1	0	0	0.1	0.9	0	0	1	1.18	-3.57	-4.75
37	1	0	0	0	1	0	0	1	1.1	-3.63	-4.73
38	1	0	0	1	0	0	0.0666	0.9334	1.6	-3.8	-5.4
39	0	1	0	1	0	0	0	1	1.53	-4.23	-5.76
40	0	0.97	0.03	1	0	0	0	1	1.53	-4.04	-5.57
41	0	0.93	0.07	1	0	0	0	1	1.54	-3.89	-5.43
42	0	0.83	0.17	1	0	0	0	1	1.56	-3.77	-5.33
43	0	0.9	0.1	1	0	0	0	1	1.55	-3.85	-5.4
44	0.16	0.79	0.05	1	0	0.16	0	0.84	1.58	-3.87	-5.45

45	0	0.83	0.17	1	0	0.2	0	0.8	1.6	-3.8	-5.4
46	0.16	0.79	0.05	1	0	0	0	1	1.54	-3.93	-5.46
47	0.16	0.79	0.05	1	0	0.15	0	0.85	1.62	-3.86	-5.48
48	0.16	0.79	0.05	1	0	0.05	0	0.95	1.57	-3.9	-5.47
49	0.16	0.79	0.05	1	0	0.1	0	0.9	1.59	-3.89	-5.48
50	0.1196	0.8004	0.08	1	0	0.1196	0	0.8804	1.6	-4.1	-5.7
51	0.15	0.85	0	1	0	0.15	0	0.85	1.73	-3.92	-5.65
52	0.85	0.15	0	1	0	0.05	0	0.95	1.58	-3.86	-5.44
53	0.1615	0.7885	0.05	1	0	0.17	0	0.83	1.7	-3.9	-5.6
54	0.083	0.747	0.17	1	0	0.13	0	0.87	1.6	-4.2	-5.8
55	0.1425	0.8075	0.05	1	0	0.1425	0	0.8575	1.6	-3.9	-5.5
56	0.14	0.81	0.05	1	0	0.15	0	0.85	1.6	-3.87	-5.47
57	1	0	0	1	0	0	0	1	1.5	-3.9	-5.4
58	0	0.9	0.1	1	0	0	0	1	1.48	-3.87	-5.35
59	1	0	0	0	1	1	0	0	2.13	-3.42	-5.67
60	1	0	0	1	0	0	0	1	1.59	-4.36	-5.93
61	0	0	1	0	1	0	0	1	1.25	-4.38	-5.69
62	0	1	0	0	1	0	0	1	1.24	-4.12	-5.34
63	0.1425	0.8075	0.05	1	0	0.1425	0	0.8575	1.62	-3.85	-5.47
64	1	0	0	1	0	0.3	0	0.7	1.96	-4.29	-6.25
65	0	0	1	1	0	0.25	0	0.75	1.87	-3.59	-5.46
66	0.153	0.747	0.1	1	0	0.17	0	0.83	1.6	-4.2	-5.8
67	0.16	0.79	0.05	1	0	0.17	0	0.83	1.63	-3.91	-5.54
68	0.1235	0.8265	0.05	1	0	0.13	0	0.87	1.6	-4.1	-5.7
69	0.17	0.83	0	1.1	0	0.167	0	0.933	1.5	-3.9	-5.4
70	0.14	0.81	0.05	1	0	0.15	0	0.85	1.6	-4.2	-5.8
71	0.16	0.79	0.05	1	0	0.17	0	0.83	1.6	-3.9	-5.5
72	1	0	0	1	0	0	0.05	0.95	1.5	-3.88	-5.38
73	1	0	0	1	0	0	0.05	0.95	1.63	-3.8	-5.43
74	0.17	0.83	0	1	0	0.12	0	0.88	1.58	-4.04	-5.62

75	0.15	0.75	0.1	1	0	0.12	0	0.88	1.59	-4.06	-5.65
76	0.5	0.5	0	1	0	0.5	0	0.5	1.5	-3.93	-5.43
77	1	0	0	0.5	0.5	0	0	1	1.22	-3.82	-5.04
78	1	0	0	0.5	0.5	0	0	1	1.3	-3.62	-4.92
79	1	0	0	0.25	0.75	0	0	1	1.27	-3.49	-4.76
80	1	0	0	0	1	0	0	1	1.37	-3.28	-4.65
81	0.13	0.74	0.1	1	0	0.13	0	0.83	1.6	-4.1	-5.7
82	0	0.9	0.1	1	0	0	0	1	1.55	-3.83	-5.38
83	0.153	0.747	0.1	1	0	0.17	0	0.83	1.57	-3.86	-5.43
84	0.7	0.3	0	1	0	0	0	1	1.57	-3.83	-5.4
85	0.1615	0.7885	0.05	1	0	0.17	0	0.83	1.7	-3.7	-5.4
86	0.1235	0.8265	0.05	1	0	0.13	0	0.87	1.63	-4.22	-5.85
87	0	0.95	0.05	1	0	0	0	1	1.51	-3.95	-5.46
88	0.6	0.4	0	1	0	0	0	1	1.6	-3.6	-5.2
89	0.8	0.2	0	1	0	0.04	0	0.96	1.6	-3.93	-5.53
90	0.075	0.875	0.05	1	0	0.075	0	0.925	1.5	-3.9	-5.4
91	0.133	0.779	0.05	1	0	0.15	0	0.85	1.6	-3.9	-5.5
92	0.1425	0.8075	0.05	1	0	0.15	0	0.85	1.6	-4.15	-5.75
93	0.4	0.6	0	0.4	0.6	0	0	1	1.22	-4	-5.22
94	0.7	0.3	0	1	0	0	0	1	1.5	-3.9	-5.4
95	0.15	0.8	0.05	1	0	0.083	0	0.917	1.57	-3.99	-5.56
96	0.5	0.5	0	0.5	0.5	0	0	1	1.2	-4	-5.2
97	0.1615	0.7885	0.05	1	0	0.1	0	0.9	1.7	-3.7	-5.4
98	0.1425	0.8075	0.05	1	0	0.15	0	0.85	1.7	-3.8	-5.5
99	0.05	0.075	0.875	1	0	0.075	0	0.925	1.6	-3.85	-5.45
100	0.4	0.6	0	0.4	0.6	0.1	0	0.9	1.4	-3.94	-5.34
101	0.05	0.95	0	1	0	0.05	0	0.95	1.5	-4	-5.5
102	0.8	0.2	0	1	0	0.033	0	0.967	1.59	-4.01	-5.6
103	1	0	0	1	0	0	1	0	3.09	-3.95	-7.04

Table S3. 13-dimensional feature database for ML prediction models(PCE、Voc、Jsc、FF)

ID	Cation A			Cation B			Halogen X		Bandgap (eV)	H (eV)	L (eV)	electron mobility (cm ² V ⁻¹ S ⁻¹)	hole mobility (cm ² V ⁻¹ S ⁻¹)	PCE (%)	Voc (V)	Jsc (mA/cm ²)	FF
	MA	FA	Cs	Pb	Sn	Br	Cl	I									
1	0.15	0.85	0	1	0	0.15	0	0.85	1.6	0.3	0.15	0.000033	0.000742	15.36	1.06	22.35	0.67
2	0.15	0.85	0	1	0	0.15	0	0.85	1.6	0.25	0.15	0.000033	0.000965	18.57	1.11	23.05	0.73
3	0.15	0.85	0	1	0	0.15	0	0.85	1.6	0.2	-0.05	0.000033	0.00012	13.2	1.05	22.4	0.66
4	0.15	0.85	0	1	0	0.15	0	0.85	1.6	0.21	-0.05	0.000033	0.00046	17	1.08	23.4	0.75
5	0.14	0.81	0.05	1	0	0.15	0	0.85	1.55	0.49	0.07	0.000033	0.000174	18.57	1.07	25.02	0.6967
6	0.14	0.81	0.05	1	0	0.15	0	0.85	1.55	0.51	0.07	0.000033	0.000322	19.22	1.09	24.42	0.7205
7	1	0	0	1	0	0	0	1	1.5	0.05	0.17	0.000033	0.00017	17.08	1.1	21.43	0.72
8	1	0	0	1	0	0	0	1	1.5	0.28	0.27	0.000033	0.0000581	14.07	0.953	20.21	0.7309
9	1	0	0	1	0	0	0	1	1.5	0.08	0.27	0.000033	0.000153	15.62	1.031	21.13	0.7174
10	1	0	0	1	0	0	0	1	1.5	0.04	0.27	0.000033	0.0000397	13.09	1.021	19.95	0.6425
11	1	0	0	1	0	0	0	1	1.5	0.08	0.27	0.000033	0.0000878	14.54	0.938	20.67	0.7493
12	0.15	0.85	0	1	0	0.15	0	0.85	1.48	0.05	0.08	0.000033	4.808E-05	15.66	1.04	20.14	0.74
13	1	0	0	1	0	0	0	1	1.5	0.37	0.07	0.000033	0.00015	16.77	1.023	21.17	0.7744
14	1	0	0	1	0	0	0	1	1.5	0.45	0.07	0.000033	0.00002	14.98	1.012	20.58	0.7418
15	0.15	0.85	0	1	0	0.15	0	0.85	1.6	0.35	0.15	0.000033	0.0000825	11.9	0.95	21.3	0.67
16	0.15	0.85	0	1	0	0.15	0	0.85	1.6	0.42	0.15	0.000033	0.000681	19.4	1.15	23.4	0.77
17	0.15	0.85	0	1	0	0.15	0	0.85	1.6	0.52	0.15	0.000033	0.000148	17.4	1.13	23.1	0.72
18	1	0	0	1	0	0	0	1	1.55	0.18	0.25	0.000033	0.000532	12.52	0.94	20.56	0.648
19	1	0	0	1	0	0	0	1	1.55	0.18	0.25	0.000033	0.00126	13.82	0.94	21.46	0.684
20	1	0	0	1	0	0	0	1	1.5	0.21	0.27	0.000033	0.00135	16.99	1.08	22.16	0.71
21	1	0	0	1	0	0	0	1	1.5	0.21	0.27	0.000033	0.00669	18.6	1.06	23.09	0.76
22	1	0	0	1	0	0	0	1	1.5	0.21	0.27	0.000033	0.0000905	15.23	0.98	22.85	0.68
23	1	0	0	1	0	0	0	1	1.5	0.33	0.07	0.000033	0.0000279	14.7	0.99	20.1	0.74
24	1	0	0	1	0	0	0	1	1.5	0.28	0.07	0.000033	0.000107	18	1.1	20.6	0.794
25	0.15	0.85	0	1	0	0.15	0	0.85	1.6	0.36	0.15	0.000033	0.000306	17.78	1.099	22.689	0.713
26	0.15	0.85	0	1	0	0.15	0	0.85	1.6	0.43	0.15	0.000033	0.000158	18.59	1.108	22.418	0.749
27	0.15	0.85	0	1	0	0.15	0	0.85	1.6	0.51	0.15	0.000033	0.000103	15	1.08	22.01	0.65
28	0.15	0.85	0	1	0	0.15	0	0.85	1.6	0.43	0.15	0.000033	0.000358	19.8	1.13	23.52	0.76
29	1	0	0	1	0	0	0	1	1.5	0.15	0.07	0.000033	0.0000109	13.23	0.967	19.06	0.71

30	1	0	0	1	0	0	0	1	1.5	0.3	0.07	0.000033	0.000143	16.61	0.987	22.32	0.75
31	1	0	0	1	0	0	0	1	1.51	0.37	0.28	0.000033	0.00157	18.58	1.08	23.2	0.7414
32	1	0	0	1	0	0	0	1	1.5	0.29	0.09	0.000033	0.000667	15.4	1.027	21.33	0.702
33	0.15	0.85	0	1	0	0.15	0	0.85	1.6	0.31	0.05	0.000033	0.000344	16.09	1.085	21.96	0.675
34	1	0	0	1	0	0	0	1	1.58	0.27	0.09	0.000033	0.0001	13.9	1.03	21.6	0.624
35	1	0	0	1	0	0	0	1	1.55	0.21	0.1	0.000033	0.00031	18.2	1.09	22.2	0.75
36	1	0	0	1	0	0	0	1	1.55	0.23	0.1	0.000033	0.00028	17.2	1.09	21.6	0.73
37	1	0	0	1	0	0	0	1	1.5	0.21	0.27	0.000033	0.00028	14.8	1.05	21.6	0.69
38	1	0	0	1	0	0	0	1	1.5	0.1	0.27	0.000033	0.00017	13.3	0.99	19.1	0.7
39	1	0	0	1	0	0	0	1	1.5	0.25	0.07	0.000033	0.000877	13.5	0.906	21.5	0.693
40	0.15	0.85	0	1	0	0.15	0	0.85	1.6	0.35	-0.05	0.000033	0.00012	18.9	1.13	21.71	0.77
41	0.15	0.85	0	1	0	0.15	0	0.85	1.6	0.27	-0.05	0.000033	0.00011	17.5	1.09	20.85	0.77
42	1	0	0	1	0	0	0	1	1.5	0.24	0.1	0.000033	0.00573	18.46	1.08	22.79	0.75
43	1	0	0	1	0	0	0	1	1.5	0.18	0.1	0.000033	0.00135	17.82	1.06	22.42	0.75
44	0.15	0.85	0	1	0	0.15	0	0.85	1.6	0.41	-0.05	0.000033	0.00026	19.03	1.13	21.7	0.78
45	0.15	0.85	0	1	0	0.15	0	0.85	1.6	0.31	-0.05	0.000033	0.000011	14.87	1.11	19.31	0.69
46	0.15	0.81	0	1	0	0.15	0	0.8367	1.73	0.56	0.08	0.000033	0.0000865	13.26	0.96	21.39	0.631
47	0.1615	0.7885	0.05	1	0	0.17	0	0.83	1.73	0.43	0.38	0.000033	0.00378	19.29	1.1	23.6	0.74
48	1	0	0	1	0	0	0	1	1.5	0.01	0.07	0.000033	0.0037	15.88	0.98	23.7	0.683
49	1	0	0	1	0	0	0	1	1.5	0.06	0.07	0.000033	0.00058	13.57	0.88	23.1	0.662
50	0.1425	0.8075	0.05	1	0	0.15	0	0.85	1.7	0.3	0.2	0.000033	0.0062	18.5	0.99	23.4	0.66
51	0.15	0.85	0	1	0	0.15	0	0.85	1.73	0.41	0.08	0.000033	0.0000172	14.29	1.02	19.6	0.71
52	1	0	0	1	0	0	0	1	1.52	0.29	0.09	0.000033	0.0000714	15.45	0.97	24	0.663
53	0.15	0.85	0	1	0	0.15	0	0.85	1.6	0.55	-0.05	0.000033	0.0000152	11.3	0.98	17.2	0.67
54	0.15	0.85	0	1	0	0.15	0	0.85	1.6	0.47	-0.05	0.000033	0.00043	14.5	1	21.4	0.66
55	0.15	0.85	0	1	0	0.15	0	0.85	1.73	0.37	0.08	0.000033	0.00065	12.26	1.04	17.92	0.66
56	1	0	0	1	0	0	0	1	1.5	0.41	0.17	0.000033	0.000173	13.93	1.07	20.41	0.63
57	0.15	0.85	0	1	0	0.15	0	0.85	1.6	0.52	0.1	0.000033	0.0000502	12.52	1.02	20.01	0.6
58	0.15	0.85	0	1	0	0.15	0	0.85	1.6	0.54	0.1	0.000033	0.0000821	13.66	1.04	20.62	0.64
59	0.15	0.85	0	1	0	0.15	0	0.85	1.6	0.55	0.1	0.000033	0.000114	15.74	1.1	21	0.68
60	0.15	0.85	0	1	0	0.15	0	0.85	1.6	0.28	0.1	0.000033	0.00047	18.42	1.15	21.89	0.73
61	1	0	0	1	0	0	0	1	1.51	0.26	0.08	0.000033	0.000321	15.84	0.98	22.11	0.731
62	1	0	0	1	0	0	0	1	1.51	0.28	0.08	0.000033	0.000233	12.83	1.03	19.59	0.636
63	1	0	0	1	0	0	0	1	1.51	0.25	0.08	0.000033	0.000318	15.11	1.04	19.88	0.731

64	1	0	0	1	0	0	0	1	1.51	0.25	0.08	0.000033	0.0000575	11.65	0.95	19.74	0.621
65	1	0	0	1	0	0	0	1	1.51	0.21	0.08	0.000033	0.000358	17	1.02	22.7	0.734
66	0	1	0	1	0	0	0	1	1.48	0.43	0.08	0.000033	0.0065904	23.44	1.152	26.04	0.7813
67	0	1	0	1	0	0	0	1	1.48	0.21	0.08	0.000033	0.0074748	24.82	1.164	26.35	0.809
68	0	1	0	1	0	0	0	1	1.48	0.34	0.08	0.000033	0.0072902	24.5	1.161	26.34	0.8015
69	1	0	0	1	0	0	0	1	1.5	0.16	0.07	0.000033	0.00102	12.1	0.91	20.9	0.64
70	0.15	0.85	0	1	0	0.15	0	0.85	1.56	0.42	0.48	0.000033	0.00019	10.6	0.895	18.5	0.638
71	0.15	0.85	0	1	0	0.15	0	0.85	1.6	0.28	0.15	0.000033	0.000289	15.36	1.072	21.609	0.663
72	1	0	0	1	0	0	0	1	1.5	0.18	0.07	0.000033	0.000204	16.6	0.99	22.82	0.7334
73	1	0	0	1	0	0	0	1	1.5	0.21	0.07	0.000033	0.000946	18.03	1.06	22.79	0.7439
74	0.1425	0.8075	0.05	1	0	0.15	0	0.85	1.59	0.24	0.27	0.000033	0.0023	14.57	1.09	19.41	0.69
75	0.1425	0.8075	0.05	1	0	0.15	0	0.85	1.59	0.37	0.27	0.000033	0.00052	12.02	1.06	18.23	0.62
76	0	0	1	1	0	1	0	0	2.3	0.44	0.9	0.000033	0.00957	10.03	1.578	7.652	0.8306
77	0	0	1	1	0	1	0	0	2.3	0.47	0.9	0.000033	0.00856	8.5	1.537	7.27	0.767
78	0	0	1	1	0	1	0	0	2.3	0.27	0.9	0.000033	0.00816	7.67	1.477	7.12	0.7293
79	0.14	0.81	0.05	1	0	0.15	0	0.85	1.6	0.58	0.1	0.000033	0.0003	16.52	1.02	23.01	0.7
80	0.14	0.81	0.05	1	0	0.15	0	0.85	1.6	0.29	0.1	0.000033	0.00046	18.47	1.05	23.46	0.75
81	1	0	0	1	0	0	0	1	1.5	0.06	0.3	0.000033	0.000083	15.59	1.024	20.81	0.732
82	0.15	0.85	0	1	0	0.15	0	0.85	1.73	0.95	0.18	0.000033	0.000384	13.83	0.99	22.36	0.62
83	0	0	1	1	0	1	0	0	2.3	0.5	0.9	0.000033	0.007443	8.53	1.524	7.19	0.779
84	0	0	1	1	0	1	0	0	2.3	0.37	0.9	0.000033	0.007672	9.4	1.532	7.2	0.852
85	0	0	1	1	0	1	0	0	2.3	0.32	0.9	0.000033	0.006819	8.31	1.518	7.03	0.778
86	0	0	1	1	0	1	0	0	2.3	0.21	0.9	0.000033	0.005655	7.76	1.519	7.09	0.72
87	0.16	0.79	0.05	1	0	0.16	0	0.84	1.58	0.25	0.13	0.000033	0.000288	16.83	1.13	20.86	0.7155
88	0.16	0.79	0.05	1	0	0.16	0	0.84	1.58	0.15	0.13	0.000033	0.00615	17.22	1.05	21.51	0.7637
89	1	0	0	1	0	0	0	1	1.5	0.44	0.32	0.000992	0.00384	15.58	1	22.09	0.7039
90	0.14	0.81	0.05	1	0	0.15	0	0.85	1.5	0.16	0.4	0.000992	0.000112	16.78	1.11	21.58	0.695
91	0.14	0.81	0.05	1	0	0.15	0	0.85	1.5	0.19	0.4	0.000992	0.000132	18.45	1.13	22.34	0.727
92	1	0	0	1	0	0	0	1	1.5	0.27	0.27	0.000992	0.00003	13.3	0.96	21.5	0.638
93	1	0	0	1	0	0	0	1	1.5	0.16	0.27	0.000992	0.00038	19.2	1.07	22.8	0.776
94	1	0	0	1	0	0	0	1	1.5	0.05	0.27	0.000992	0.00057	19.7	1.09	22.8	0.785
95	0.08	0.92	0	1	0	0.08	0	0.92	1.62	0.4	0.12	0.000992	0.023	16.83	1.05	21.6	0.741
96	0.08	0.92	0	1	0	0.08	0	0.92	1.62	0.55	0.12	0.000992	0.0001	18.76	1.07	24.1	0.726
97	1	0	0	1	0	0	0	1	1.5	0.16	0.57	0.000992	0.00454	18.6	1.11	22.63	0.7405

98	1	0	0	1	0	0	0	1	1.5	0.28	0.3	0.000992	0.000105	13.57	0.97	20.67	0.6829
99	1	0	0	1	0	0	0	1	1.5	0.27	0.3	0.000992	0.000426	14.52	0.98	21.08	0.6984
100	0.8	0.2	0	1	0	0	0.07	0.93	1.5	0.24	0.7	0.000992	0.021	18.1	0.998	22.18	0.819
101	0.1425	0.8075	0.05	1	0	0.15	0	0.85	1.6	0.15	0.55	0.000992	0.000219	19.05	1.09	24.2	0.7243
102	0.1425	0.8075	0.05	1	0	0.15	0	0.85	1.6	0.15	0.55	0.000992	0.000208	18.04	1.06	24.1	0.7052
103	0.1425	0.8075	0.05	1	0	0.15	0	0.85	1.6	0.16	0.55	0.000992	0.000202	16.83	1.02	24.08	0.6839
104	0.1235	0.8265	0.05	1	0	0.13	0	0.87	1.6	0.62	0.12	0.000992	0.0024	15.02	0.981	22.16	0.6916
105	0.1235	0.8265	0.05	1	0	0.13	0	0.87	1.6	0.46	0.12	0.000992	0.0053	16.5	1.006	23.76	0.6907
106	0.1235	0.8265	0.05	1	0	0.13	0	0.87	1.6	0.23	0.12	0.000992	0.0031	15.76	0.989	23.83	0.6692
107	1	0	0	1	0	0	0	1	1.5	0.11	0.47	0.000992	0.005101	16.25	1.05	21.52	0.7
108	1	0	0	1	0	0	0	1	1.5	0.31	0.47	0.000992	0.004243	16.13	1.04	20.35	0.68
109	0.133	0.779	0.05	1	0	0.15	0	0.85	1.6	0.2	0.3	0.000369	0.00286	18.48	1.1	22.16	0.759
110	0.133	0.779	0.05	1	0	0.15	0	0.85	1.6	0.6	0.3	0.000369	0.000729	15.91	1.09	19.71	0.743
111	0	0.83	0.17	1	0	0.2	0	0.8	1.6	0.14	0.2	0.000369	0.000117	13.65	1.02	18.84	0.71
112	0	0.83	0.17	1	0	0.2	0	0.8	1.6	0.07	0.2	0.000369	0.000116	15.44	1.04	18.82	0.79
113	0	0.83	0.17	1	0	0.2	0	0.8	1.6	0.04	0.2	0.000369	0.000107	15.71	1.05	18.79	0.79
114	1	0	0	1	0	0	0	1	1.5	0.22	0.1	0.000369	0.00043	18.12	1.04	22.95	0.76
115	0.85	0.15	0	1	0	0.05	0	0.95	1.58	0.24	0.34	0.000369	0.00873	15.22	1.054	20.99	0.688
116	0.85	0.15	0	1	0	0.05	0	0.95	1.58	0.04	0.34	0.000369	0.0144	20.05	1.111	22.73	0.794
117	0.7	0.3	0	1	0	0	0	1	1.5	0.35	0.3	0.000369	0.000445	18.17	1.069	20.83	0.816
118	1	0	0	1	0	0	0	1	1.5	0.18	0.1	0.000369	0.015	16.85	1.02	22.11	0.7114
119	1	0	0	1	0	0	0	1	1.5	0.1	0.1	0.000369	0.013	19.05	1.05	22.53	0.7904
120	1	0	0	1	0	0	0	1	1.5	0.05	0.1	0.000369	0.0077	14.8	1.01	20.15	0.6819
121	1	0	0	1	0	0	0	1	1.5	0.4	0	0.000369	0.0000434	15.53	1.02	20.26	0.753
122	1	0	0	1	0	0	0	1	1.5	0.35	0	0.000369	0.0000129	14.01	0.97	20.21	0.7173
123	1	0	0	1	0	0	0	1	1.5	0.35	0.1	0.000369	0.00142	14.8	1.03	21.1	0.72
124	1	0	0	1	0	0	0	1	1.5	0.32	0.1	0.000369	0.00241	14.9	1.03	21.7	0.7
125	1	0	0	1	0	0	0	1	1.5	0.13	0.1	0.000369	0.00175	16.7	1.06	22.4	0.72
126	1	0	0	1	0	0	0	1	1.5	-0.1	0.3	0.000369	0.000499	17.47	1.02	21.82	0.781
127	1	0	0	1	0	0	0	1	1.51	0.07	0.07	0.000369	0.000021	16.32	1.07	21.49	0.71

128	1	0	0	1	0	0	0	1	1.51	0.06	0.07	0.000369	0.000051	14.63	0.96	21.55	0.71
129	1	0	0	1	0	0	0	1	1.5	0.06	0.4	0.000369	0.000063	14.15	0.99	19.85	0.7169
130	1	0	0	1	0	0	0	1	1.5	0.01	0.4	0.000369	0.000296	18.23	1.07	22.96	0.7423
131	1	0	0	1	0	0	0	1	1.6	0.2	0.1	0.000369	4.579E-05	14.86	1.01	19.88	0.7179
132	1	0	0	1	0	0	0	1	1.6	0.16	0.1	0.000369	0.0001073	16.24	1.04	20.3	0.7547
133	1	0	0	1	0	0	0	1	1.6	0.29	0.1	0.000369	6.513E-05	14.69	1.01	19.17	0.7241
134	1	0	0	1	0	0	0	1	1.5	0.25	0.2	0.000369	0.00715	15.5	0.95	21.03	0.775
135	1	0	0	1	0	0	0	1	1.5	0.16	0.2	0.000369	0.00586	14.52	1	18.66	0.7784
136	0.1615	0.7885	0.05	1	0	0.17	0	0.83	1.6	0.46	-0.2	0.000369	3.61E-06	12.9	1.11	16.93	0.6887
137	0.1615	0.7885	0.05	1	0	0.17	0	0.83	1.6	0.49	-0.2	0.000369	0.0000142	16.95	1.09	20.7	0.7509
138	1	0	0	1	0	0	0	1	1.3	0.23	0.36	0.000033	0.000465	5.44	0.716	15.18	0.5007
139	1	0	0	0.75	0.25	0	0	1	1.24	0.02	0.26	0.000033	0.000465	7.37	0.728	15.82	0.6401
140	1	0	0	0.5	0.5	0	0	1	1.17	-0.18	0.39	0.000033	0.000465	7.27	0.584	20.64	0.6032
141	1	0	0	0.25	0.75	0	0	1	1.17	-0.34	0.55	0.000033	0.000465	3.74	0.376	17.55	0.5664
142	1	0	0	0	1	0.333	0	0.667	1.56	0.3	0.3	0.000033	0.000465	5.48	0.77	14.38	0.5
143	1	0	0	0	1	0.667	0	0.333	1.75	0.31	0.48	0.000033	0.000465	5.73	0.82	12.3	0.57
144	1	0	0	0	1	1	0	0	2.15	0.32	0.87	0.000033	0.000465	4.27	0.88	8.26	0.59
145	0.4	0.6	0	0.4	0.6	0	0	1	1.22	0.2	-0.1	0.000369	0.00033	14.19	0.73	27.14	0.716
146	0	0	1	0.4	0.6	0.2	0	0.8	1.35	0.21	-0.04	0.000369	0.00033	11.67	0.85	18.88	0.729
147	0	0	1	0.4	0.6	0	0	1	1.3	-0.04	0.24	0.000369	0.00033	6.79	0.62	15.58	0.703
148	0	0	1	0.4	0.6	0.1	0	0.9	1.33	0.09	0.14	0.000369	0.00033	7.46	0.64	16.85	0.687
149	0	0	1	0.4	0.6	0.333	0	0.667	1.42	0.48	-0.16	0.000369	0.00033	7.72	0.8	14.21	0.681
150	1	0	0	0.95	0.05	0	0	1	1.5	0.22	0.08	0.000369	0.00033	16.57	1	22.42	0.74
151	1	0	0	0.9	0.1	0	0	1	1.46	0.02	0.24	0.000369	0.00033	17.74	0.99	23.31	0.77
152	1	0	0	1	0	0	0	1	1.6	0.35	0.05	0.000369	0.00033	15.36	1.01	20.74	0.73
153	1	0	0	1	0	0	0	1	1.6	0.3	0.1	0.00048	0.00033	16.3	0.99	21.17	0.79
154	1	0	0	1	0	0	0	1	1.6	0.3	0	0.00035	0.00033	15.77	0.96	20.98	0.79
155	1	0	0	1	0	0	0	1	1.6	0.3	0.1	0.00037	0.00033	15.66	0.88	21.56	0.8
156	0.5	0.5	0	0.5	0.5	0	0	1	1.2	0.2	0	0.000369	0.00033	10.7	0.58	28.3	0.635
157	0	0.95	0.05	1	0	0	0	1	1.51	0.24	0.1	0.000992	0.000465	18.04	1.08	22.7	0.735

158	0	0	1	1	0	0.33	0	0.67	1.92	0.86	0.27	0.000992	0.000465	11.9	1.06	14.7	0.757
159	0.1196	0.8004	0.08	1	0	0.1196	0	0.8804	1.6	0.54	0	0.000033	0.000465	19.94	1.112	23.29	0.765
160	0.15	0.85	0	1	0	0.15	0	0.85	1.73	0.49	0.18	0.000033	0.000465	18.8	1.09	22.35	0.773
161	0.14	0.81	0.05	1	0	0.15	0	0.85	1.6	0.58	0.1	0.000033	0.000465	16.52	1.02	23.01	0.7
162	0.1615	0.7885	0.05	1	0	0.17	0	0.83	1.61	0.2	0.29	0.000992	0.000465	17.21	1.07	21.64	0.7396
163	0.8	0.2	0	1	0	0.04	0	0.96	1.6	0.33	0.18	0.000033	0.000465	15.85	1.09	20.05	0.73
164	0.1425	0.8075	0.05	1	0	0.15	0	0.85	1.6	0.53	0.3	0.000992	0.000465	17.6	1.071	22.38	0.734
165	0	0	1	1	0	0.33	0	0.67	1.91	0.46	0.32	0.000033	0.0012	13.45	1.177	14.25	0.802
166	0	0	1	1	0	0.67	0	0.33	2.07	0.42	0.75	0.000992	0.000465	9.86	1.267	10.69	0.71
167	0	0	1	1	0	0	0	1	1.68	-0.03	0.66	0.000033	0.000465	15.1	1.05	20.03	0.72
168	0	0	1	1	0	0.33	0	0.67	1.92	0.94	0.24	0.000992	0.00856	14.08	1.174	15.24	0.787
169	0	0	1	1	0	0.33	0	0.67	1.9	0.3	0.9	0.000992	0.000465	11.12	1.11	13.99	0.7158
170	0	0	1	1	0	0.33	0	0.67	1.91	0.54	0.32	0.000033	0.00856	12.96	1.16	15.18	0.738
171	0	0	1	1	0	0.67	0	0.33	2.05	0.42	0.41	0.000033	0.000465	7.81	1.19	10.7	0.611
172	0	0	1	1	0	0.33	0	0.67	1.91	0.46	0.21	0.000992	0.000465	13.09	1.06	15.99	0.7712
173	0	0	1	1	0	0.33	0	0.67	1.53	0.21	0.4	0.000992	0.000465	13.2	1.22	14.5	0.704
174	0	0	1	1	0	1	0	0	2.31	0.42	0.64	0.000033	0.000465	6.79	1.301	6.76	0.7708
175	0.8	0.2	0	1	0	0.033	0	0.967	1.59	0.12	0.09	0.00008	0.00574	17.5	1.02	24.11	0.7146
176	0.1615	0.7885	0.05	1	0	0.17	0	0.83	1.63	0.65	0.28	0.00008	0.000376	15.47	1.02	21.24	0.7136
177	0.1425	0.8075	0.05	1	0	0.1425	0	0.8575	1.6	0.25	0.32	0.000033	0.000465	17.17	1.08	22.08	0.72
178	0.15	0.8	0.05	1	0	0.083	0	0.917	1.57	0.25	0.32	0.000992	0.000465	19.1	1.09	23.1	0.76
179	0.1425	0.8075	0.05	1	0	0.15	0	0.85	1.65	0.65	0.23	0.000992	0.000465	18.23	1.124	23.29	0.7
180	0.5	0.5	0	0.5	0.5	0	0	1	1.2	0.2	0.5	0.000992	0.00856	5.7	0.35	27.6	0.59
181	0.14	0.81	0.05	1	0	0.15	0	0.85	1.62	0.83	-0.46	0.000033	0.000465	18.5	1.14	21.92	0.75
182	0.1425	0.8075	0.05	1	0	0.15	0	0.85	1.7	0.3	0.2	0.000033	0.000465	18.5	0.99	23.4	0.66
183	0.1615	0.7885	0.05	1	0	0.17	0	0.83	1.5	0.2	0.3	0.000033	0.000465	19.6	1.13	23.2	0.75
184	1	0	0	1	0	0	0	1	1.5	0.2	0.03	0.000033	0.000465	13.8	1.07	19.47	0.661
185	1	0	0	1	0	0	0.05	0.95	1.5	0.3	0.1	0.000369	0.00033	14.2	0.94	19.6	0.77
186	1	0	0	1	0	0	0.05	0.95	1.55	0.1	0.15	0.000369	0.00033	15.12	0.99	19.58	0.78
187	1	0	0	1	0	0	0.05	0.95	1.55	0.08	0.25	0.000033	0.000465	17.14	1.08	21.45	0.74

188	1	0	0	1	0	0	0.05	0.95	1.63	0.21	0.15	0.000033	0.000465	15.15	1.036	19.1	0.77
189	0.13	0.74	0.1	1	0	0.13	0	0.83	1.6	0.48	0	0.000033	0.000465	18.77	1.097	22.59	0.758
190	0.153	0.747	0.1	1	0	0.17	0	0.83	1.57	0.16	0.14	0.000033	0.000465	19.6	1.11	23.52	0.7506
191	0.1235	0.8265	0.05	1	0	0.13	0	0.87	1.63	0.63	0.16	0.000992	0.000465	19.14	1.098	22.21	0.785
192	0.135	0.765	0.1	1	0	0.15	0	0.85	1.611	0.28	0.32	0.000033	0.000465	15.71	1.061	21.28	0.6955
193	0.14	0.81	0.05	1	0	0.15	0	0.85	1.612	0.18	0.41	0.000033	0.000465	17.1	1.054	21.7	0.7548
194	0.15	0.85	0	1	0	0.15	0	0.85	1.62	0.23	0.37	0.000033	0.000465	15.24	1.027	21.47	0.6916
195	1	0	0	1	0	1	0	0	2.3	0.48	1.09	0.000033	0.000465	0.21	0.91	0.35	0.6522
196	1	0	0	1	0	0	0	1	1.5	0.18	0.21	0.000033	0.000465	17.43	1.06	22.13	0.7
197	1	0	0	1	0	0	0	1	1.5	0.4	0.01	0.00136	0.000465	16.45	1.04	21.37	0.74
198	1	0	0	1	0	0	0	1	1.5	0.2	0.5	0.000012	0.000465	11.7	0.99	17.4	0.679
199	1	0	0	1	0	0	0	1	1.53	0.26	0.08	0.000369	0.00033	18.84	1.1	21.41	0.8
200	1	0	0	1	0	0	0	1	1.53	0.26	0.35	0.000104	0.00033	16.45	1.06	20.16	0.77
201	1	0	0	1	0	0	0	1	1.5	0.4	0.01	0.00024	0.00033	15.04	0.93	21.49	0.7494
202	1	0	0	1	0	0	0	1	1.5	0.4	-0.04	0.000085	0.00033	12.64	0.95	19.85	0.6692
203	1	0	0	1	0	0	0	1	1.6	0.4	-0.1	0.00119	0.00033	17.03	1.07	22.37	0.712
204	1	0	0	1	0	0	0.05	0.95	1.5	0.1	0.08	0.0005	0.00033	15.5	0.96	21.4	0.76
205	1	0	0	1	0	0	0.05	0.95	1.5	0.1	0.19	0.000018	0.00033	13.8	0.93	20.7	0.71
206	1	0	0	1	0	0	0.05	0.95	1.5	0.1	0.06	0.00033	0.00033	16	0.97	21.9	0.75
207	1	0	0	1	0	0	0.05	0.95	1.5	0.1	0.21	0.000017	0.00033	14	0.94	21	0.71
208	1	0	0	1	0	0	0	1	1.55	0.35	0.3	0.000369	0.00033	14.3	0.9	22.47	0.7072
209	1	0	0	1	0	0	0	1	1.5	0.04	0.06	0.0004	0.00041	14.11	1.054	20.74	0.65
210	1	0	0	1	0	0	0.05	0.95	1.55	0.25	0.11	0.000012	0.00033	10.83	0.899	17.1	0.71
211	1	0	0	1	0	0	0	1	1.5	0.1	0	0.000685	0.00033	14.7	0.94	20.96	0.744
212	1	0	0	1	0	0	0	1	1.5	0.1	0	0.000983	0.00033	16.6	0.96	21.89	0.788
213	1	0	0	1	0	0	0	1	1.53	0.26	0.4	9.27E-05	0.00033	16.37	1.06	20.87	0.74
214	1	0	0	1	0	0	0	1	1.53	0.26	0.13	0.000256	0.00033	19.37	1.11	22.27	0.79
215	1	0	0	1	0	0	0	1	1.6	0.3	0.1	0.000334	0.00033	15.74	0.91	21.1	0.82
216	1	0	0	1	0	0	0	1	1.6	0.3	0.1	0.000132	0.00033	16.01	0.93	21	0.82
217	1	0	0	1	0	0	0	1	1.6	0.3	0.1	0.000458	0.00033	17.22	0.94	22.1	0.83

218	1	0	0	1	0	0	0	1	1.6	0.3	0.1	0.000768	0.00033	17.77	0.96	22.3	0.83
219	1	0	0	1	0	0	0	1	1.6	0.3	0.1	0.000621	0.00033	17.08	0.92	22.1	0.84
220	0.15	0.85	0	1	0	0.15	0	0.85	1.51	0.17	0.07	0.000033	0.000537	17.71	1.05	21.26	0.79
221	0.15	0.85	0	1	0	0.15	0	0.85	1.51	0.12	0.07	0.000033	0.000679	18.48	1.11	21.01	0.79
222	0.15	0.85	0	1	0	0.15	0	0.85	1.51	0.21	0.07	0.000033	0.000117	13.2	0.99	19.5	0.68
223	1	0	0	1	0	0	0.05	0.95	1.55	0.1	0.17	0.000298	0.00033	14	0.93	20.7	0.73
224	0.1615	0.7885	0.05	1	0	0.17	0	0.83	1.59	0.3	0.21	0.00361	0.000465	20.92	1.122	23.85	0.782
225	0.1615	0.7885	0.05	1	0	0.17	0	0.83	1.59	0.3	0.47	0.00121	0.000465	19.12	1.098	22.77	0.765
226	0.1615	0.7885	0.05	1	0	0.17	0	0.83	1.5	0.2	0.3	0.000033	0.000465	19.6	1.13	23.2	0.75
227	0.12	0.83	0.05	1	0	0.15	0	0.85	1.61	0.48	0.14	0.000033	0.000465	17.92	1.11	22.23	0.7261
228	1	0	0	1	0	0	0	1	1.5	0.2	0	0.000369	0.0012	17.2	1.09	22.2	0.706
229	0.15	0.85	0	1	0	0	0	1	1.56	0.31	0.09	0.000033	0.000465	20	1.08	24.69	0.7501
230	0	0	1	1	0	0	0	1	1.7	0.1	0.7	0.0004	0.000465	12.22	1.14	15.31	0.7
231	0.1425	0.8075	0.05	1	0	0.15	0	0.85	1.6	0.4	-0.1	0.00419	0.0012	20.86	1.136	22.94	0.801
232	0.1425	0.8075	0.05	1	0	0.15	0	0.85	1.6	0.4	0	0.00315	0.0012	20.14	1.113	22.87	0.792
233	0.05	0.95	0	1	0	0.05	0	0.95	1.5	0.3	0.53	0.00008	0.000249	17.69	1	23.04	0.768
234	0.05	0.95	0	1	0	0.05	0	0.95	1.5	0.3	-0.17	0.0006	0.000249	20.89	1.08	23.85	0.811
235	0.05	0.95	0	1	0	0.05	0	0.95	1.5	0.3	0.04	0.0008	0.000249	21.63	1.1	24.25	0.811
236	0.05	0.95	0	1	0	0.05	0	0.95	1.5	0.3	0.09	0.0009	0.000249	22.13	1.1	24.38	0.825
237	1	0	0	1	0	0	0	1	1.5	0.55	-0.03	0.000369	0.00033	12.7	0.81	21.4	0.731
238	1	0	0	1	0	0	0	1	1.5	0.25	0.23	3.72E-05	0.000465	13	0.98	19.8	0.672
239	1	0	0	1	0	0	0	1	1.5	0.25	0.02	5.27E-05	0.000465	16.8	1.05	21.6	0.745
240	1	0	0	1	0	0	0	1	1.5	0.11	0.13	0.000169	0.000465	20.34	1.1	23.57	0.7813
241	1	0	0	1	0	0	0	1	1.5	0.11	0.16	0.000033	0.000465	16.57	1.03	22.81	0.7017
242	1	0	0	1	0	0	0	1	1.5	0.35	0.3	0.000369	0.00084	16.29	1	20.49	0.79
243	1	0	0	1	0	0	0	1	1.53	0.02	0.1	0.000369	0.000331	16.4	1.04	21.94	0.72
244	1	0	0	1	0	0	0.05	0.95	1.6	0.17	0.33	0.000771	0.00033	14.1	0.97	20.2	0.72
245	0.1425	0.8075	0.05	1	0	0.15	0	0.85	1.6	0.4	0.19	0.00042	0.0012	18.7	1.08	22.5	0.767
246	0.1425	0.8075	0.05	1	0	0.15	0	0.85	1.6	0.4	0.11	0.0005	0.0012	19.9	1.11	23	0.783
247	0.1425	0.8075	0.05	1	0	0.15	0	0.85	1.6	0.4	0	0.00035	0.0012	19.3	1.1	22.7	0.778

248	1	0	0	1	0	0	0.05	0.95	1.5	0.1	0.04	0.00048	0.00033	15.4	0.97	21.4	0.74
-----	---	---	---	---	---	---	------	------	-----	-----	------	---------	---------	------	------	------	------

Table S4. 11-dimensional feature database for ML models explanation

ID	Cation A			Cation B			Halogen X		Bandgap (eV)	H (eV)	L (eV)	PCE (%)	Voc (V)	Jsc (mA/cm ²)	FF
	MA	FA	Cs	Pb	Sn	Br	Cl	I							
1	1	0	0	0.75	0.25	0	0	1	1.24	0.02	0.26	7.37	0.728	15.82	0.6401
2	1	0	0	0.5	0.5	0	0	1	1.17	-0.18	0.39	7.27	0.584	20.64	0.6032
3	1	0	0	0.25	0.75	0	0	1	1.17	-0.34	0.55	3.74	0.376	17.55	0.5664
4	0	0	1	1	0	0.33	0	0.67	1.91	0.46	0.32	13.45	1.177	14.25	0.802
5	0	0	1	1	0	1	0	0	2.3	0.37	0.9	8.42	1.45	7.47	0.7743
6	0	0	1	1	0	1	0	0	2.3	0.43	0.9	7.79	1.4	7.37	0.7549
7	0	0	1	1	0	1	0	0	2.3	0.48	0.9	6.66	1.37	6.48	0.7502
8	0.1615	0.7885	0.05	1	0	0.17	0	0.83	1.61	0.16	0	19.37	1.138	22.55	0.7544
9	0.1615	0.7885	0.05	1	0	0.17	0	0.83	1.61	0.16	0.12	19.14	1.141	22.7	0.7398

10	0	0	1	1	0	0.33	0	0.67	1.91	0.53	0.38	10.01	1.21	13.35	0.62
11	0	0	1	1	0	0.67	0	0.33	2.07	0.42	0.75	9.86	1.267	10.69	0.71
12	0	0	1	1	0	0.67	0	0.33	2.07	0.52	0.65	7.29	1.165	9.88	0.63
13	1	0	0	0	1	0.667	0	0.333	1.75	0.31	0.48	5.73	0.82	12.3	0.57
14	1	0	0	0	1	1	0	0	2.15	0.32	0.87	4.27	0.88	8.26	0.59
15	0	0.95	0.05	1	0	0	0	1	1.51	0.24	0.1	18.04	1.08	22.7	0.735
16	0	0.95	0.05	1	0	0	0	1	1.51	0.24	0.21	14.6	1.05	21.43	0.649
17	0	0.95	0.05	1	0	0	0	1	1.51	0.24	0.03	20.41	1.11	24.55	0.75
18	0.15	0.85	0	1	0	0.15	0	0.85	1.73	0.6	0.18	15.5	1.066	20.34	0.713
19	0.15	0.85	0	1	0	0.15	0	0.85	1.73	0.27	0.18	18.2	1.106	21.31	0.772
20	0.15	0.85	0	1	0	0.15	0	0.85	1.73	0.28	0.18	18.5	1.065	21.88	0.795
21	0.15	0.85	0	1	0	0.15	0	0.85	1.73	0.49	0.18	18	1.042	23.23	0.743
22	1	0	0	1	0	0	0	1	1.5	0.2	0.2	16.2	1.01	21.81	0.735
23	1	0	0	1	0	0	0	1	1.5	0.2	0.1	18.5	1.04	22.85	0.7804
24	0	0	1	1	0	1	0	0	2.3	0.35	0.9	9.21	1.46	7.89	0.8
25	0.15	0.85	0	1	0	0.15	0	0.85	1.51	0.32	0.15	18.51	1.11	21.94	0.7631
26	0.15	0.85	0	1	0	0.15	0	0.85	1.51	0.39	0.15	15.36	1.04	20.68	0.7142
27	1	0	0	1	0	0	0	1	1.5	0.2	0.25	17.35	1.089	23.06	0.691
28	1	0	0	1	0	0	0	1	1.5	0.2	0.12	19.19	1.105	24.39	0.712
29	0	0	1	1	0	1	0	0	2.4	0.9	1	9.01	1.444	8.54	0.731
30	0.1615	0.7885	0.05	1	0	0.17	0	0.83	1.61	0.2	0.29	17.21	1.07	21.64	0.7396
31	0.1615	0.7885	0.05	1	0	0.17	0	0.83	1.61	0.2	0.12	18.45	1.09	21.82	0.7761
32	0.1615	0.7885	0.05	1	0	0.17	0	0.83	1.61	0.2	0.13	18.36	1.08	21.61	0.7817
33	0.6	0.4	0	1	0	0	0	1	1.6	-0.02	0.15	15.14	0.964	23.41	0.67
34	1	0	0	1	0	0	0	1	1.6	0.3	0.62	17.04	1.06	22.26	0.7207
35	1	0	0	1	0	0	0	1	1.6	0.3	0.53	16.99	1.1	21.67	0.7142
36	0.15	0.85	0	1	0	0.15	0	0.85	1.6	0.68	-0.05	15.5	1.05	21.1	0.696
37	0.15	0.85	0	1	0	0.15	0	0.85	1.6	0.67	-0.05	17.4	1.07	22.7	0.714
38	0.15	0.85	0	1	0	0.15	0	0.85	1.6	0.43	-0.05	16.7	1.07	22.2	0.703
39	1	0	0	1	0	0	0	1	1.51	0.16	0.07	12.97	0.98	20.68	0.64

40	1	0	0	1	0	0	0	1	1.5	0.4	0.32	11.02	0.883	20.9	0.5973
41	1	0	0	1	0	0	0	1	1.5	0.44	0.32	15.58	1	22.09	0.7039
42	1	0	0	1	0	0	0	1	1.5	0.48	0.32	12.7	0.94	20.78	0.6507
43	1	0	0	1	0	0	0	1	1.5	0.54	0.32	11.34	0.932	19.77	0.6169
44	0.8	0.2	0	1	0	0.04	0	0.96	1.6	0.33	0.1	18.42	1.12	21.31	0.77
45	0.8	0.2	0	1	0	0.04	0	0.96	1.6	0.33	0.18	15.85	1.09	20.05	0.73
46	1	0	0	1	0	0	0	1	1.5	0.3	0.3	14.06	0.985	20.81	0.685
47	1	0	0	1	0	0	0	1	1.5	0.31	0.3	14.53	1.03	20.9	0.68
48	0.15	0.85	0	1	0	0.15	0	0.85	1.6	0.53	-0.05	13.18	1	19.18	0.69
49	0.15	0.85	0	1	0	0.15	0	0.85	1.6	0.32	-0.05	15.4	1.07	20.12	0.72
50	0.15	0.85	0	1	0	0.15	0	0.85	1.6	0.29	-0.05	16.95	1.09	20.82	0.75
51	1	0	0	1	0	0	0	1	1.5	0.2	0.3	10.9	1.06	18.1	0.568
52	1	0	0	1	0	0	0	1	1.5	0.2	0.1	13.7	1.08	21.2	0.601
53	1	0	0	1	0	0	0	1	1.5	0.13	0.47	15.92	0.94	21.81	0.696
54	1	0	0	1	0	0	0	1	1.5	0.23	0.47	10.95	0.83	19.89	0.643
55	0	0	1	1	0	0	0	1	1.7	0.1	0.7	12.22	1.14	15.31	0.6998
56	0.15	0.85	0	1	0	0.15	0	0.85	1.6	0.08	0.4	14.27	1.03	19.68	0.706
57	0.15	0.85	0	1	0	0.15	0	0.85	1.6	0.03	0.4	18.08	1.09	22.23	0.744
58	0.15	0.85	0	1	0	0.15	0	0.85	1.51	0.34	0.15	19.3	1.14	24.1	0.69
59	0.15	0.85	0	1	0	0.15	0	0.85	1.51	0.26	0.15	18.7	1.08	22.5	0.769
60	1	0	0	1	0	0	0	1	1.59	0.28	0.09	16.37	1.109	21.07	0.704
61	1	0	0	1	0	0	0	1	1.59	0.08	0.09	18.85	1.125	22.21	0.754
62	1	0	0	1	0	0	0	1	1.59	0.19	0.09	17.71	1.114	21.86	0.727
63	0.15	0.85	0	1	0	0.15	0	0.85	1.6	0.97	0.33	18.05	1.04	23.09	0.75
64	0.15	0.85	0	1	0	0.15	0	0.85	1.6	0.5	0.33	19.38	1.05	23.8	0.78
65	0.075	0.875	0.05	1	0	0.075	0	0.925	1.5	0.21	0.3	19.13	1.05	23.75	0.77
66	0.075	0.875	0.05	1	0	0.075	0	0.925	1.5	0.28	0.3	14.65	0.94	22.78	0.69
67	0.075	0.875	0.05	1	0	0.075	0	0.925	1.5	0.33	0.3	15.22	1.01	22.76	0.66
68	0.075	0.875	0.05	1	0	0.075	0	0.925	1.5	0.18	0.3	18.86	1.11	23.13	0.74
69	0	0	1	1	0	0.333	0	0.667	1.91	0.66	0.06	8.59	1.127	11.84	0.6437

70	0	0	1	1	0	0.333	0	0.667	1.91	0.66	-0.04	13.43	1.201	14.92	0.7497
71	0.075	0.875	0.05	1	0	0.075	0	0.925	1.5	0.27	0.1	20.42	1.1	24.96	0.744
72	0.075	0.875	0.05	1	0	0.075	0	0.925	1.5	0.3	0.1	17.2	0.94	25.14	0.728
73	0.075	0.875	0.05	1	0	0.075	0	0.925	1.5	0.1	0.1	15.4	1.075	24.15	0.593
74	0.075	0.875	0.05	1	0	0.075	0	0.925	1.5	0.16	0.1	20.84	1.115	25.1	0.745
75	0.1615	0.7885	0.05	1	0	0.17	0	0.83	1.6	0.39	0.28	15.09	0.94	23.51	0.68
76	0.1615	0.7885	0.05	1	0	0.17	0	0.83	1.6	0.71	0.28	13.47	0.91	22.99	0.64
77	0.1615	0.7885	0.05	1	0	0.17	0	0.83	1.6	0.74	0.28	12.37	0.89	22.88	0.61
78	0.1615	0.7885	0.05	1	0	0.17	0	0.83	1.6	0.77	0.28	11.5	0.85	22.11	0.61
79	0	0	1	1	0	0.333	0	0.667	1.92	0.8	0.05	13.56	1.11	15.33	0.817
80	0	0	1	1	0	0.333	0	0.667	1.92	0.57	0.05	13.21	1.21	14.19	0.772
81	0	0	1	1	0	0.333	0	0.667	1.92	0.61	0.05	14.12	1.2	14.62	0.817
82	0	0	1	1	0	0.333	0	0.667	1.92	0.63	0.05	14.95	1.2	15.28	0.825
83	1	0	0	1	0	0	0	1	1.5	0.21	0.07	17.51	1.03	23.5	0.7225
84	0.15	0.85	0	1	0	0.15	0	0.85	1.73	0.37	0.28	16.58	1.07	20.85	0.74
85	0.15	0.85	0	1	0	0.15	0	0.85	1.73	0.38	0.28	15.43	1.04	20.67	0.72
86	0.15	0.85	0	1	0	0.15	0	0.85	1.73	0.39	0.28	18.45	1.09	21.7	0.78
87	0.15	0.85	0	1	0	0.15	0	0.85	1.73	0.4	0.28	17.11	1.07	21.28	0.75
88	1	0	0	1	0	0	0	1	1.5	0.14	0.18	14.63	0.994	21.94	0.6701
89	0.133	0.779	0.05	1	0	0.15	0	0.85	1.6	0.2	0.3	18.48	1.1	22.16	0.759
90	0.133	0.779	0.05	1	0	0.15	0	0.85	1.6	0.6	0.3	15.91	1.09	19.71	0.743
91	0.133	0.779	0.05	1	0	0.15	0	0.85	1.6	-0.3	0.3	9.46	0.96	13.58	0.726
92	0.15	0.85	0	1	0	0.15	0	0.85	1.6	0.45	0.15	16.9	1.05	22.2	0.726
93	0.15	0.85	0	1	0	0.15	0	0.85	1.6	0.47	0.15	19.3	1.1	23.2	0.758
94	0.16	0.79	0.05	1	0	0.16	0	0.84	1.58	0.25	0.13	16.83	1.13	20.86	0.7155
95	0.16	0.79	0.05	1	0	0.16	0	0.84	1.58	0.15	0.13	17.22	1.05	21.51	0.7637
96	0.1425	0.8075	0.05	1	0	0.15	0	0.85	1.6	0.53	0.3	17.6	1.071	22.38	0.734
97	0.1425	0.8075	0.05	1	0	0.15	0	0.85	1.6	0.53	0.11	20.4	1.124	23.22	0.7818
98	0	0	1	1	0	0.33	0	0.67	1.9	0.4	0.43	12.1	1.12	14.41	0.75
99	1	0	0	1	0	0	0	1	1.55	0.08	0.45	17.07	1.06	21.72	0.7414

100	1	0	0	1	0	0	0	1	1.55	0.08	0.27	16.63	1.09	21.49	0.7123
101	0.16	0.79	0.05	1	0	0	0	1	1.54	0.26	0.11	20.5	1.04	25.9	0.76
102	0.16	0.79	0.05	1	0	0.05	0	0.95	1.57	0.27	0.14	20.5	1.07	25.3	0.76
103	0.16	0.79	0.05	1	0	0.1	0	0.9	1.59	0.28	0.15	21.3	1.11	24.7	0.78
104	0.16	0.79	0.05	1	0	0.15	0	0.85	1.62	0.28	0.18	19.9	1.11	23.6	0.76
105	0	0	1	1	0	0.33	0	0.67	1.92	0.86	0.27	11.9	1.06	14.7	0.757
106	0.15	0.85	0	1	0	0.15	0	0.85	1.59	0.16	0.3	20.02	1.11	23.52	0.7668
107	0.15	0.85	0	1	0	0.15	0	0.85	1.59	0.16	0.22	21.77	1.16	23.76	0.7913
108	1	0	0	1	0	0	0	1	1.5	0.2	0.2	16.83	1.07	21.89	0.71
109	1	0	0	1	0	0	0	1	1.5	0.27	0.21	15.77	1.03	21.32	0.7164
110	1	0	0	1	0	0	0	1	1.5	0.27	-0.09	17.07	1.03	21.55	0.7683
111	1	0	0	1	0	0	0	1	1.5	0.27	0.02	18.83	1.07	22.22	0.7903
112	1	0	0	1	0	0	0	1	1.5	0.2	0.43	17.21	1.07	22.47	0.716
113	1	0	0	1	0	0	0	1	1.5	0.2	0.22	19.46	1.17	22.74	0.731
114	1	0	0	1	0	0	0	1	1.6	0.3	0.1	10.53	0.99	16.69	0.6373
115	1	0	0	1	0	0	0	1	1.5	0.2	0.38	13.3	1.02	20.86	0.62
116	0.1196	0.8004	0.08	1	0	0.1196	0	0.8804	1.6	0.54	0	19.94	1.112	23.29	0.765
117	0.1196	0.8004	0.08	1	0	0.1196	0	0.8804	1.6	0.32	0	15.88	1.01	22.95	0.685
118	0.15	0.85	0	1	0	0.15	0	0.85	1.73	0.49	0.18	18.8	1.09	22.35	0.773
119	0.15	0.85	0	1	0	0.15	0	0.85	1.73	0.27	0.18	16.3	1.013	20.56	0.783
120	1	0	0	1	0	0	0	1	1.5	0.2	0.4	13.04	1.025	19	0.67
121	1	0	0	1	0	0	0	1	1.5	0.2	0.3	18.3	1.05	22.3	0.75
122	0	0	1	1	0	0	0	1	1.68	-0.03	0.66	15.1	1.05	20.03	0.72
123	0.1615	0.7885	0.05	1	0	0.17	0	0.83	1.7	0.26	0	18.47	1.123	23.08	0.713
124	0.1615	0.7885	0.05	1	0	0.17	0	0.83	1.7	0.23	0	17.33	1.111	23.06	0.678
125	0.1615	0.7885	0.05	1	0	0.17	0	0.83	1.7	0.3	0	14.36	1.04	20.65	0.668
126	0.1615	0.7885	0.05	1	0	0.17	0	0.83	1.7	0.42	0	17.2	1.073	22.86	0.701
127	0	0	1	1	0	0.33	0	0.67	1.92	0.94	0.24	14.08	1.174	15.24	0.787
128	0	0	1	1	0	0.33	0	0.67	1.92	0.78	0.24	14.82	1.269	15.42	0.757
129	1	0	0	1	0	0	0	1	1.5	0.1	0.3	13.27	0.88	23.43	0.64

130	0.7	0.3	0	1	0	0	0	1	1.57	0.25	0.1	21.02	1.135	23.05	0.804
131	1	0	0	1	0	0	0	1	1.5	0.06	0.3	15.59	1.024	20.81	0.732
132	0.14	0.81	0.05	1	0	0.15	0	0.85	1.6	0.58	0.1	16.52	1.02	23.01	0.7
133	0.14	0.81	0.05	1	0	0.15	0	0.85	1.6	0.29	0.1	18.47	1.05	23.46	0.75
134	1	0	0	1	0	0	0	1	1.51	0.21	0.07	16.7	1.04	21.21	0.76
135	1	0	0	1	0	0	0	1	1.51	0.15	0.07	18.27	1.06	21.7	0.79
136	1	0	0	1	0	0	0	1	1.51	0.22	0.07	16.93	1.07	20.74	0.76
137	0.1425	0.8075	0.05	1	0	0.1425	0	0.8575	1.6	0.25	0.32	17.17	1.08	22.08	0.72
138	0.1425	0.8075	0.05	1	0	0.1425	0	0.8575	1.6	0.25	0.02	19.12	1.09	23.08	0.76
139	1	0	0	1	0	0	0	1	1.6	0.8	0.2	10.8	0.91	17.7	0.669
140	1	0	0	1	0	0	0	1	1.6	0.3	0.2	18	1.06	22.8	0.745
141	1	0	0	1	0	0	0	1	1.6	0.5	0.2	17	1.05	22.7	0.712
142	1	0	0	1	0	0	0	1	1.45	0.06	0.58	16.01	1.02	22.05	0.7124
143	1	0	0	1	0	0	0	1	1.45	0.06	0.21	18.03	1.06	23.64	0.7211
144	0.1615	0.7885	0.05	1	0	0.17	0	0.83	1.6	0.11	-0.08	13.77	0.99	20.75	0.67
145	0.1615	0.7885	0.05	1	0	0.17	0	0.83	1.6	0.11	-0.03	18.08	1.08	23.27	0.72
146	0.1615	0.7885	0.05	1	0	0.17	0	0.83	1.6	0.11	0.04	16.21	1.05	22.4	0.69
147	0.1615	0.7885	0.05	1	0	0.17	0	0.83	1.6	0.11	0.12	15.46	1.01	22.89	0.67
148	0	0	1	1	0	0.33	0	0.67	1.9	0.3	0.9	11.12	1.11	13.99	0.7158
149	0.15	0.85	0	1	0	0.15	0	0.85	1.75	0.41	0.28	14.9	0.99	19.5	0.77
150	0.15	0.85	0	1	0	0.15	0	0.85	1.75	0.39	0.28	18.4	1.07	22.1	0.78
151	0.15	0.85	0	1	0	0.15	0	0.85	1.75	0.45	0.28	19.6	1.09	23.1	0.78
152	0.4	0.6	0	0.4	0.6	0	0	1	1.22	0.2	-0.1	14.19	0.73	27.14	0.716
153	0.4	0.6	0	0.4	0.6	0	0	1	1.22	0.03	-0.1	15.85	0.783	27.22	0.7436
154	0	0	1	1	0	1	0	0	2.3	0.47	0.9	8.5	1.537	7.27	0.767
155	0	0	1	1	0	1	0	0	2.3	0.45	0.9	9.22	1.571	7.48	0.7846
156	0	0	1	1	0	1	0	0	2.3	0.44	0.9	10.03	1.578	7.652	0.8306
157	0	0	1	1	0	1	0	0	2.3	0.31	0.9	8.34	1.516	7.32	0.7506
158	0	0	1	1	0	1	0	0	2.3	0.27	0.9	7.67	1.477	7.12	0.7293
159	1	0	0	1	0	0	0	1	1.6	0.1	0.3	15.18	1.08	19.23	0.7309

160	0	0	1	1	0	1	0	0	2.3	0.5	0.9	6.49	1.36	7.02	0.68
161	0.7	0.3	0	1	0	0	0	1	1.5	0.5	0.3	13.7	0.85	20.67	0.78
162	0.7	0.3	0	1	0	0	0	1	1.5	0.35	0.3	18.17	1.069	20.83	0.816
163	0.15	0.8	0.05	1	0	0.083	0	0.917	1.57	0.25	0.32	19.1	1.09	23.1	0.76
164	0.15	0.8	0.05	1	0	0.083	0	0.917	1.57	0.39	0.18	16.6	1.07	22.9	0.68
165	0.1425	0.8075	0.05	1	0	0.15	0	0.85	1.65	0.65	0.23	18.23	1.124	23.29	0.7
166	0.1425	0.8075	0.05	1	0	0.15	0	0.85	1.65	0.65	0.34	19.15	1.131	23.83	0.71
167	1	0	0	1	0	0	0	1	1.6	0.18	0.21	17.43	1.101	21.42	0.739
168	0.1425	0.8075	0.05	1	0	0.15	0	0.85	1.59	0.24	0.27	14.57	1.09	19.41	0.69
169	0.1425	0.8075	0.05	1	0	0.15	0	0.85	1.59	0.37	0.27	12.02	1.06	18.23	0.62
170	1	0	0	1	0	0	0	1	1.51	0.22	0.38	18.14	1.11	23.11	0.7011
171	1	0	0	1	0	0	0	1	1.5	0.2	0.23	16.47	1	23.03	0.7065
172	1	0	0	1	0	0	0	1	1.5	0.2	0.29	12.23	0.96	22.43	0.5681
173	0.14	0.81	0.05	1	0	0.15	0	0.85	1.6	0.27	0.26	18.18	1.1	22.12	0.7292
174	0.14	0.81	0.05	1	0	0.15	0	0.85	1.6	0.27	0.32	14.75	1.06	20.88	0.6555
175	0	0.9	0.1	1	0	0	0	1	1.47	0.15	0.26	19.09	1.06	24.31	0.7412
176	0	0.9	0.1	1	0	0	0	1	1.47	0.15	0.32	15.97	1.03	23.4	0.6629
177	0	0.9	0.1	1	0	0	0	1	1.47	0.15	0.41	16.06	1	22.18	0.7243
178	0	0	1	1	0	0.33	0	0.67	1.91	0.54	0.32	12.96	1.16	15.18	0.738
179	1	0	0	1	0	0	0	1	1.5	0.18	0.07	16.6	0.99	22.82	0.7334
180	1	0	0	1	0	0	0	1	1.5	0.21	0.07	18.03	1.06	22.79	0.7439
181	0.1615	0.7885	0.05	1	0	0.17	0	0.83	1.55	0.25	0.1	19.44	1.095	22.6	0.7852
182	0.1615	0.7885	0.05	1	0	0.17	0	0.83	1.55	0.35	0.1	17.84	1.038	22.97	0.7475
183	0.1615	0.7885	0.05	1	0	0.17	0	0.83	1.55	0.23	0.1	17.93	1.085	22.62	0.7302
184	0.1615	0.7885	0.05	1	0	0.17	0	0.83	1.55	0.2	0.1	18.62	1.086	22.64	0.7574
185	1	0	0	1	0	0	0	1	1.5	0.27	0.06	12.4	1.031	19.76	0.61
186	1	0	0	1	0	0	0	1	1.5	0.2	0.06	11.96	1.036	19.35	0.6
187	1	0	0	1	0	0	0	1	1.5	0.17	0.06	13.52	1.043	20.28	0.64
188	1	0	0	1	0	0	0	1	1.5	0.04	0.06	14.11	1.054	20.74	0.65
189	1	0	0	1	0	0	0	1	1.5	0.18	0.06	14.61	1.047	20.58	0.68

190	0.15	0.85	0	1	0	0.15	0	0.85	1.56	0.42	0.48	16.8	1.07	23	0.728
191	0.15	0.85	0	1	0	0.15	0	0.85	1.56	0.26	0.48	18.3	1.105	23.5	0.748
192	0.15	0.85	0	1	0	0.15	0	0.85	1.6	0.52	0.1	12.52	1.02	20.01	0.6
193	0.15	0.85	0	1	0	0.15	0	0.85	1.6	0.54	0.1	13.66	1.04	20.62	0.64
194	0.15	0.85	0	1	0	0.15	0	0.85	1.6	0.55	0.1	15.74	1.1	21	0.68
195	0.15	0.85	0	1	0	0.15	0	0.85	1.6	0.28	0.1	18.42	1.15	21.89	0.73
196	0.15	0.85	0	1	0	0.15	0	0.85	1.58	0.44	0.3	19.9	1.1	23.4	0.827
197	0.15	0.85	0	1	0	0.15	0	0.85	1.58	0.06	0.3	21.2	1.14	23.4	0.823
198	0.15	0.85	0	1	0	0.15	0	0.85	1.58	-0.05	0.3	17.3	1.13	23.4	0.703
199	1	0	0	1	0	0	0	1	1.5	0.18	0.07	10.3	0.92	18.58	0.6
200	1	0	0	1	0	0	0	1	1.5	0.16	0.07	12.1	0.91	20.9	0.64
201	0	0	1	1	0	0.33	0	0.67	1.92	1.05	0.3	13.34	1.12	15.78	0.755
202	1	0	0	1	0	0	0	1	1.4	0.08	-0.02	14.89	1.03	22.5	0.64
203	0.5	0.5	0	0.5	0.5	0	0	1	1.2	0.2	0.5	5.7	0.35	27.6	0.59
204	0.5	0.5	0	0.5	0.5	0	0	1	1.2	0.2	0.1	9	0.48	28.7	0.656
205	1	0	0	1	0	0	0	1	1.6	0.1	0.3	12.3	1.04	18.2	0.647
206	1	0	0	1	0	0	0	1	1.5	0.23	0.1	11.62	0.96	21.49	0.569
207	1	0	0	1	0	0	0	1	1.51	0.26	0.08	15.84	0.98	22.11	0.731
208	1	0	0	1	0	0	0	1	1.51	0.28	0.08	12.83	1.03	19.59	0.636
209	1	0	0	1	0	0	0	1	1.51	0.25	0.08	15.11	1.04	19.88	0.731
210	1	0	0	1	0	0	0	1	1.51	0.25	0.08	11.65	0.95	19.74	0.621
211	1	0	0	1	0	0	0	1	1.51	0.21	0.08	17	1.02	22.7	0.734
212	0.1615	0.7885	0.05	1	0	0.1	0	0.9	1.7	0.79	0.18	17.28	1.024	22.95	0.7349
213	0.1615	0.7885	0.05	1	0	0.1	0	0.9	1.7	0.19	0.18	19.58	1.095	23.29	0.7681
214	0.1615	0.7885	0.05	1	0	0.1	0	0.9	1.7	0.05	0.18	20.94	1.135	23.61	0.7816
215	0.14	0.81	0.05	1	0	0.15	0	0.85	1.62	0.83	-0.46	18.5	1.14	21.92	0.75
216	0.14	0.81	0.05	1	0	0.15	0	0.85	1.62	0.83	-0.02	19.88	1.16	22.42	0.76
217	1	0	0	1	0	0	0	1	1.53	0.24	0.5	16.55	1.09	21.1	0.7197
218	1	0	0	1	0	0	0	1	1.53	0.24	0.36	18.52	1.1	22.46	0.7495
219	0	0	1	1	0	0.67	0	0.33	2.05	0.42	0.41	7.81	1.19	10.7	0.611

220	0	0	1	1	0	0.33	0	0.67	1.9	0.44	0.58	13.45	1.22	15.07	0.7318
221	0	0	1	1	0	0.33	0	0.67	1.9	0.44	0.09	14.11	1.2	15.44	0.7615
222	0	0	1	1	0	0.33	0	0.67	1.91	0.46	0.21	13.09	1.06	15.99	0.7712
223	1	0	0	1	0	0	0	1	1.5	0.2	0.04	16.81	1.057	22.49	0.7076
224	1	0	0	1	0	0	0	1	1.5	0.21	0.27	16.32	1.01	22.08	0.72
225	1	0	0	1	0	0	0	1	1.5	0.18	0.21	17.43	1.06	22.13	0.7
226	1	0	0	1	0	0	0	1	1.5	0.18	0.09	19.75	1.15	23.83	0.75
227	0.15	0.85	0	1	0	0.15	0	0.85	1.6	0.55	-0.05	11.3	0.98	17.2	0.67
228	0.15	0.85	0	1	0	0.15	0	0.85	1.6	0.47	-0.05	14.5	1	21.4	0.66
229	1	0	0	1	0	0	0	1	1.5	0.4	0.3	16.23	1.03	22.33	0.7
230	1	0	0	1	0	0	0	1	1.5	0.42	0.6	11.9	0.93	22.2	0.574
231	1	0	0	1	0	0	0	1	1.5	0.27	0.27	13.3	0.96	21.5	0.638
232	1	0	0	1	0	0	0	1	1.5	0.16	0.27	19.2	1.07	22.8	0.776
233	1	0	0	1	0	0	0	1	1.5	0.05	0.27	19.7	1.09	22.8	0.785
234	1	0	0	1	0	1	0	0	2.3	0.48	1.09	0.21	0.91	0.35	0.6522
235	1	0	0	1	0	1	0	0	2.3	0.48	0.59	5.98	1.38	7.07	0.6129
236	0.15	0.85	0	1	0	0.15	0	0.85	1.6	0.64	-0.05	13.6	1.05	20.8	0.65
237	0.15	0.85	0	1	0	0.15	0	0.85	1.6	0.57	-0.05	19.2	1.11	24.3	0.75
238	0.15	0.85	0	1	0	0.15	0	0.85	1.6	0.53	-0.05	18.2	1.06	23.7	0.76
239	0	0	1	1	0	0.33	0	0.67	1.53	0.21	0.4	13.2	1.22	14.5	0.704
240	0	0	1	1	0	1	0	0	2.31	0.42	0.64	6.79	1.301	6.76	0.7708
241	1	0	0	1	0	0	0	1	1.52	0.24	0.09	18.13	1.01	24.97	0.716
242	1	0	0	1	0	0	0	1	1.52	0.3	0.09	18.22	1.09	23.95	0.7035
243	1	0	0	1	0	0	0	1	1.5	0.2	0.03	13.8	1.07	19.47	0.661
244	0.1425	0.8075	0.05	1	0	0.15	0	0.85	1.7	0.3	0.2	18.5	0.99	23.4	0.66
245	0.1425	0.8075	0.05	1	0	0.15	0	0.85	1.7	0.4	0.2	15.2	1.08	23	0.73
246	1	0	0	1	0	0	0	1	1.5	0.2	0.1	15.87	1.018	22.2	0.702
247	0	0	1	1	0	0	0	1	1.73	0.18	0.25	9.26	0.99	14.6	0.644
248	1	0	0	1	0	0	0	1	1.5	0.01	0.07	15.88	0.98	23.7	0.683
249	1	0	0	1	0	0	0	1	1.5	0.06	0.07	13.57	0.88	23.1	0.662

250	0	0	1	1	0	0.33	0	0.67	1.92	0.8	0.05	13.56	1.11	15.33	0.817
251	0	0	1	1	0	0.33	0	0.67	1.92	0.57	0.05	13.21	1.21	14.19	0.772
252	0	0	1	1	0	0.33	0	0.67	1.92	0.61	0.05	14.12	1.2	14.62	0.817
253	0	0	1	1	0	0.33	0	0.67	1.92	0.63	0.05	14.95	1.2	15.28	0.825
254	0.15	0.85	0	1	0	0.15	0	0.85	1.6	0.34	0.08	15.82	1.04	21.76	0.699
255	0.05	0.075	0.875	1	0	0.075	0	0.925	1.6	0.27	0.15	19.4	1.093	24.36	0.729
256	0.05	0.075	0.875	1	0	0.075	0	0.925	1.6	0.18	0.15	21	1.115	24.31	0.774
257	0.15	0.85	0	1	0	0.15	0	0.85	1.6	0.27	0.15	15.75	1.05	21.71	0.69
258	0.15	0.85	0	1	0	0.15	0	0.85	1.6	0.43	0.15	14.47	1.04	22.08	0.63
259	1	0	0	1	0	0	0	1	1.5	0.11	0.07	9.33	0.92	15.81	0.64
260	1	0	0	1	0	0	0	1	1.5	0.21	0.07	15.49	1.06	19.49	0.75
261	1	0	0	1	0	0	0	1	1.5	0.18	0.1	17.82	1.06	22.42	0.75
262	1	0	0	1	0	0	0	1	1.5	0.18	0.34	12.42	1	20.4	0.61
263	1	0	0	1	0	0	0	1	1.55	0.01	0.12	17.23	1.13	22.53	0.6736
264	1	0	0	1	0	0	0	1	1.55	0.23	0.12	15.59	1.05	22.05	0.6727
265	1	0	0	1	0	0	0	1	1.5	0.21	0.27	14.8	1.05	21.6	0.69
266	1	0	0	1	0	0	0	1	1.5	0.1	0.27	13.3	0.99	19.1	0.7
267	1	0	0	1	0	0	0	1	1.5	0.21	0.57	18.67	1.09	23.38	0.7326
268	1	0	0	1	0	0	0	1	1.5	0.28	0.09	16.7	1.042	21.92	0.728
269	1	0	0	1	0	0	0	1	1.6	0.28	0.3	17.12	1.04	22.24	0.74
270	1	0	0	1	0	0	0	1	1.5	0.28	0.3	13.57	0.97	20.67	0.6829
271	1	0	0	1	0	0	0	1	1.5	0.27	0.3	14.52	0.98	21.08	0.6984
272	1	0	0	1	0	0	0	1	1.51	0.28	0.28	15.76	1.04	22.7	0.6674
273	0.8	0.2	0	1	0	0	0.07	0.93	1.5	0.4	0.7	15.5	1.027	20.85	0.723
274	0.15	0.85	0	1	0	0.15	0	0.85	1.6	0.43	0.15	18.59	1.108	22.418	0.749
275	1	0	0	1	0	0	0	1	1.57	0.26	0.39	15.65	1.05	21.51	0.7424
276	1	0	0	1	0	0	0	1	1.5	0.21	0.14	14.1	0.958	20.6	0.71
277	0.15	0.85	0	1	0	0.15	0	0.85	1.6	0.52	0.15	19.18	1.11	23.04	0.75
278	1	0	0	1	0	0	0	1	1.55	0.21	0.32	17.92	1.07	22.68	0.738
279	0.15	0.85	0	1	0	0.15	0	0.85	1.6	0.42	0.15	19.4	1.15	23.4	0.77

280	0.15	0.85	0	1	0	0.15	0	0.85	1.6	0.52	0.15	17.4	1.13	23.1	0.72
281	0.15	0.85	0	1	0	0.15	0	0.85	1.6	0.6	0.1	16.08	1.08	22.31	0.6666
282	1	0	0	1	0	0	0	1	1.51	-0.04	0.07	16.42	1.1	21.11	0.7072
283	1	0	0	1	0	0	0	1	1.51	0.22	0.07	16.81	1.1	21.44	0.7133
284	0.1615	0.7885	0.05	1	0	0.17	0	0.83	1.5	0.2	0.3	19.6	1.13	23.2	0.75
285	1	0	0	1	0	0	0	1	1.51	0.21	0.28	13.97	0.997	19.02	0.7363
286	1	0	0	1	0	0	0	1	1.5	0.2	0.4	16.22	1.1	21.34	0.702
287	1	0	0	1	0	0	0	1	1.5	0.21	0.07	15.08	1.04	21.52	0.6719
288	0.15	0.85	0	1	0	0.15	0	0.85	1.73	0.45	0.08	17.8	1.09	22.7	0.77
289	0.5	0.5	0	0.5	0.5	0	0	1	1.25	0.2	0.35	12.93	0.66	27.15	0.72
290	0.4	0.6	0	0.4	0.6	0.1	0	0.9	1.4	0.04	0.56	7.04	0.5	21.64	0.66
291	0.4	0.6	0	0.4	0.6	0	0	1	1.25	0.71	-0.06	14.02	0.75	27.22	0.69
292	1	0	0	0.5	0.5	0	0	1	1.17	0.5	0.06	11.6	0.61	27.79	0.68
293	0	0	1	0.4	0.6	0.2	0	0.8	1.35	0.21	-0.04	11.67	0.85	18.88	0.729
294	0	0	1	0.4	0.6	0	0	1	1.3	-0.04	0.24	6.79	0.62	15.58	0.703
295	0	0	1	0.4	0.6	0.1	0	0.9	1.33	0.09	0.14	7.46	0.64	16.85	0.687
296	0	0	1	0.4	0.6	0.333	0	0.667	1.42	0.48	-0.16	7.72	0.8	14.21	0.681
297	1	0	0	1	0	0	0	1	1.6	0.35	0.05	15.36	1.01	20.74	0.73
298	0.5	0.5	0	0.5	0.5	0	0	1	1.2	0.2	0	10.7	0.58	28.3	0.635
299	1	0	0	0.5	0.5	0.2	0	0.8	1.35	0.01	-0.02	15.45	0.89	23.14	0.75
300	0.25	0.75	0	0	1	0	0	1	1.33	-0.12	0.95	7.48	0.58	21	0.619
301	0	1	0	0	1	0	0	1	1.36	-0.12	0.98	5.93	0.48	20.9	0.588
302	0	1	0	0	1	0	0	1	1.4	0.7	0	5.59	0.46	20.68	0.588
303	1	0	0	1	0	0	0.0666	0.9334	1.6	0.1	0.7	15.7	1.05	19.5	0.764
304	1	0	0	1	0	0	0	1	1.5	0.21	0.3	12.01	0.956	18.76	0.671
305	1	0	0	1	0	0	0	1	1.5	0.165	0.3	15.86	1.018	20.5	0.749
306	1	0	0	1	0	0	0	1	1.5	0.14	0.3	16.77	1.025	21.14	0.758
307	0	0.85	0.15	1	0	0.1	0	0.9	1.6	0.095	0.4	20.67	1.112	23.19	0.801
308	1	0	0	1	0	0	0	1	1.5	0.05	0.4	13.47	0.983	19.17	0.696
309	1	0	0	1	0	0	0	1	1.5	0.04	0.4	15.83	1	20.86	0.759

310	1	0	0	1	0	0	0	1	1.5	0.02	0.4	17.85	1.02	22.19	0.788
311	1	0	0	1	0	0	0	1	1.5	0.3	0.4	13.16	0.869	20.07	0.754
312	1	0	0	1	0	0	0	1	1.5	0.2	0	18.31	1.119	22.13	0.7397
313	1	0	0	1	0	0	0	1	1.6	0.4	-0.1	17.3	1.08	22.7	0.7
314	1	0	0	1	0	0	0	1	1.6	0.4	0.1	16.8	1.1	22.5	0.678
315	1	0	0	1	0	0	0	1	1.5	0.4	0	12.01	0.92	21.02	0.761
316	1	0	0	1	0	0	0	1	1.5	0.08	0	15.34	1	21.06	0.7815
317	1	0	0	1	0	0	0	1	1.56	0.07	0	10	1	17.99	0.65
318	1	0	0	1	0	0	0	1	1.56	0.06	0	11	1.01	18.4	0.67
319	1	0	0	1	0	0	0	1	1.56	0.05	0	12	1.03	19.05	0.73
320	1	0	0	1	0	0	0	1	1.56	0.02	0	14	1.03	19.6	0.7525
321	1	0	0	1	0	0	0	1	1.56	0	0	16.6	1.04	20.09	0.782
322	1	0	0	1	0	0	0	1	1.56	0.08	0	13.9	1.02	18.23	0.732
323	1	0	0	1	0	0	0	1	1.56	0.26	0	15.9	1.03	20.33	0.72
324	1	0	0	1	0	0	0	1	1.53	0.03	0	20.05	1.14	22.6	0.784
325	1	0	0	1	0	0	0	1	1.53	0.13	0	17.92	1.06	22.27	0.757
326	1	0	0	1	0	0	0	1	1.53	0.46	0.08	18	1.09	21.47	0.77
327	1	0	0	1	0	0	0	1	1.53	0.46	0.35	15.86	1.05	20.34	0.74
328	1	0	0	1	0	0	0	1	1.5	0.43	0.3	9.52	0.826	17.45	0.66
329	1	0	0	1	0	0	0	1	1.5	0.265	0.3	14.28	1.031	18.21	0.761
330	1	0	0	1	0	0	0	1	1.6	0.08	0.1	18.39	1.134	21.618	0.7501
331	1	0	0	1	0	0	0	1	1.6	0.19	0.1	17.89	1.109	21.256	0.759
332	1	0	0	1	0	0	0	1	1.6	0.3	0.1	15.05	1.057	20.531	0.6938
333	1	0	0	1	0	0	0	1	1.5	0.4	0	11.82	0.969	19.3	0.63
334	1	0	0	1	0	0	0	1	1.5	0.14	0.13	15.27	1.022	20.6	0.73
335	1	0	0	1	0	0	0	1	1.5	0.26	0	11.4	0.85	20.28	0.66
336	1	0	0	1	0	0	0	1	1.5	0.02	0	15.14	1	20.79	0.7279
337	1	0	0	1	0	0	0	1	1.5	0.38	0.3	11.66	0.92	19.24	0.6612
338	1	0	0	1	0	0	0	1	1.5	0.13	0.3	17.3	1.1	21.9	0.7156
339	1	0	0	1	0	0	0	1	1.51	0.04	0.07	10.23	0.85	19.73	0.61

340	1	0	0	1	0	0	0	1	1.51	0.03	0.07	10.23	0.83	22.13	0.62
341	1	0	0	1	0	0	0	1	1.51	0.02	0.07	10.42	0.82	20.17	0.63
342	1	0	0	1	0	0	0	1	1.5	0.13	0.07	15.7	1.09	20.6	0.7
343	1	0	0	1	0	0	0	1	1.5	0.14	0.06	18	1.057	21.9	0.778
344	1	0	0	1	0	0	0	1	1.5	0.14	0.1	15.9	1.025	20.9	0.745
345	1	0	0	1	0	0	0	1	1.55	-0.01	0.45	15	1.09	20	0.69
346	1	0	0	1	0	0	0	1	1.55	0.13	0.45	11	0.91	17.3	0.7
347	1	0	0	1	0	0	0	1	1.5	0.14	0.58	16.87	1.015	21.39	0.78
348	1	0	0	1	0	0	0	1	1.55	0.35	0.3	13.7	0.91	21.05	0.7072
349	1	0	0	1	0	0	0	1	1.55	0.35	0.35	11.8	0.9	21.74	0.6286
350	0.05	0.95	0	1	0	0.05	0	0.95	1.5	0.3	0.53	17.69	1	23.04	0.768
351	0.05	0.95	0	1	0	0.05	0	0.95	1.5	0.3	-0.17	20.89	1.08	23.85	0.811
352	0.05	0.95	0	1	0	0.05	0	0.95	1.5	0.3	0.04	21.63	1.1	24.25	0.811
353	0.05	0.95	0	1	0	0.05	0	0.95	1.5	0.3	0.09	22.13	1.1	24.38	0.825
354	1	0	0	1	0	0	0	1	1.6	0.45	0.3	15.92	0.99	22.03	0.73
355	1	0	0	1	0	0	0	1	1.6	0.2	0.3	16.23	0.99	21.57	0.76
356	1	0	0	1	0	0	0	1	1.6	0.09	0.3	18.38	1.07	22.02	0.78
357	0	0.83	0.17	1	0	0.2	0	0.8	1.6	0.14	0.2	13.65	1.02	18.84	0.71
358	0	0.83	0.17	1	0	0.2	0	0.8	1.6	0.07	0.2	15.44	1.04	18.82	0.79
359	0	0.83	0.17	1	0	0.2	0	0.8	1.6	0.04	0.2	15.71	1.05	18.79	0.79
360	1	0	0	1	0	0	0	1	1.5	0.5	0.2	14.18	0.956	19.35	0.7667
361	1	0	0	1	0	0	0	1	1.6	0.08	0.11	17.7	1.26	18.2	0.768
362	1	0	0	1	0	0	0	1	1.5	0.26	0.3	18.9	1.08	23.01	0.77
363	1	0	0	1	0	0	0	1	1.5	0.32	0.3	16.47	1.02	22.12	0.73
364	0	0	1	1	0	0.33	0	0.67	1.91	0.06	0.72	10.38	1.11	11.94	0.783
365	1	0	0	1	0	0	0	1	1.5	0	0.3	16.9	1.05	21.45	0.75
366	1	0	0	1	0	0	0	1	1.5	0.14	0.1	15.52	1.027	20.99	0.72
367	1	0	0	1	0	0	0	1	1.5	0.14	0.13	16.55	1.027	21.46	0.75
368	1	0	0	1	0	0	0	1	1.5	0.2	0.4	13.61	0.99	20.52	0.67
369	1	0	0	1	0	0	0	1	1.5	0.21	0.4	14.98	0.98	20.66	0.74

370	1	0	0	1	0	0	0	1	1.5	0.19	0.4	15.52	0.98	21.4	0.74
371	1	0	0	1	0	0	0	1	1.5	0.13	0.4	16.99	0.99	22.58	0.76
372	1	0	0	1	0	0	0	1	1.5	0.1	0.4	17.76	0.97	23.18	0.79
373	0.85	0.15	0	1	0	0.05	0	0.95	1.58	0.24	0.34	15.22	1.054	20.99	0.688
374	0.85	0.15	0	1	0	0.05	0	0.95	1.58	0.04	0.34	20.05	1.111	22.73	0.794
375	0	1	0	0	1	0	0	1	1.38	-0.05	0.54	5.12	0.37	22.06	0.627
376	1	0	0	1	0	0	0	1	1.5	0.4	0.1	12.6	0.9	20.76	0.674
377	1	0	0	1	0	0	0	1	1.5	0.3	0.1	13.37	1.02	22.87	0.573
378	1	0	0	1	0	0	0	1	1.5	0.22	0.1	18.12	1.04	22.95	0.76
379	0.7	0.3	0	1	0	0	0	1	1.58	-0.1	0.68	14.75	0.94	22.18	0.7102
380	1	0	0	1	0	0.034	0.016	0.95	1.58	0.4	-0.09	19.23	1.12	21.77	0.7882
381	1	0	0	1	0	0.034	0.016	0.95	1.58	0.42	-0.09	20.84	1.17	22.38	0.7947
382	1	0	0	1	0	0.034	0.016	0.95	1.58	0.4	-0.09	21.08	1.19	22.23	0.7861
383	1	0	0	1	0	0.034	0.016	0.95	1.58	0.32	-0.09	21.56	1.19	22.23	0.8171
384	1	0	0	1	0	0	0	1	1.5	0.14	0.1	15.27	1.022	20.6	0.73
385	1	0	0	1	0	0	0	1	1.5	0.14	-0.03	16.29	1.013	21.68	0.74
386	1	0	0	1	0	0	0	1	1.6	0.2	0.1	16.76	1.01	21.69	0.7687
387	1	0	0	1	0	0	0	1	1.6	0.1	0.1	18.96	1.06	22.94	0.7776
388	1	0	0	1	0	0	0	1	1.5	0.19	0.3	12.9	0.91	17.5	0.79
389	1	0	0	1	0	0	0	1	1.5	0.19	0.3	12.1	0.9	17.5	0.77
390	1	0	0	1	0	0	0	1	1.5	0.18	0.3	15.6	1	19.5	0.79
391	1	0	0	1	0	0	0	1	1.5	0.13	0.3	14.4	0.94	19.9	0.79
392	1	0	0	1	0	0	0	1	1.5	0.03	0.3	16.9	1.04	19.8	0.8
393	1	0	0	1	0	0	0	1	1.5	0.08	0.3	14.4	0.98	18.1	0.8
394	1	0	0	1	0	0	0	1	1.6	0.4	0.3	18.7	1.09	22.5	0.762
395	0.7	0.3	0	1	0	0	0	1	1.62	0.34	-0.03	14.8	1.11	19.72	0.67
396	0.7	0.3	0	1	0	0	0	1	1.62	0.3	0.01	17.01	1.12	21	0.73
397	0.7	0.3	0	1	0	0	0	1	1.62	0.26	0.05	20.3	1.12	23	0.75
398	0.7	0.3	0	1	0	0	0	1	1.62	-0.08	0.39	13	1.1	16.7	0.65
399	1	0	0	1	0	0	0	1	1.5	-0.04	0	16.55	1.001	22.52	0.73

400	1	0	0	1	0	0	0	1	1.5	0.11	0	12.41	0.933	21.4	0.622
401	1	0	0	1	0	0	0	1	1.5	0.25	0.3	17.6	1.08	21.75	0.75
402	0.1425	0.8075	0.05	1	0	0.1425	0	0.8575	1.62	0.15	0.05	12.67	1.02	17.01	0.73
403	0.1425	0.8075	0.05	1	0	0.1425	0	0.8575	1.62	0.02	0.05	17.34	1.01	22.59	0.76
404	1	0	0	1	0	0	0	1	1.5	0.1	0.2	18.2	1.1	22.7	0.732
405	1	0	0	1	0	0	0	1	1.6	0.3	0.1	16.3	0.99	21.17	0.79
406	1	0	0	1	0	0	0	1	1.6	0.3	0	15.77	0.96	20.98	0.79
407	1	0	0	1	0	0	0	1	1.6	0.3	0.1	15.66	0.88	21.56	0.8
408	1	0	0	1	0	0	0	1	1.5	0.1	0.1	14.4	1.05	19.4	0.71
409	1	0	0	1	0	0	0	1	1.6	0.4	-0.1	17.38	1.084	22.67	0.707
410	1	0	0	1	0	0	0	1	1.5	0.4	0	15.53	1.02	20.26	0.753
411	1	0	0	1	0	0	0	1	1.5	0.35	0	14.01	0.97	20.21	0.7173
412	1	0	0	1	0	0	0	1	1.5	0.2	0.3	14.5	0.96	18.9	0.8
413	1	0	0	1	0	0	0	1	1.5	0.35	0.1	12.19	0.97	18.69	0.6716
414	1	0	0	1	0	0	0	1	1.5	0.18	0.1	17.56	1.06	22.6	0.7318
415	1	0	0	1	0	0	0	1	1.5	0.1	0.1	19.64	1.08	22.78	0.8043
416	1	0	0	1	0	0	0	1	1.5	0	0.3	15.24	1.07	22.43	0.635
417	1	0	0	1	0	0	0	1	1.5	0.24	0.1	16.67	1.049	21.48	0.743
418	1	0	0	1	0	0	0	1	1.5	0.15	0.1	18.76	1.097	21.96	0.781
419	1	0	0	1	0	0	0	1	1.5	0.5	0	13.44	0.95	19.47	0.725
420	1	0	0	1	0	0	0	1	1.5	0.2	0	18.79	1.09	23.29	0.742
421	1	0	0	1	0	0	0	1	1.5	0.08	-0.03	16.29	1.05	20.57	0.7515
422	1	0	0	1	0	0	0	1	1.5	0.01	-0.03	14.75	1.02	19.63	0.7381
423	1	0	0	1	0	0	0	1	1.5	0.39	0.1	14.4	0.913	21	0.751
424	1	0	0	1	0	0	0	1	1.5	0.35	0.1	14.6	0.961	20.8	0.726
425	1	0	0	1	0	0	0	1	1.5	0.32	0.1	16.7	0.99	21.8	0.773
426	1	0	0	1	0	0	0	1	1.5	0.1	-0.09	16.59	1.04	20.91	0.76
427	0.1615	0.7885	0.05	1	0	0.17	0	0.83	1.63	0.65	0.28	15.47	1.02	21.24	0.7136
428	0.1615	0.7885	0.05	1	0	0.17	0	0.83	1.63	0.41	0.28	18.3	1.1	21.95	0.757
429	0	1	0	0	1	0	0	1	1.35	0.59	0.26	4.83	0.422	19.92	0.5751

430	1	0	0	1	0	0	0	1	1.5	0.2	0	13.9	0.97	18.9	0.75
431	1	0	0	1	0	0	0	1	1.5	0.33	-0.1	13.53	0.98	19.15	0.721
432	1	0	0	1	0	0	0	1	1.5	0.26	-0.1	15.67	1.05	20.15	0.741
433	1	0	0	1	0	0	0	1	1.5	-0.18	0.2	11.86	0.922	18.87	0.681
434	1	0	0	1	0	0	0	1	1.5	0.14	0.1	14.78	1.02	20.46	0.71
435	1	0	0	1	0	0	0	1	1.5	0.14	0.07	15.13	1.015	20.68	0.72
436	1	0	0	1	0	0	0	1	1.5	0.14	0.06	17.1	1.045	21.34	0.77
437	0	0	1	1	0	0.33	0	0.67	2	0.5	0.2	8.31	0.92	12.92	0.686
438	1	0	0	1	0	0	0	1	1.5	0.3	0.1	14.4	1.04	19.66	0.707
439	1	0	0	1	0	0	0	1	1.5	0.24	0.02	13.2	0.96	19.6	0.7
440	1	0	0	1	0	0	0	1	1.5	0.12	0.02	15.3	1.05	20.1	0.73
441	1	0	0	1	0	0	0	1	1.5	0.3	0.1	15.51	0.993	20.39	0.77
442	1	0	0	1	0	0	0	1	1.5	0.3	0.1	15.73	0.93	22.1	0.79
443	1	0	0	1	0	0	0	1	1.5	0.8	0.28	13.5	0.99	18.7	0.746
444	1	0	0	1	0	0	0	1	1.53	0.02	0.1	16.4	1.04	21.94	0.72
445	1	0	0	1	0	0	0	1	1.53	0.23	0.1	12.1	1	18.06	0.67
446	1	0	0	1	0	0	0	1	1.52	0.15	0.07	13.33	1.01	20.22	0.65
447	1	0	0	1	0	0	0	1	1.5	0.2	0.1	14.3	1.04	20.96	0.658
448	1	0	0	1	0	0	0	1	1.5	0.42	0.3	15.35	1.06	18.52	0.7853
449	1	0	0	1	0	0	0	1	1.5	0.24	0.3	16.26	1.07	19.2	0.7903
450	1	0	0	1	0	0	0	1	1.5	0.5	0.1	13.5	0.92	20.3	0.77
451	1	0	0	1	0	0	0	1	1.5	0.5	0.3	12.39	0.89	19.28	0.723
452	1	0	0	1	0	0	0	1	1.5	-0.1	0.3	17.47	1.02	21.82	0.781
453	1	0	0	1	0	0	0	1	1.5	0.3	0.3	13.13	0.903	19.35	0.751
454	0.8	0.2	0	1	0	0.033	0	0.967	1.59	0.12	0.09	17.5	1.02	24.11	0.7146
455	0	1	0	0	1	0	0	1	1.4	0.7	-0.18	7.09	0.47	22.45	0.678
456	0	1	0	0	1	0	0	1	1.4	0.7	-0.16	6.56	0.44	22.34	0.673
457	0	1	0	0	1	0	0	1	1.4	0.7	-0.28	5.9	0.4	22.17	0.662
458	0	1	0	0	1	0	0	1	1.4	0.7	-0.36	5.29	0.36	21.96	0.674
459	1	0	0	0.75	0.25	0	0	1	1.38	0.04	0.32	14.35	0.82	22.44	0.78

460	1	0	0	0.5	0.5	0	0	1	1.3	0.08	0.28	3.68	0.52	11.07	0.64
461	1	0	0	0.25	0.75	0	0	1	1.27	0.24	0.41	2.36	0.36	11.12	0.59
462	0	1	0	0.5	0.5	0	0	1	1.17	0.5	0.06	11.6	0.61	27.79	0.68
463	0.5	0.5	0	0.5	0.5	0	0	1	1.25	0.2	0.35	14.18	0.67	28.35	0.74

Table S5. Performance comparison and parameters of Bandgap prediction models (using Table S2 as the database)

Models	Hyperparameters	Bandgap		
		Train RMSE(eV)	Test RMSE(eV)	r value(Test)
Bandgap _{LR}		0.0933	0.102	0.88
Bandgap _{KNN}	'algorithm':'ball_tree', 'n_neighbors': 2, 'weights': 'uniform'	0.0585	0.12	0.86
Bandgap _{SVR}	'C':0.2,'degree':1,'epsilon': 0.05, 'gamma':0.2, 'kernel': 'poly'	0.0952	0.105	0.88
Bandgap _{MLP}	hidden_layer_sizes=(4,),solver='lbfgs',max_iter=50,verbose=True,	0.0716	0.076	0.94
Bandgap _{RF}	n_estimators=20,max_features='auto',max_depth=10,min_samples_split=2,min_samples_leaf=1,	0.0404	0.0764	0.94
Bandgap _{GBDT}	n_estimators=90,max_depth =3,	0.0328	0.0794	0.94
Bandgap _{XGBoost}	'colsample_bytree':0.7, 'gamma':0, 'learning_rate': 0.1,'max_depth':2, 'min_child_weight':3, 'n_estimators':300, 'reg_alpha':0, 'reg_lambda':1, 'subsample': 0.8	0.044	0.064	0.96

Table S6. Performance comparison and parameters of CBM prediction models (using Table S2 as the database)

Models	Hyperparameters	CBM		
		Train RMSE(eV)	Test RMSE(eV)	Train RMSE(eV)
CBM _{LR}		0.198	0.211	0.32
CBM _{KNN}	'algorithm':'kd_tree', 'n_neighbors': 6, 'weights': 'uniform'	0.176	0.192	0.41
CBM _{SVR}	'C':0.2,'degree':2,'epsilon': 0.1, 'gamma':0.5, 'kernel': 'rbf'	0.151	0.162	0.63
CBM _{MLP}	hidden_layer_sizes=(8,),solver='lbfgs',max_iter=25,verbose=True,	0.163	0.165	0.62
CBM _{RF}	n_estimators=10,max_features='sqrt',max_depth=60,min_samples_split=5,min_samples_leaf=1,	0.131	0.149	0.70
CBM _{GBDT}	n_estimators=20,max_depth =3,	0.135	0.145	0.74
CBM _{XGBoost}	'colsample_bytree':0.5, 'gamma':0.1,'learning_rate': 0.15,'max_depth':4, 'min_child_weight':3, 'n_estimators':5000, 'reg_alpha':0, 'reg_lambda':1, 'subsample': 0.9	0.134	0.133	0.78

Table S7. Performance comparison and parameters of VBM prediction models (using Table S2 as the database)

Models	Hyperparameters	VBM		
		Train RMSE(eV)	Test RMSE(eV)	r value(Test)
VBM _{LR}		0.2	0.2124	0.52
VBM _{KNN}	'algorithm':'kd_tree', 'n_neighbors': 4, 'weights': 'uniform'	0.191	0.205	0.58
VBM _{SVR}	'C':0.3,'degree':1,'epsilon': 0.1, 'gamma':0.2, 'kernel': 'rbf'	0.194	0.201	0.59
VBM _{MLP}	hidden_layer_sizes=(8,),solver='lbfgs',max_iter=25,verbose=True,	0.173	0.191	0.69
VBM _{RF}	n_estimators=80,max_features='sqrt',max_depth=60,min_samples_split=5,min_samples_leaf=1,	0.141	0.193	0.64
VBM _{GBDT}	n_estimators=30,max_depth =2,	0.162	0.184	0.68
VBM _{XGBoost}	'colsample_bytree':0.7, 'gamma':0.1,'learning_rate': 0.15,'max_depth':4, 'min_child_weight':4, 'n_estimators':5000, 'reg_alpha':0, 'reg_lambda':2, 'subsample': 0.9	0.149	0.178	0.71

Table S8. Performance comparison and parameters of PCE prediction models (using Table S3 as the database)

Models	Hyperparameters	PCE		
		Train RMSE(%)	Test RMSE(%)	r value(Test)
PCE _{LR}		2.26	2.99	0.61
PCE _{KNN}	'algorithm':'ball_tree', 'n_neighbors':3,'weights': 'uniform'	1.61	1.82	0.81
PCE _{SVR}	'C':0.3,'degree':1,'epsilon': 1, 'gamma':0.5, 'kernel': 'poly'	2.33	1.83	0.81
PCE _{MLP}	hidden_layer_sizes=(16,10,16),solver='lbfgs',max_iter=15,verbose=True,	2.02	2.06	0.77
PCE _{RF}	n_estimators=50,max_features='auto',max_depth=10,min_samples_split=3,min_samples_leaf=1,	1.15	1.58	0.86
PCE _{GBDT}	n_estimators=60,max_depth =2,	1.66	1.75	0.82
PCE _{XGBoost}	'colsample_bytree':0.3, 'gamma':0,'learning_rate': 0.1,'max_depth':4, 'min_child_weight':3, 'n_estimators':100, 'reg_alpha':0.3, 'reg_lambda':9, 'subsample': 1	1.53	1.76	0.83

Table S9. Performance comparison and parameters of Voc prediction models (using Table S3 as the database)

Models	Hyperparameters	Voc		
		Train RMSE(V)	Test RMSE(V)	r value(Test)
Voc _{LR}		0.077	0.093	0.76
Voc _{KNN}	'algorithm':'ball_tree', 'n_neighbors': 4, 'weights': 'uniform'	0.062	0.061	0.89
Voc _{SVR}	'C':0.1,'degree':2,'epsilon':0.01, 'gamma':0.1, 'kernel': 'poly'	0.054	0.065	0.88
Voc _{MLP}	hidden_layer_sizes=(16,10,16),solver='lbfgs',max_iter=20,verbose=True,	0.052	0.063	0.89
Voc _{RF}	n_estimators=500,max_features='sqrt',max_depth=10,min_samples_split=3,min_samples_leaf=1,	0.036	0.051	0.93
Voc _{GBDT}	n_estimators=90,max_depth =2,	0.044	0.06	0.9
Voc _{XGBoost}	'colsample_bytree':0.5, 'gamma':0,'learning_rate': 0.15,'max_depth':6, 'min_child_weight':3, 'n_estimators':100, 'reg_alpha':0.3, 'reg_lambda':1, 'subsample': 0.8	0.044	0.055	0.92

Table S10. Performance comparison and parameters of Jsc prediction models (using Table S3 as the database)

Models	Hyperparameters	Jsc		
		Train RMSE(mA/cm ²)	Test RMSE(mA/cm ²)	r value (Test)
Jsc _{LR}		1.72	1.09	0.95
Jsc _{KNN}	'algorithm':'ball_tree', 'n_neighbors':3,'weights': 'uniform'	1.21	1.32	0.93
Jsc _{SVR}	'C':0.1,'degree':2,'epsilon':0.001, 'gamma':0.1, 'kernel': 'linear'	1.77	1.05	0.96
Jsc _{MLP}	hidden_layer_sizes=(16,10,16),solver='lbfgs',max_iter=50,verbose=True,	1.32	1.39	0.92
Jsc _{RF}	n_estimators=50,max_features='auto',max_depth=10,min_samples_split=3,min_samples_leaf=1,	0.85	1.04	0.96
Jsc _{GBDT}	n_estimators=40,max_depth =3,	1.09	1.09	0.95
Jsc _{XGBoost}	'colsample_bytree':0.6, 'gamma':0,'learning_rate': 0.15,'max_depth':4, 'min_child_weight':4, 'n_estimators':50, 'reg_alpha':0,'reg_lambda':2, 'subsample': 1	0.88	1.14	0.95

Table S11. Performance comparison and parameters of FF prediction models (using Table S3 as the database)

Models	Hyperparameters	FF		
		Train RMSE	Test RMSE	r value(Test)
FF _{LR}		0.044	0.073	0.18
FF _{KNN}	'algorithm':'ball_tree', 'n_neighbors':17,'weights': 'uniform'	0.049	0.053	0.4
FF _{SVR}	'C':0.1,'degree':2,'epsilon':0.1, 'gamma':0.1, 'kernel': 'poly'	0.049	0.053	0.42
FF _{MLP}	hidden_layer_sizes=(16,10,16),solver='lbfgs',max_iter=50,verbose=True,	0.036	0.052	0.5
FF _{RF}	n_estimators=20,max_features='sqrt',max_depth=110,min_samples_split=5,min_samples_leaf=3,	0.034	0.046	0.63
FF _{GBDT}	n_estimators=50,max_depth =2,	0.036	0.048	0.55
FF _{XGBoost}	'colsample_bytree':0.5, 'gamma':0,'learning_rate': 0.05,'max_depth':4, 'min_child_weight':3,	0.033	0.047	0.58

	'n_estimators':200, 'reg_alpha':0.2,'reg_lambda':1, 'subsample': 0.8			
--	----------------------------------------------------------------------	--	--	--

Table S12. Performance comparison and parameters of PCE prediction models (using Table S4 as the database)

Models	Hyperparameters	PCE		
		Train RMSE(%)	Test RMSE(%)	r value(Test)
PCE_LR11		2.5	2.46	0.66
PCE_KNN11	'algorithm':'brute', 'n_neighbors':5,'weights': 'uniform'	2.07	2.51	0.66
PCE_SVR11	'C':0.1,'degree':1,'epsilon': 1, 'gamma':0.1, 'kernel': 'linear'	2.53	2.37	0.69
PCE_MLP11	hidden_layer_sizes=(11,6,3),solver='sgd',max_iter=100,verbose=True,	2.32	2.54	0.66
PCE_RF11	n_estimators=80,max_features='sqrt',max_depth=10,min_samples_split=5,min_samples_leaf=1,	1.76	2.35	0.7
PCE_GBDT11	n_estimators=90,max_depth =2,	2	2.38	0.69
PCE_XGBoost11	'colsample_bytree':0.5, 'gamma':0.4,'learning_rate': 0.05,'max_depth':6, 'min_child_weight':4, 'n_estimators':100, 'reg_alpha':0.1, 'reg_lambda':2, 'subsample': 1	1.73	2.41	0.69

Table S13. Comparison of experimental and predicted values under the combination of the two ML models

Cation A		Cation B		Halogen X			Bandgap Ex (eV)	Bandgap ML (eV)	PCE Ex (%)	Voc Ex (V)	Jsc Ex (mA/cm ²)	FF Ex	PCE ML (%)	Voc ML (V)	Jsc ML (mA/cm ²)	FF ML	
MA	FA	Cs	Pb	Sn	Br	Cl	I										
1	0	0	1	0	0	0	1	1.6	1.581502	16.3	0.99	21.17	0.79	15.90446	0.981209	21.30387	0.749705
1	0	0	1	0	0	0	1	1.6	1.581502	15.77	0.96	20.98	0.79	14.86277	0.952024	21.2981	0.756693
1	0	0	1	0	0	0	1	1.6	1.581502	15.66	0.88	21.56	0.8	15.90466	0.981844	21.27503	0.752011
0	0.95	0.05	1	0	0	0	1	1.51	1.523595	18.04	1.08	22.7	0.735	21.0508	1.089474	23.7397	0.760971
0	0	1	1	0	0.33	0	0.67	1.92	1.850436	11.9	1.06	14.7	0.757	12.3995	1.132871	14.04643	0.734232
0.1196	0.8004	0.08	1	0	0.1196	0	0.8804	1.6	1.615064	19.94	1.112	23.29	0.765	18.22941	1.083353	22.85674	0.729074
0.15	0.85	0	1	0	0.15	0	0.85	1.73	1.655762	18.8	1.09	22.35	0.773	17.90319	1.0708	21.98143	0.710344
0.14	0.81	0.05	1	0	0.15	0	0.85	1.6	1.63968	16.52	1.02	23.01	0.7	16.42632	1.074114	21.79004	0.69536
0.1615	0.7885	0.05	1	0	0.17	0	0.83	1.61	1.663576	17.21	1.07	21.64	0.7396	17.71787	1.083623	21.97226	0.760296
0.8	0.2	0	1	0	0.04	0	0.96	1.6	1.593959	15.85	1.09	20.05	0.73	17.32797	1.026834	21.96074	0.710577

0.1425	0.8075	0.05	1	0	0.15	0	0.85	1.6	1.63968	17.6	1.071	22.38	0.734	17.47007	1.063854	22.60644	0.718991
0	0	1	1	0	0.33	0	0.67	1.91	1.850436	13.45	1.177	14.25	0.802	12.90903	1.152692	14.37381	0.741291
0	0	1	1	0	0.67	0	0.33	2.07	2.047736	9.86	1.267	10.69	0.71	8.437973	1.182351	9.424363	0.71147
0	0	1	1	0	0.33	0	0.67	1.9	1.850436	11.12	1.11	13.99	0.7158	12.97618	1.130248	14.34873	0.7327
0	0	1	1	0	0.33	0	0.67	1.91	1.850436	12.96	1.16	15.18	0.738	12.92672	1.132573	14.99102	0.752072
0	0	1	1	0	0.67	0	0.33	2.05	2.047736	7.81	1.19	10.7	0.611	8.372737	1.179525	9.840347	0.703819
0	0	1	1	0	0.33	0	0.67	1.91	1.850436	13.09	1.06	15.99	0.7712	12.895	1.110278	14.67555	0.743155
0	0	1	1	0	0.33	0	0.67	1.53	1.850436	13.2	1.22	14.5	0.704	12.81501	1.133153	14.20203	0.734232
0	0	1	1	0	1	0	0	2.31	2.36875	6.79	1.301	6.76	0.7708	7.334707	1.308892	6.250547	0.704955
0.8	0.2	0	1	0	0.033	0	0.967	1.59	1.593185	17.5	1.02	24.11	0.7146	17.04749	1.008389	22.01539	0.722328
0.1615	0.7885	0.05	1	0	0.17	0	0.83	1.63	1.663576	15.47	1.02	21.24	0.7136	15.8915	1.066212	21.65612	0.70292
0.1425	0.8075	0.05	1	0	0.1425	0	0.8575	1.6	1.621688	17.17	1.08	22.08	0.72	16.33664	1.071123	21.32501	0.698035
0.15	0.8	0.05	1	0	0.083	0	0.917	1.57	1.541032	19.1	1.09	23.1	0.76	18.18149	1.083692	22.39099	0.742921
0.1425	0.8075	0.05	1	0	0.15	0	0.85	1.65	1.63968	18.23	1.124	23.29	0.7	16.97356	1.064916	22.30922	0.715771
0.5	0.5	0	0.5	0.5	0	0	1	1.2	1.26856	5.7	0.35	27.6	0.59	7.42404	0.534912	24.74449	0.679321
0.14	0.81	0.05	1	0	0.15	0	0.85	1.62	1.63968	18.5	1.14	21.92	0.75	17.96391	1.078346	22.7075	0.714209
0.1425	0.8075	0.05	1	0	0.15	0	0.85	1.7	1.63968	18.5	0.99	23.4	0.66	17.84793	1.077565	22.3472	0.718653

Table S14. Weight of features to principal components in interpretable dimensionality reduction of PCE_{RF}

Variance contribution rate	MA weight	FA weight	Cs weight	Pb weight	Sn weight	Br weight	Cl weight	I weight	Bandgap weight	H weight	L weight	electron mobility weight	hole mobility weight
Component1 0.340258	0.0013 26	0.16641 1	0.0072 76	0.0954 03	0.4825 3	0.0610 77	5.20E-0 6	0.0676 57	0.104344	1.83E-0 7	0.0122 94	0.000398	0.00127 9
Component2 0.258105	0.0033 6	0.7352 82	0.0013 13	0.0308 3	0.1607 08	0.0002 46	5.89E-0 5	0.0002 78	0.01225	1.27E-0 5	0.0020 64	0.001111	0.05248 7

Table S15. The average effective masses(relative to the electron mass m₀) for holes (m_h*) and electrons (m_e*), the reduced effective masses (μ) and binding energies of exciton (E_b) for MA_xFA_{1-x}PbI₃

MAPbI ₃	MA _{0.75} FA _{0.25} P	MA _{0.5} FA _{0.5} P	MA _{0.25} FA _{0.75} P	FAPbI ₃
--------------------	-----------------------------------------	---------------------------------------	-----------------------------------------	--------------------

	bI ₃	bI ₃	bI ₃	
m _h */ m _e *	0.27/0.17 0.28/0.17	0.16/0.12	0.15/0.11	0.13/0.10 -/0.098 ^[13]
(m ₀)	[11]			
μ (m ₀)	0.102 0.1 ^[11]	0.068	0.065	0.055
E _b (meV)	19.50 19 ^[12]	11.09	9.61	5.5 5.3 ^[14]
				4.57

TableS16: Meaning of abbreviations

Abbreviation	Meaning	Abbreviation	Meaning
PSCs	Perovskite solar cells	ML	Machine learning
CBM	Conduction band minimum	SHAP	SHapley Additive exPlanations
VBM	Valence band maximum	CNN	Convolutional neural networks
PCE	Power conversion efficiency	LR	Linear regression
LOMO	Lowest unoccupied molecular level	KNN	K-nearest neighbors
HOMO	Highest occupied molecular level	SVR	Support vector regression
SCLC	Space-charge-limited current method	RF	Random forest
DFT	Density functional theory	MLP	Multilayer Perceptron
VASP	Vienna <i>ab initio</i> simulation package	GBDT	Gradient Boosting Decision Tree
r value	Pearson's correlation coefficient	XGBoost	Xtreme Gradient Boosting
RMSE	Root mean square error	PCA	Principal component analysis

TableS17: Explanation and method of SHAP analysis

	Explanation	Method
Figure 5	Influence of a single feature on SHAP values (local feature explanation)	SHAP part of code abstract
Figure 6	Influence of two-feature interaction on SHAP values (local feature explanation)	SHAP part of code abstract
Figure 7 Figure S2, S5, S6	Overall feature importance ranking (global explanation)	SHAP part of code abstract
Figure 8	Interpretable dimensionality reduction (local feature explanation)	Interpretable dimensionality reduction part of code abstract
Figure 9 Figure S8	Features that play a major influence in a single sample (local sample explanation)	SHAP part of code abstract

Table S18. Number of Features, Observations and Missing values in Databases

	Features	Number Features	Number Observations	Number Missing values
TableS2	MA, FA, Cs, Pb, Sn, Br, Cl, I,	8	103	0
TableS3	MA, FA, Cs, Pb, Sn, Br, Cl, I, Bandgap, H, L, electron mobility, hole mobility	13	248	0
TableS4	MA, FA, Cs, Pb, Sn, Br, Cl, I, Bandgap, H, L	11	463	0

Table S19. Overview of explanation for features

Features (descriptors)	Explanation
MA, FA, Cs, Pb, Sn, Br, Cl, I	Representing the chemical compositions of ABX ₃ -type perovskites
Bandgap	Representing the influence of the absorber layer bandgap on the electrical parameters of PSCs
H, L	Representing the energy loss at the interface (absorber layer/ transport layer) H=HTL _{HOMO} -Perovskite _{VBM} L= Perovskite _{CBM} -ETL _{LOMO}
electron mobility, hole mobility	Representing the carrier transport capacity of the transport layer

Table S20. Comparison between predicted and experimental values of band gap

Perovskites	EX(eV)	ML(eV)	Ref
MA _{0.15} FA _{0.85} PbI ₃	1.55	1.53	23
MA _{0.1} FA _{0.85} Cs _{0.05} Pb(I _{0.95} Br _{0.05}) ₃	1.55	1.51	24
FAPbBr ₃	2.29	2.28	25
FA _{0.55} MA _{0.45} Cs _{0.05} Pb _{0.5} Sn _{0.5} I ₃	1.25	1.21	26
FA _{0.9} MA _{0.1} Pb _{0.7} Sn _{0.3} I _{2.7} Br _{0.3}	1.34	1.3	27

Table S21. Comparison between predicted and experimental values of PCE

Perovskites	HTM	ETM	PCE _{EX} (%)	PCE _{ML} (%)
(FAPbI ₃) _{0.85} (MAPbBr ₃) _{0.15}	tpa-tFBTD	TiO ₂	18.3 ^[28]	17.42
(FAPbI ₃) _{0.95} (MAPbBr ₃) _{0.05}	PT-HP	SnO ₂	19.09 ^[29]	18.95
FA _{0.9} MA _{0.1} Pb _{0.7} Sn _{0.3} I _{2.7} Br _{0.3}	PEDOT:PSS	PCBM	14.41 ^[27]	14.36

Table S22. Influence of shrinking feature scale on SVR predicted PCE

Features	Train RMSE (%)	Test RMSE (%)	r value (Test)
Bandgap, H, L	3.45	2.75	0.44
Bandgap, H, L, electron mobility, hole mobility	3.31	2.69	0.47
MA, FA, Cs, Pb, Sn, Br, Cl, I, Bandgap, H, L	2.45	1.88	0.8
MA, FA, Cs, Pb, Sn, Br, Cl, I, Bandgap, H, L, electron mobility, hole mobility	2.33	1.83	0.81

Table S23. A comparative overview of predicted performance for PCE

Data Source	ML algorithms	prediction object	Performance(r value)
Literature	Kernel ridge regression	Organic solar cells	0.78 ^[30]
Literature	k-Nearest Neighbours	Organic solar cells	0.72 ^[31]
Literature	Boosted regression tree	Organic solar cells	0.71 ^[32]
Literature	Random forest	Perovskite solar cells	0.86 (This work)

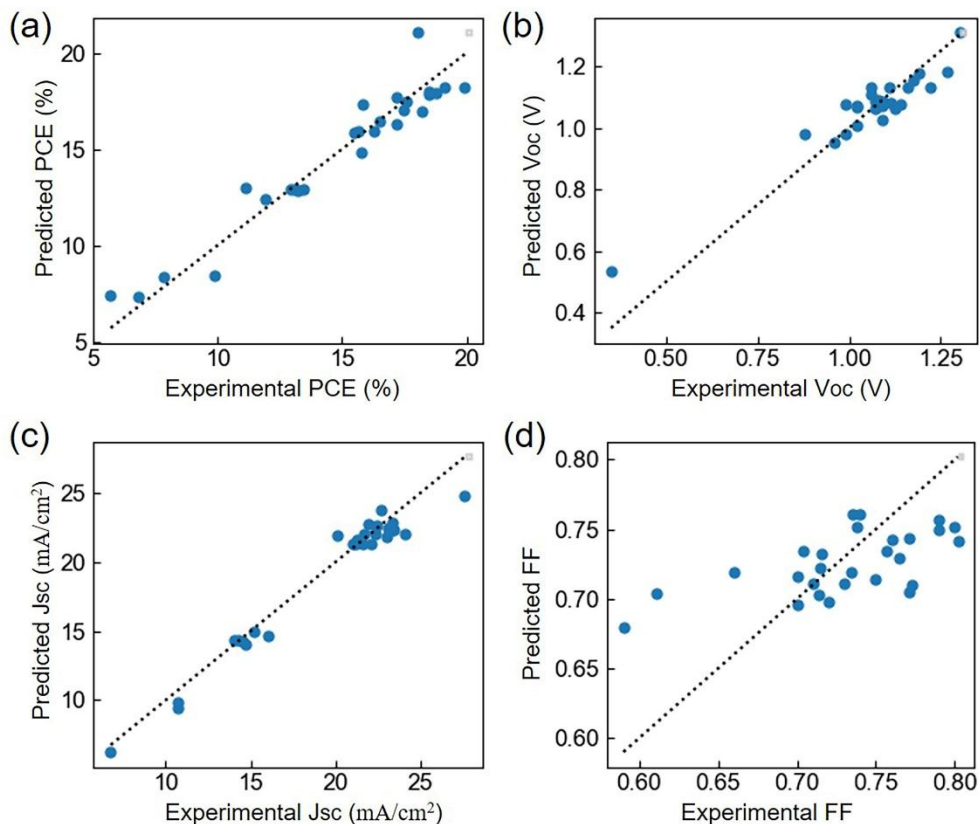


Figure S1. Performances of electricity parameter prediction model by the RF algorithm using predicted

values of bandgap、CBM and VBM. The 27 sets of experimental data in the figure are derived from TableS3. (a) Predicted PCE versus Experimental PCE. (b) Predicted Voc versus Experimental Voc. (c) Predicted Jsc versus Experimental Jsc. (d) Predicted FF versus Experimental FF.

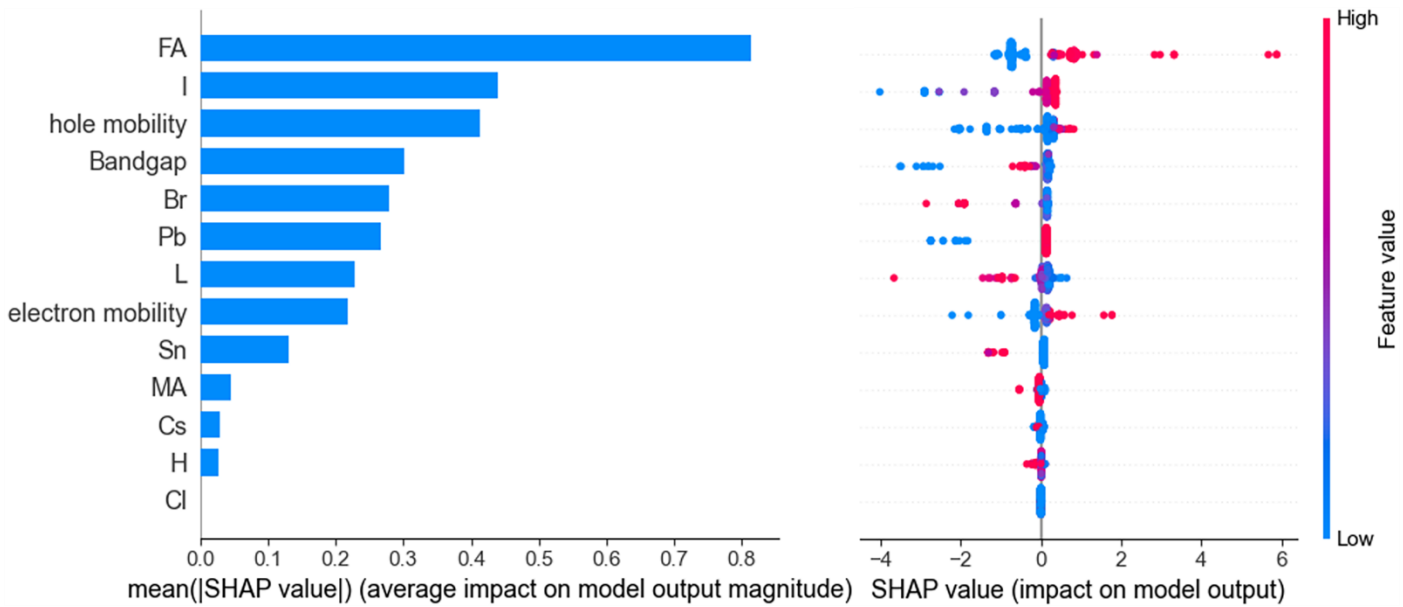


Figure S2. Feature importance ranking plot based on SHAP value(for PCE_{GBDT}). Left: bar chart of the average absolute value of the SHAP value magnitude. Right: each point represents a sample, and each row represents a feature. The order of the features is in descending order of the average absolute value of the SHAP value. Crowded places indicate a large number of samples accumulated. The color indicates the size of the feature value (red indicates high feature value, blue indicates low feature value), and the horizontal axis represents positive and negative SHAP values.

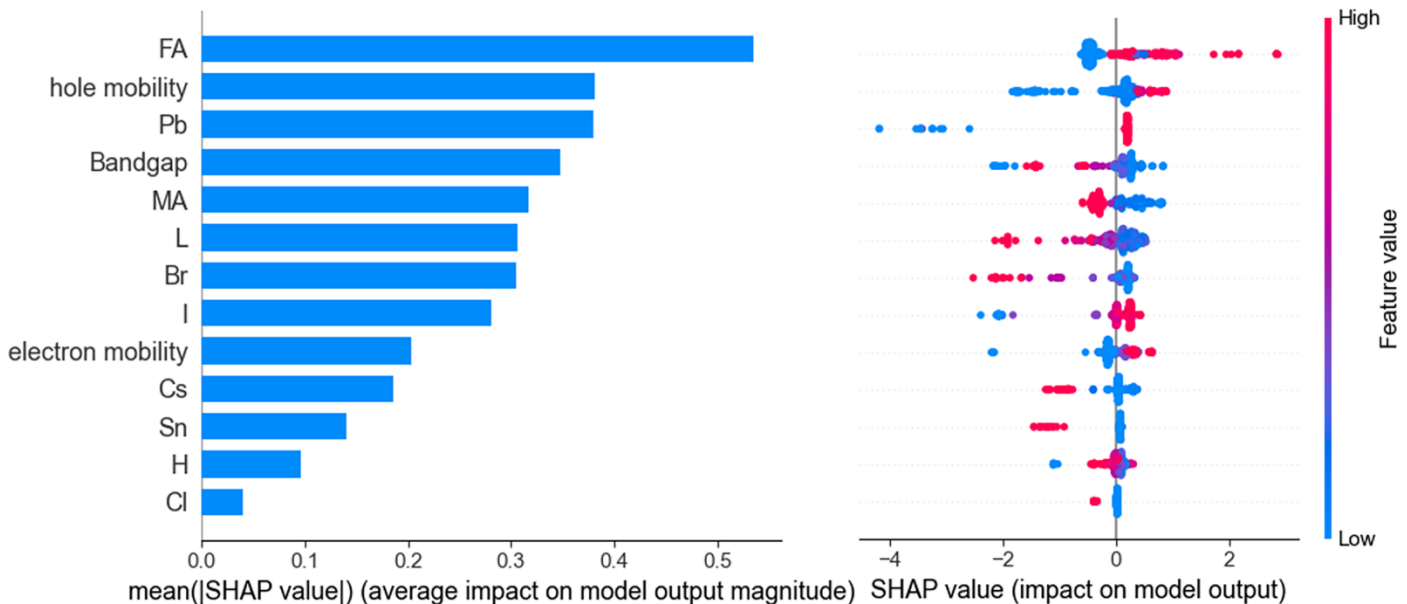


Figure S3. Feature importance ranking plot based on SHAP value(for PCE_{XGBoost}). Left: bar chart of the average absolute value of the SHAP value magnitude. Right: each point represents a sample, and each row represents a feature. The order of the features is in descending order of the average absolute value of the SHAP value. Crowded places indicate a large number of samples accumulated. The color indicates the size of the feature value (red indicates high feature value, blue indicates low feature value), and the

horizontal axis represents positive and negative SHAP values.

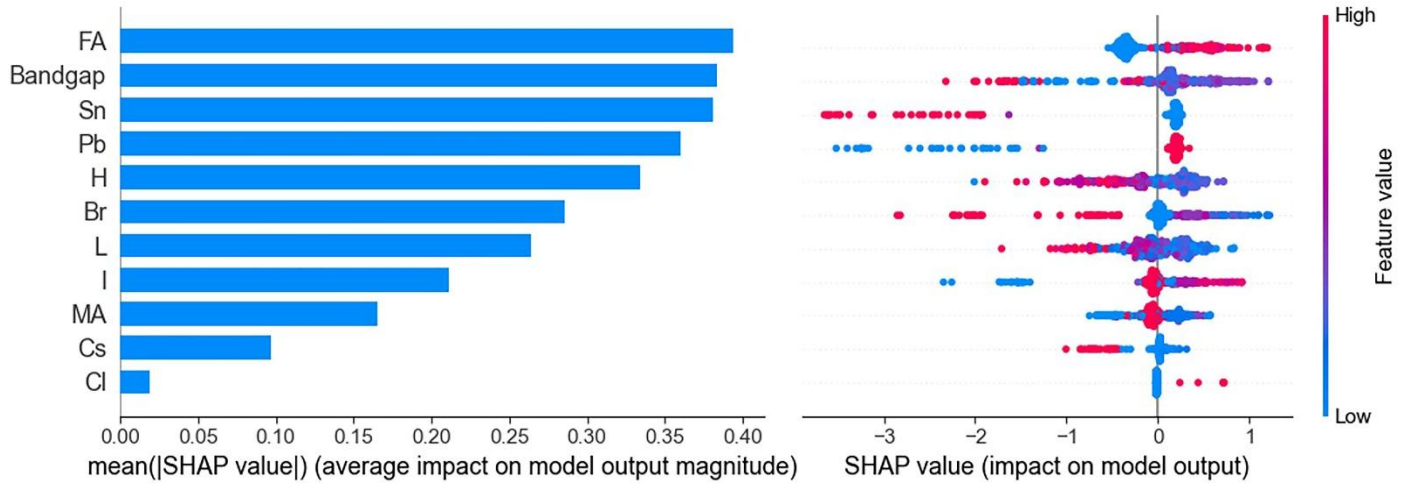


Figure S4. Feature importance ranking plot based on SHAP value(for PCE_{RF11}). Left: bar chart of the average absolute value of the SHAP value magnitude. Right: each point represents a sample, and each row represents a feature. The order of the features is in descending order of the average absolute value of the SHAP value. Crowded places indicate a large number of samples accumulated. The color indicates the size of the feature value (red indicates high feature value, blue indicates low feature value), and the horizontal axis represents positive and negative SHAP values.

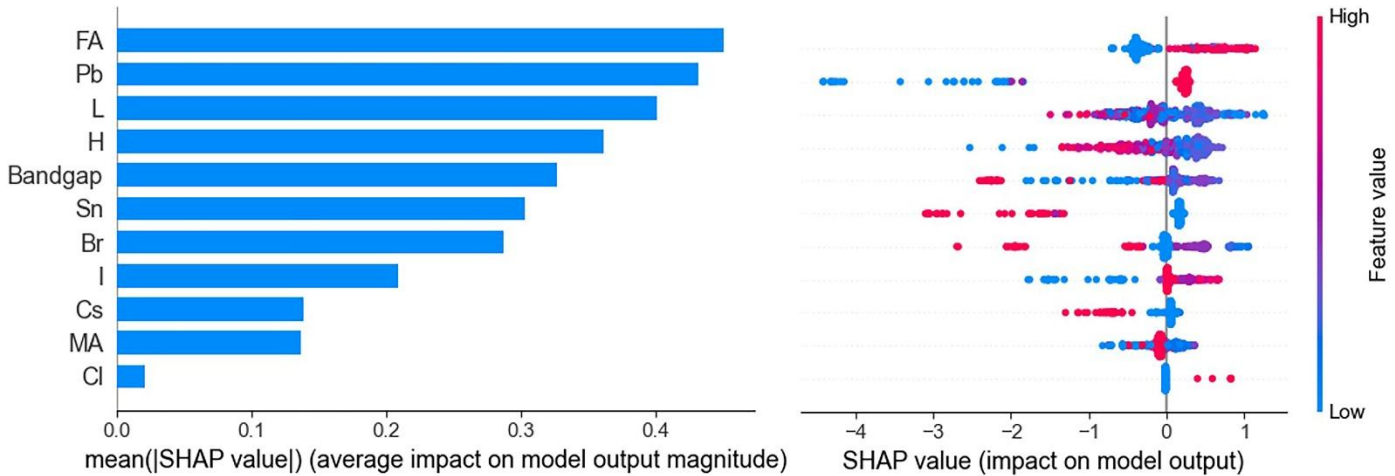


Figure S5. Feature importance ranking plot based on SHAP value(for PCE_{XGBoost11}). Left: bar chart of the average absolute value of the SHAP value magnitude. Right: each point represents a sample, and each row represents a feature. The order of the features is in descending order of the average absolute value of the SHAP value. Crowded places indicate a large number of samples accumulated. The color indicates the size of the feature value (red indicates high feature value, blue indicates low feature value), and the horizontal axis represents positive and negative SHAP values.

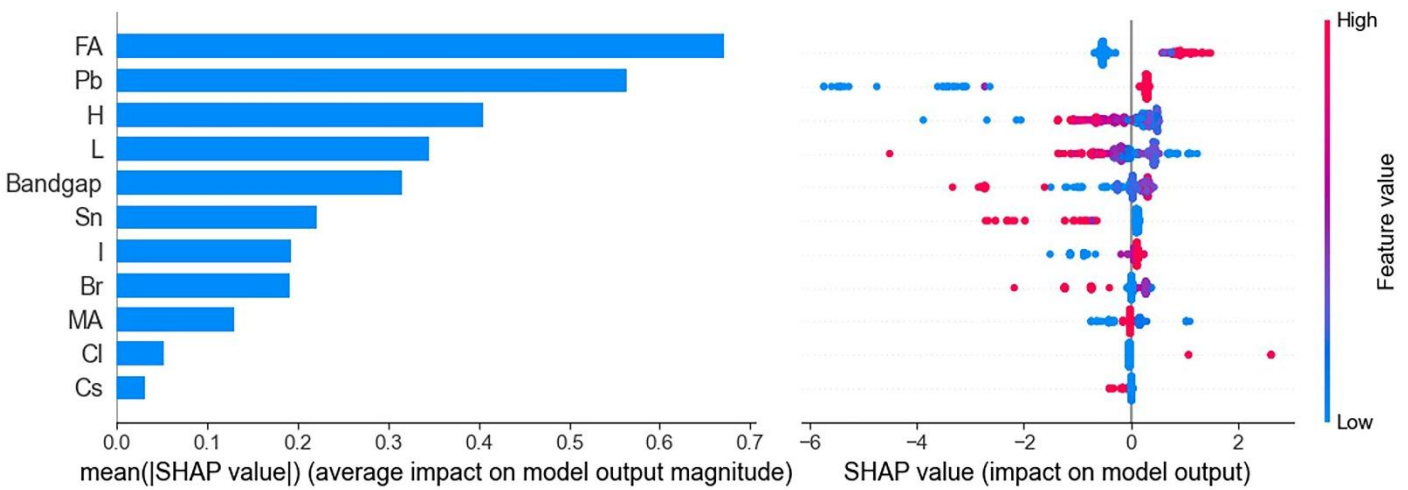


Figure S6. Feature importance ranking plot based on SHAP value(for PCE_{GBDT11}). Left: bar chart of the average absolute value of the SHAP value magnitude. Right: each point represents a sample, and each row represents a feature. The order of the features is in descending order of the average absolute value of the SHAP value. Crowded places indicate a large number of samples accumulated. The color indicates the size of the feature value (red indicates high feature value, blue indicates low feature value), and the horizontal axis represents positive and negative SHAP values.

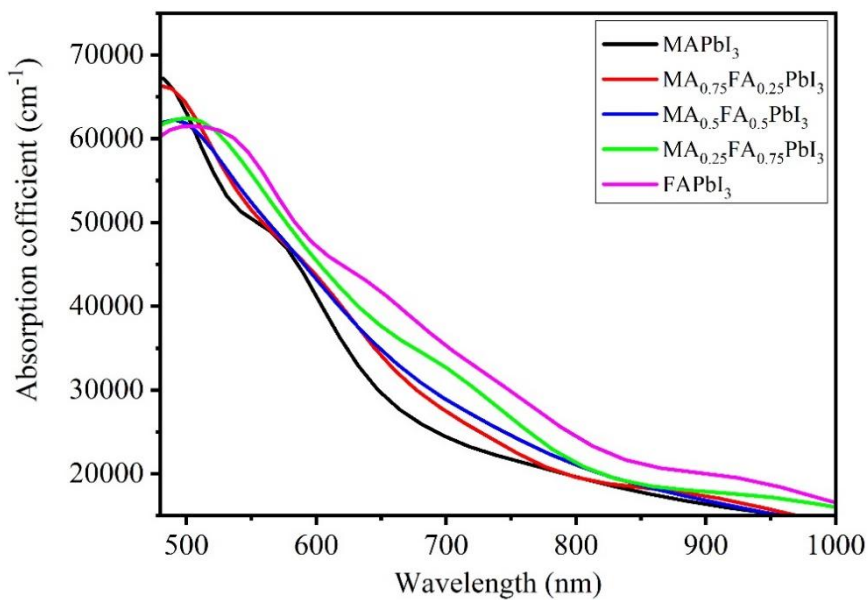


Figure S7. Absorption spectra of MA_xFA_{1-x}PbI₃.

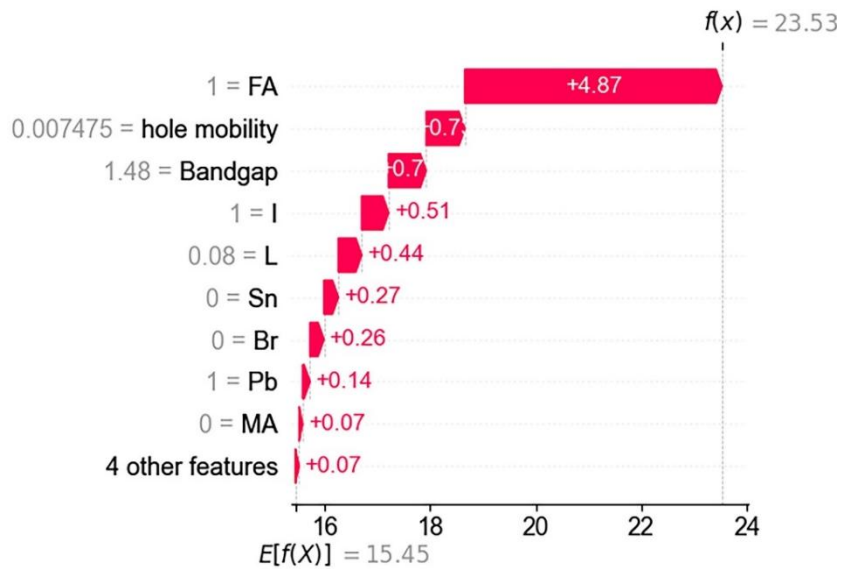


Figure S8. Evaluation process of a single sample. Perovskite composition is FAPbI₃

Mathematical part

$$RMSE = \sqrt{\frac{1}{N} \sum_{t=1}^N (observed_t - predicted_t)^2} \quad (1)$$

N represents the volume of data

$$r = \frac{\sum_{i=1}^n (\phi_i - \bar{\phi})(\varphi_i - \bar{\varphi})}{\sqrt{\sum_{i=1}^n (\phi_i - \bar{\phi})^2} \sqrt{\sum_{i=1}^n (\varphi_i - \bar{\varphi})^2}} \quad (2)$$

ϕ_i and φ_i are experimental value and predicted value of the i-th sample, $\bar{\phi}$ and $\bar{\varphi}$ are the mean value of experimental values and predicted values.

Hardware and time cost part

Hardware:

RAM:16 GB

GPU: NVIDIA GeForce GTX 970M

CPU: Intel(R) Core (TM) i7-6700HQ @ 2.60GHz(8-core)

Time cost:

ML: The training time of the 49 ML models are less than 1 min, and the calculation time are determined according to the input amount, and each 100 types are less than 20s. The time required for “GridSearchCV” and “Fivefold cross-validation” are determined by the grid search space and database. For TableS2, MLP,

SVR, KNN GBDT and RF are all less than 3 h; Xgboost about 20 h. For TableS3 and TableS4, M MLP, SVR, KNN GBDT and RF are all less than 4 h; Xgboost about 28 h.

DFT calculations

In the present work, all DFT calculations used the projector augmented-wave (PAW) method,^[15] as implemented in the VASP code.^[16] All structural relaxation and optical properties were calculated by Perdew-Burke-Ernzerhof (PBE) exchange correlation function.^[17] After the convergence test, the calculation parameters were selected as: the cutoff energy 500 eV and the electron energy convergence criterion 1×10^{-6} eV. The atomic position is relaxed until the force is less than 0.001 eV/Å. The $2 \times 2 \times 2$ and $3 \times 3 \times 3$ k -point grid samplings in Brillouin zone were used for structural optimization and optical properties calculations, respectively. Because lead belongs to heavy metals, there is a strong relativistic effect between lead and halogen atoms.^[18] Thus, the spin orbit coupling (SOC) effect is considered in all DFT calculations in this work. In cubic MAPbI₃ cells, Pb²⁺ at B site forms the Pb-I octahedron with the surrounding six I⁻ ions and MA⁺ is positioned at a corner. MAPbI₃ unit cell was increased to 2*2*2 supercell.

According to the effective mass approximation theory, the carriers of semiconductors are mainly generated by thermal excitation, and the excited holes and electrons are mainly located at VBM and CBM, respectively. The formula of carrier effective mass is as follows:^[19-21]

$$m^* = \hbar^2 \left[\frac{\partial^2 E(k)}{\partial k^2} \right]^{-1} \quad (3)$$

where k is the wave vector, $E(k)$ is the eigenvalue of the energy band and \hbar is the reduced Planck constant. A Coulomb-bound electron-hole pair produced by a photon absorbing by solid is called an exciton. Based on Mott-Wannier exciton model, the exciton binding energy E_b is calculated by Eq.(4):

$$E_b = \frac{\mu e^4}{(4\pi\epsilon_0)^2 2\hbar^2 \epsilon_{eff}^2 n^2} = 13.6 \frac{\mu}{\epsilon_{eff}^2} \quad (4)$$

where ϵ_0 is the vacuum dielectric constant, μ is reduced effective mass derived from the formula $1/\mu = 1/m_e^* + 1/m_h^*$, ϵ_{eff} is the dielectric constant and 13.6 eV is the Rydberg energy or ionization energy of the ground state H atom.

For the calculation of optical properties, the complex dielectric function and the Kramers-Kronig relationship are used.^[22] The absorption coefficient $\alpha(\omega)$ is defined as follows:

$$\alpha(\omega) = \sqrt{2\omega} \left[\sqrt{\epsilon_1(\omega)^2 + \epsilon_2(\omega)^2} - \epsilon_1(\omega) \right]^{1/2}$$

(5)

where ω is the optical frequency, $\varepsilon_1(\omega)$ and $\varepsilon_2(\omega)$ are the real part and imaginary part of the complex dielectric function $\varepsilon(\omega)$, respectively

Code abstract

Prepare some needed libraries

```
import numpy as np
import pandas as pd
import matplotlib.pyplot as plt
from sklearn.model_selection import train_test_split
from sklearn.preprocessing import StandardScaler
from sklearn.model_selection import cross_val_score, GridSearchCV
from sklearn import metrics
from sklearn.ensemble import RandomForestRegressor
from sklearn.ensemble import GradientBoostingRegressor
from sklearn.neural_network import MLPRegressor
from sklearn.svm import SVR
import xgboost as xgb
from sklearn.linear_model import LinearRegression
from sklearn.neighbors import KNeighborsRegressor
import shap
from scipy import stats
from sklearn.decomposition import PCA
```

Read data and standardized data

```
df = pd.read_csv()
X_train, X_test, y_train, y_test = train_test_split(X, Y, test_size=0.2, random_state=10)
scaler = StandardScaler()
scaler.fit(X_train)
X_train_stand = scaler.transform(X_train)
X_test_stand = scaler.transform(X_test)
```

gridsearch and cv select model

KNN

```
param_grid = {'weights': ['uniform'], 'n_neighbors': range(2,20), 'algorithm': ['ball_tree', 'kd_tree', 'brute']}
```

SVR

```
param_grid = {'kernel': ['linear', 'poly', 'rbf', 'sigmoid'], 'degree': [1, 2, 3], 'gamma': [0.01, 0.05, 0.1, 0.2, 0.5, 0.6, 0.8], 'C': [0.1, 0.2, 0.3, 0.4, 0.5, 1], 'epsilon': [0.5, 1, 2]}
```

MLP

```
param_grid = {"hidden_layer_sizes": [(4,),(8,), (11,6,3), (16,10,16)], "solver": ['sgd', 'lbfgs', 'adam'],
              "max_iter": [15,25,50,100,1000],
              "verbose": [True]}
```

```

        }
RF
param_grid = {'n_estimators': [5,10,20,30,40,50,60,70,80,90,100,500,1000,1500,2000,3000,5000],
              'max_features': ['auto', 'sqrt'],
              'max_depth': max_depth,
              'min_samples_split': [2,3,5],
              'min_samples_leaf': [1,2,3],
              'bootstrap': [True]}

GDBT
param_grid = {'n_estimators': [5,10,20,30,40,50,60,70,80,90,100,500,1000,1500,2000],
              'max_depth': range(1,10)}

XGBoost
param_grid={ 'learning_rate': [0.001,0.005,0.1,0.15,0.35,0.5],
             'n_estimators': [50,100,200,300,500,700],
             'max_depth': [4,5,6,7,8],
             'min_child_weight': [3,4,6,7],
             'subsample': [0.6,0.7,0.8,0.9,1],
             'colsample_bytree': [0.3,0.4,0.5,0.6,0.7,0.8,0.9],
             'gamma': [0,0.1,0.2,0.3,0.4,0.6],
             'reg_alpha': [0,0.1,0.2,0.3],
             'reg_lambda': [1,2,5,7,9]
           }

knn_regressor = KNeighborsRegressor()
svr_regressor = SVR()
nn_regressor = MLPRegressor()
rf_regressor = RandomForestRegressor()
gb_regressor = GradientBoostingRegressor()
xgb_regressor = xgb.sklearn.XGBRegressor()
model = GridSearchCV(estimator=knn_regressor/svr_regressor/ nn_regressor / rf_regressor / gb_regressor /
/xgb_regressor, scoring='neg_root_mean_squared_error', param_grid = param_grid, cv=5,
verbose=3, n_jobs=-1, return_train_score=True)
model.fit(X_train_stand, y_train)
print(model.cv_results_)
dfresult=pd.DataFrame(model.cv_results_)
dfresult.to_csv()

```

fit and predict

```

lr_regressor/knn_regressor/svr_regressor/ nn_regressor / rf_regressor / gb_regressor /
xgb_regressor.fit(X_train_stand, y_train)
y_train_hat = lr_regressor/knn_regressor/svr_regressor/ nn_regressor / rf_regressor / gb_regressor /
xgb_regressor.predict(X_train_stand)
y_test_hat = lr_regressor/knn_regressor/svr_regressor/ nn_regressor / rf_regressor / gb_regressor /
xgb_regressor.predict(X_test_stand)

```

plot

```
fontsize = 12
```

```

plt.figure(figsize=(3.5,3))
plt.style.use('default')
plt.rc('xtick', labelsize=fontsize)
plt.rc('ytick', labelsize=fontsize)
plt.rcParams['font.family']="Arial"
a = plt.scatter(y_train, y_train_hat, s=25,c='#b2df8a')
plt.plot([y_train.min(), y_train.max()], [y_train.min(), y_train.max()], 'k:', lw=1.5)
plt.xlabel('Observation', fontsize=fontsize)
plt.ylabel('Prediction', fontsize=fontsize)
plt.tick_params(direction='in')
plt.title(("Train RMSE: {:.2e}".format(np.sqrt(metrics.mean_squared_error(y_train, y_train_hat))),\
           "Test RMSE: {:.2e}".format(np.sqrt(metrics.mean_squared_error(y_test, y_test_hat)))),\
           fontsize=fontsize)
b = plt.scatter(y_test, y_test_hat, s=25,c='#1f78b4')
plt.legend((a,b),("Train",'Test'),fontsize=fontsize,handletextpad=0.1,borderpad=0.1)
plt.rcParams['font.family']="Arial"
plt.tight_layout()
plt.show()
print ('r:', stats.pearsonr(y_test, y_test_hat))

```

SHAP

```

model.fit(X,Y)
explainer = shap.TreeExplainer(model)
shap_values = explainer.shap_values(X)
shap_explainer = explainer(X)
shap_explainer.base_values=shap_explainer.base_values[0][0]
shap_explainer.data=shap_explainer.data[]
shap_explainer.values=shap_explainer.values[]
print(shap_values.shape)
print(X.values.shape)
print(shap_explainer)
shap.initjs()
shap.dependence_plot(' feature1', shap_values,X,interaction_index='feature2',show = False)
shap.dependence_plot(' feature1', shap_values, X, interaction_index=None,show = False)
shap.plots.waterfall(shap_explainer, show = False)
shap.summary_plot(shap_values,X, plot_type="bar",show = False)
shap.summary_plot(shap_values,X,plot_type = "dot",show = False)~
plt.rcParams['font.sans-serif'] = "Arial"
plt.rcParams.update({'font.size': 80})
plt.tight_layout()
plt.show()

```

Interpretable dimensionality reduction

```

def embedding_plot(embedding, values, label, alpha=1.0, show=True):
    f = plt.figure(figsize=(3,3),dpi=500)
    plt.scatter(embedding[:,0],
                embedding[:,1],

```

```

s=10,
c=values,
linewidth=0, alpha=alpha, cmap=shap.plots.colors.red_blue)
cb = plt.colorbar(label=label, aspect=40, orientation="horizontal")
cb.set_alpha(1)
cb.draw_all()
cb.outline.set_linewidth(0)
cb.ax.tick_params('x', length=0)
cb.ax.xaxis.set_label_position('top')
plt.gca().axis("off")
if show:
    plt.show()
model.fit(X, Y)
explainer = shap.TreeExplainer(model)
shap_values = explainer.shap_values(X)
print(shap_values.shape)
pca=PCA(n_components=2)
pca.fit(shap_values)
print(pca.explained_variance_ratio_)
print(pca.components_)
components=np.array(pca.components_)
cc=components*components
print(components*components)
dfc=pd.DataFrame(cc,index=pca.explained_variance_ratio_,columns=names[:13])
dfc.to_csv(' ')
shap_pca = PCA(n_components=2).fit_transform(shap_values)
embedding_plot(shap_pca, shap_values.sum(1), " difference with average value of PCE ", show=False)
np.save('rf_shap_pca.npy',shap_pca)
np.save('shap_values.npy',shap_values.sum(1))
for i in range(13):
    embedding_plot(shap_pca, shap_values[:,i], names[i], show=False)
plt.savefig(' ')

```

References

- [1] Q. Jiang, g, L. Q. Zhang, H. L. Wang, X. L. Yang, J. H. Meng, H. Liu, Z. G. Yin, J. L. Wu, X. W. Zhang and J. B. You, *Nat. Energy.* **2017**, 2, 16177.
- [2] Y. Dong, , R. X. Yang, K. Wang , C. C. Wu, X. J. Zhu, J. S. Feng, X. D. Ren, G. J. Fang, S. Priya and S. Z. Liu, *Nat. Commun.* **2018**, 9, 3239.
- [3] C. Ge, W.T. Wu, L. Hu, Y. H. Hua, Y. H. Zhou, W. S. Li and X. K. Gao, *Org. Electron.* **2018**, 61, 113.
- [4] W. Chu, J. Y. Yang, Q. H. Jiang, X. Li and J. W. Xin, *Applied. Surface Science.* **2018**, 440, 1116.
- [5] X. W. Hu, C. Liu, Z. Y. Zhang, X. F. Jiang,J. Garcia, C. Sheehan, L. L. Shui, S. Priya, G. F. Zhou, S. Zhang and K. Wang, *Adv Sci.* **2020**, 7, 202001285.
- [6] Ra, A.et al.High-performance dopant-free conjugated small molecule-based hole-transport materials for perovskite solar cells - ScienceDirect.*Nano Energy.* **2018**, 44, 191.
- [7] B. Gil, J. Kim, K. Park, J. Cho and B. Park, *Nanomaterials.* **2020**, 10, 1669.
- [8] A. E. Labban, H. Chen , M. Kirkus , J. Barbe ,S. D. Gobbo , M. Neophytou , I. McCulloch and J. Eid

Adv. Energy. Mater. **2016**, *6*, 1502101.

- [9] Y. Liu, B. He, J.I. Duan, Y. Y. Zhao, Y. Ding, M. X. Tang, H. Y. Chen and Q. W. Tang. *J. Mater. Chem. A.* **2019**, *7*, 12635.
- [10] X. Yin, , J.H. Han, Y. Zhou, Y.C. Gu, M.Q. Tai, H. Nan, Y. Y. Zhou, J. B Li and H. Lin, *J. Mater. Chem. A.* **2019**, *7*, 5666.
- [11] P . Umari, E.Mosconi and F. D. Angelis. *Sci. Reports.* **2014**, *4*, 4467.
- [12] P . Umari, E.Mosconi and F. D. Angelis. *J. Phys. Chem. Lett.* **2018**, *9*, 620.
- [13] Y. Liu, J. Wang, N. Zhu, W. Liu, C. C Wu, C. Y. Liu, L. X. Xiao, Z. J. Chen, and S. F. Wang, *Optics. Letters.* **2019**, *44*, 3474.
- [14] C. Davies, J. Borchert, C. Q. Xia, R. L. Milot, H. Kraus, M. B. Johnston, and L. M. Herz, *J. Phys. Chem. Lett.* **2018**, *9*, 4502.
- [15] P. E. Blöchl, *Phys. Rev. B.* **1994**, *50*, 17953.
- [16] G. Kresse and J. Furthmüller, *Phys rev B.* **1996**, *54*, 11169.
- [17] J. P. Perdew, *Phys Rev Lett.* **1998**, *77*, 3865.
- [18] Y. Liang, L. Guan, X. Xu, S. Han and X. Li, *J. Phy. Chem. C.* **2020**, *124*, 6028.
- [19] Z.L. Yu, Q-R. Ma, Y-Q Zhao, B. Liu, and M-Q. Cai, *J. Phy. Chem. C.* **2018**, *122*, 9275.
- [20] W. J. Yin, J. H. Yang, J. Kang, Y. F. Yan and S.H. Wei, *J. Mater. Chem. A.* **2015**, *3*, 8926.
- [21] W. Geng, L. Zhang, Y. N. Zhang, W. M. Lau and L. M. Liu, *J. Phy. Chem. C.* **2014**, *118*, 19565.
- [22] Y. Q. Zhao, , L. J. Wu, B. Liu, L. Z. Wang, P. B. He and M.-Q. Cai, *J. Power. Sources.* **2016**, *313*, 96.
- [23] W.J. Zhao, J. Xu, K. He, Y. Cai, Y. Han, Sm. Yang, S. Zhan and D.p. Wang, *Nano. Micro. Letters.* **2021**, *13*, 1-13.
- [24] G.Q. Tong, K.L. Ono, Y.Q. Liu, H. Zhang, T.L. Bu, Y.B. Qi, *Nano. Micro. Letters.* **2021**, *13*, 1-14.
- [25] M. Rwaimi, C.G. Bailey, P.J. Shaw, T.M. Mercier, C. Krishnan, T. Rahman, P.G. Lagoudakis, R.H Horng, S. Boden, M.D.B. Charlton, *Sol. Ener. Mat. Sol. C.* **2022**, *234*, 111406.
- [26] H. Kim, J.W. Lee, G. R. Han, Y. J. Kim, S. H. Kim, S. K. Kim, S. K. Kwak and J. H. Oh, *Adv. Funct. Mater.* **2021**, *early*, 2110069.
- [27] Y. Tian a, L. Tao, C. Chen, H.F. Lu, H.P. Li, X.C. Yang and M. Cheng, *Dyes Pigments.* **2021**, *184*, 108786.
- [28] W.Q. Li, C. Shen , Z.H. Wu, Y.Y. Wang, D.Y. Ma and Y.Z. Wu, *Mater. Today. Energy.* **2022**, *23*, 100903.
- [29] X.H. Zhang, Y. Hao, S.Q. Li, J.K. Ren, Y.K. Wu, Q.J. Sun, Y.X Cui and Y.Y. Hao. *J. Phys. Chem. Lett.* **2022**, *13*, 118.
- [30] D. Padula and A.Troisi, *Adv. Energy. Mater.* **2019**, *9*, 201902463.
- [31] Z.W. Zhao, M. Cueto, Y. Geng, and A. Troisi, *Chem. Mater.* **2020**, *32*, 7777.
- [32] Y. Wu, J. Guo, R. Sun and J. Min, *npj Comput. Mate.* **2020**, *6*, 120.